

LINEAR AND STAR-LIKE SUBSTITUTED POLYCAPROLACTONES
FOR ENHANCED DELIVERY OF DOXORUBICIN

by

Katherine E. Washington



APPROVED BY SUPERVISORY COMMITTEE:

Dr. Mihaela C. Stefan, Chair

Dr. Michael C. Biewer

Dr. Jiyong Lee

Dr. Steven O. Nielsen

Copyright 2017

Katherine E. Washington

All Rights Reserved

For my family

LINEAR AND STAR-LIKE SUBSTITUTED POLYCAPROLACTONES
FOR ENHANCED DELIVERY OF DOXORUBICIN

by

KATHERINE E. WASHINGTON, BS

DISSERTATION

Presented to the Faculty of
The University of Texas at Dallas
in Partial Fulfillment
of the Requirements
for the Degree of

DOCTOR OF PHILOSOPHY IN
CHEMISTRY

THE UNIVERSITY OF TEXAS AT DALLAS

August 2017

ACKNOWLEDGMENTS

First, I would like to express my deep gratitude to my research advisor Dr. Mihaela Stefan. I will forever be grateful for her guidance and support over these years. Her intelligence, creativity, and perseverance continually inspires me to achieve more. Without her, I wouldn't have been able to achieve my full potential in graduate school. I would also like to thank my committee members for their direction and support. I would like to thank Dr. Michael Biewer for his advice and insight into my project and for taking me into his group when I was an undergraduate student, helping me to find a love of research. I would like to thank Dr. Jiyong Lee and Dr. Steven Nielsen for serving on my committee and guiding me with helpful comments and suggestions during my committee meetings.

I truly appreciate all of the members in the Stefan and Biewer labs, both past and present. It was a pleasure to work with so many intelligent, kind, and creative people. I would like to thank Dr. Jing Hao for her guidance and support and teaching me so many things in the laboratory. Without her support and encouragement, I might have never entered the PhD program. Many thanks to Dr. Elizabeth Rainbolt for her mentorship in the drug delivery projects, for teaching me so many techniques, and for her friendship. Special thanks to Dr. Jia Du, for being a great friend and colleague. I am really grateful for his support and advice. My appreciation goes to Ruvanthi Kularatne for being so wonderful to work with in the drug delivery projects and being a great friend, together we were able to learn and accomplish so much. I would also like to thank Chandima Bulumulla, Dushanthi Dissanayake, and Ruwan Gunawardhana for being so easy to work with, their friendship, and for their positive attitudes and hard work. I would like to thank Crystal Niermann for being a good friend and someone who was always excited to talk about

science. I would like to thank Yixin Ren for his help and his hard work in the lab. I would also like to thank former group members Dr. Ruvini Kularatne, Dr. Hien Nguyen, Dr. Peishen Huang, Dr. Samodha Gunathilake, Dr. Mahesh Bhatt, Dr. Harsha Magurudeniya, and Dr. Suchithra Senevirathne who helped train and mentor me as an undergraduate and new graduate student. I learned so much from all of them. My appreciation goes to the other current members of the Stefan and Biewer labs as well: Taniya Pathiranage, Vasanthi Karmegam, Lakmal Gamage, Muktadir Talukder, Justin Miller, Pooneh Soltantabar, Erika Calubaquib, John Michael Cue, and Mahesh Gedara. I am glad that I had a chance to work with everyone.

I would also like to thank all of the undergraduate students that I had an opportunity to work with, especially Matthew Gillings, Nicolette Doan, Jack Webb, and Calvin Geng who helped me so much with the synthesis of monomers and polymers.

I would like to express my gratitude to the faculty of the Chemistry and Biochemistry department as well. Special thanks to Linda Heard, Betty Maldonado, Kelli Lewis, Dr. George McDonald, and Dr. Hien Nguyen for all of their help.

Finally, I would like to thank my whole family. My gratitude goes to my husband James and daughter Naomi, who have been so supportive and never complain about how busy I am. I would like to thank my parents as well who have always supported and believed in me, and raised me to believe that I could accomplish anything I could dream of if I worked hard enough.

August 2017

LINEAR AND STAR-LIKE SUBSTITUTED POLYCAPROLACTONES FOR ENHANCED DELIVERY OF DOXORUBICIN

Katherine E. Washington, PhD
The University of Texas at Dallas, 2017

Supervising Professor: Dr. Mihaela C. Stefan

Doxorubicin is a poorly water soluble chemotherapeutic drug used in the treatment of many cancers. However, due to its toxic side effects, there has been a lot of effort to develop better delivery methods for this drug to alleviate some of the toxicity and to improve its efficacy. Encapsulation of doxorubicin in polymeric micellar drug delivery systems offers an opportunity to improve this delivery by improved solubility and more controlled release of the drug to tumor sites. Substituted poly(caprolactone)s are a desirable material to use to form amphiphilic block copolymers due to their tunable properties. Depending on the substituent used, the size, stability, degradation rate, and hydrophilicity or hydrophobicity of the micelle can be adjusted. One drawback of micelle drug delivery systems is their tendency to have low drug loading capacities. In this dissertation, several drug delivery systems were designed in order to increase the amount of doxorubicin loading in polymeric micelles.

The design and recent advances of polymeric drug delivery systems featuring polyesters is discussed in Chapter 1. Polyesters are attractive drug delivery materials due to their biocompatibility and biodegradability. Many systems have been designed using these systems

including those that are stimuli-responsive to allow more control over release and those that have targeting to allow for a better accumulation of the drug delivery vehicles at tumor sites. Different systems that have been developed in recent years using polyesters are discussed in this chapter.

Chapter 2 describes a comparison of linear and 4-arm star-like block copolymers synthesized from amphiphilic polycaprolactones with a tri(ethylene glycol) substituted polycaprolactone as the hydrophilic block and unsubstituted poly(caprolactone) as the hydrophobic segment. The linear and star-like block copolymers are compared in terms of their thermodynamic stability, degradation, size, and drug loading capabilities, with the star-like structure used as a way to improve the loading of doxorubicin.

In Chapter 3, two star-like polycaprolactones featuring either four or six arms are compared in terms of their properties and drug loading abilities. In addition, these polymers are synthesized with a tri(ethylene glycol) substituted poly(caprolactone) hydrophilic block and a ethoxy substituted hydrophobic block, which are shown to have thermally controlled drug release.

Chapter 4 focuses on improving the loading of doxorubicin in polymeric micelles through the combination loading of doxorubicin with resveratrol, a polyphenolic compound that has cardioprotective and chemosensitizing properties. Resveratrol, when loaded in combination with doxorubicin, increases the amount of doxorubicin encapsulated in the micelle significantly. This can be a way to improve loading of the chemotherapeutic drug, while also decreasing some of its toxic side effects.

TABLE OF CONTENTS

ACKNOWLEDGMENTS	v
ABSTRACT.....	vii
LIST OF FIGURES	xiii
LIST OF TABLES.....	xvii
LIST OF SCHEMES.....	xviii
CHAPTER 1 RECENT ADVANCES IN ALIPHATIC POLYESTERS FOR DRUG DELIVERY APPLICATIONS	1
1.1 Abstract	2
1.2 Introduction.....	2
1.3 Ring-Opening Polymerization	5
1.3.1 Anionic ROP	5
1.3.2 Enzymatic ROP	6
1.3.3 Coordination-insertion ROP.....	6
1.4 Polyester Nanocarriers for Drug Delivery	7
1.4.1 Polymeric nanoparticles and micelles	7
1.4.2 Polymersomes	9
1.4.3 Targeting of Drug Delivery Vehicles.....	9
1.5 Nonstimuli-responsive Polyester Nanocarriers.....	10
1.6 Stimuli-responsive Polyester Nanocarriers.....	14
1.6.1 pH Responsive.....	14
1.6.2 Reduction Sensitive.....	16
1.6.3 Temperature Responsive	20

1.6.4	Light Sensitive.....	22
1.6.5	Multi-stimuli Responsive	23
1.7	Conclusions.....	26
CHAPTER 2 SYNTHESIS OF LINEAR AND STAR-LIKE POLY(E-CAPROLACTONE)-B-POLY { Γ -2-[2-(2-METHOXY-ETHOXY)ETHOXY]ETHOXY-E-CAPROLACTONE} AMPHIPHILIC BLOCK COPOLYMERS USING ZINC UNDECYLENATE.....		29
2.1	Abstract	30
2.2	Introduction.....	30
2.3	Experimental	34
2.3.1	Materials.....	34
2.3.2	Analysis	35
2.3.3	Synthetic Procedures	36
2.3.4	Characterization	37
2.4	Results and Discussion	39
2.4.1	Synthesis and Characterization of Linear and Star-Like Polymers.....	40
2.4.2	Evidence of Self-Assembly	44
2.4.3	Drug Loading with Doxorubicin	46
2.4.4	Polymer Degradation.....	49
2.5	Conclusions.....	49
2.6	Acknowledgments.....	50
CHAPTER 3 THERMORESPONSIVE STAR-LIKE Γ -SUBSTITUTED POLY(CAPROLACTONE)S FOR MICELLAR DRUG DELIVERY		52
3.1	Abstract	53

3.2	Introduction.....	53
3.3	Experimental	55
3.3.1	Materials.....	55
3.3.2	Analysis.....	56
3.3.3	Synthetic Procedures	57
3.3.4	Determination of LCST.....	58
3.3.5	Determination of CMC.....	58
3.3.6	Preparation of Micelles	59
3.3.7	Preparation of DOX Loaded Micelles.....	59
3.3.8	DLS Analysis	60
3.3.9	Demonstration of Polymer Degradation	60
3.3.10	Biological Studies	60
3.3.11	Empty Micelle Cytotoxicity Studies	60
3.3.12	DOX Loaded Micelle Cytotoxicity Studies	61
3.3.13	Cellular Uptake	61
3.4	Results and Discussion	62
3.4.1	Polymer Synthesis	62
3.4.2	Self-Assembly and Thermoresponsivity	67
3.4.3	Size and Morphology	68
3.4.4	Doxorubicin Encapsulation	69
3.4.5	Biocompatibility and Degradation	72
3.4.6	Cytotoxicity and Cellular Uptake of DOX Loaded Micelles	74

3.5	Conclusions.....	75
3.6	Acknowledgments.....	77
CHAPTER 4 COMBINATION LOADING OF DOXORUBICIN AND RESVERATROL IN POLYMERIC MICELLES TO INCREASE LOADING EFFICIENCY AND EFFICACY.....		
4.1	Abstract.....	79
4.2	Introduction.....	79
4.3	Experimental.....	81
4.3.1	Materials.....	81
4.3.2	Analysis.....	82
4.3.3	Synthetic Procedures.....	82
4.3.4	Preparation of Micelles.....	83
4.3.5	Preparation of DOX Loaded Micelles.....	84
4.3.6	Determination of Critical Micelle Concentration (CMC).....	84
4.3.7	DLS Analysis.....	85
4.3.8	Determination of <i>In vitro</i> Drug Release.....	85
4.3.9	Biological Studies.....	85
4.3.10	Empty Micelle Cytotoxicity Studies.....	86
4.3.11	Loaded Micelle Cytotoxicity Studies.....	86
4.3.12	Cellular Uptake.....	87
4.4	Results and Discussion.....	87
4.4.1	Polymer Design and Synthesis.....	87
4.4.2	Self-assembly and Morphology.....	89
4.4.3	Drug Loading Capabilities.....	93

4.4.4	Size and Morphology of Combination Loaded Micelles	96
4.4.5	<i>In vitro</i> Drug Release	99
4.4.6	Cytotoxicity of Empty and Combination Loaded Micelles	100
4.4.7	Cellular Uptake	102
4.5	Conclusions.....	103
4.6	Acknowledgments.....	104
REFERENCES		105
BIOGRAPHICAL SKETCH		120
CURRICULUM VITAE		

LIST OF FIGURES

Figure 1.1. Types and sizes of common nanocarriers used for delivery of anti-cancer drugs.....	8
Figure 1.2. Non-stimuli responsive polyesters a) poly(hydroxypropyl methacrylamide)-g- α -tocopheryl succinate) b) poly(Lac-OCA)- <i>b</i> -poly(Tyr(alkynyl)-OCA-g-mannose c) β -CD-PLA-POEGMA 21-arm star-like polymer.....	13
Figure 1.3. pH responsive polyesters with pH responsive units highlighted in green.....	17
Figure 1.4. Reduction sensitive polyesters with reduction sensitive units in orange.	20
Figure 1.5. Thermoresponsive polyesters with thermoresponsive units highlighted in blue and their respective LCST or UCST values.	22
Figure 1.6. Light responsive polyesters with light sensitive units highlighted in purple.	24
Figure 1.7. Multi-stimuli responsive polyesters for drug delivery applications, responsive units are highlighted in various colors to clarify their functionality (pH = green, light = purple, temperature = blue, and reduction = orange.	27
Figure 2.1. ^1H NMR spectrum of linear poly(ϵ -caprolactone)- <i>b</i> -poly{ γ -2-[2-(2-methoxyethoxy)ethoxy]ethoxy- ϵ -caprolactone}	41
Figure 2.2. ^1H NMR spectrum of 4-arm star-like poly(ϵ -caprolactone)- <i>b</i> -poly{ γ -2-[2-(2-methoxyethoxy)ethoxy]ethoxy- ϵ -caprolactone}	41
Figure 2.3. SEC for linear PCL precursor (black trace) and for the linear poly(ϵ -caprolactone)- <i>b</i> -poly{ γ -2-[2-(2-methoxyethoxy)ethoxy]ethoxy- ϵ -caprolactone} diblock copolymer (red trace)	43
Figure 2.4. SEC for 4-arm star-like PCL precursor (black trace) and for the 4-arm star-like poly(ϵ -caprolactone)- <i>b</i> -poly{ γ -2-[2-(2-methoxyethoxy)ethoxy]ethoxy- ϵ -caprolactone} diblock copolymer (red trace)	43
Figure 2.5. Mark-Houwink plot for linear poly(ϵ -caprolactone)- <i>b</i> -poly{ γ -2-[2-(2-methoxyethoxy)ethoxy]ethoxy- ϵ -caprolactone} (black trace) and 4-arm star-like poly(ϵ -caprolactone)- <i>b</i> -poly{ γ -2-[2-(2-methoxyethoxy)ethoxy]ethoxy- ϵ -caprolactone} (red trace)	45
Figure 2.6. Determination of CMC of (left) linear and (right) star-like PCL- <i>b</i> -PMEEECL	46

Figure 2.7. DLS of (left) linear and (right) star-like PCL- <i>b</i> -PMEEEECL showing size differences between the empty and DOX loaded micelles.	48
Figure 2.8. TEM images of empty (a) linear and (b) star-like PCL- <i>b</i> -PMEEEECL and DOX loaded (c) linear and (d) star-like PCL- <i>b</i> -PMEEEECL, scale bars are 200 nm.	48
Figure 2.9. Degradation of linear and star-like PCL- <i>b</i> -PMEEEECL in PBS (pH 7.4) over 7 days.	50
Figure 3.1. ¹ H NMR spectrum of 4-arm star-like PECL- <i>b</i> -PMEEEECL.	64
Figure 3.2. ¹ H NMR spectrum of 6-arm star-like PECL- <i>b</i> -PMEEEECL.	65
Figure 3.3. SEC trace of 4-arm star-like PECL- <i>b</i> -PMEEEECL.	66
Figure 3.4. SEC trace of 6-arm star-like PECL- <i>b</i> -PMEEEECL.	66
Figure 3.5. Transmittance and CMC plots showing thermoresponsiveness and thermodynamic stability of 4A (A and B) and 6A (C and D) respectively.	67
Figure 3.6. Size distribution (D_h) for 4A (A) and 6A (B) polymeric micelles at 25 °C obtained from DLS.	69
Figure 3.7. TEM images of empty polymeric micelles (A) 4A and (B) 6A.	70
Figure 3.8. Absorbance spectra of DOX loaded star polymers.	71
Figure 3.9. TEM images of DOX loaded micelles (A) 4A and (B) 6A, scale bar = 200 nm. TMAFM images of DOX loaded polymeric micelles (C) 4A and (D) 6A deposited on mica-substrate, scan size: 1 μ m.	72
Figure 3.10. Size distribution (D_h) obtained through DLS for (A) 4A and (B) 6A comparing the sizes of empty and DOX loaded micelles.	73
Figure 3.11. Degradation measurements of polymer 6A under physiological conditions (37 °C, pH 7.4), the % change in molecular weight (M_n) is plotted versus time.	74
Figure 3.12. Cell viability measurements of varying concentrations of empty polymeric micelles in PBS using HeLa cells and CellTiter Blue [®] cytotoxicity kit.	74
Figure 3.13. Cell viability of HeLa cells after dosing with DOX loaded micelles above and below the LCST.	76
Figure 3.14. Uptake of 4A and 6A DOX loaded micelles in HeLa cells after incubating for 4 hours. Cell nuclei were stained with DAPI.	76

Figure 4.1. ^1H NMR spectrum of PEG- <i>b</i> -PCL.	90
Figure 4.2. SEC trace of PEG- <i>b</i> -PCL with THF as the eluent.	90
Figure 4.3. ^1H NMR spectrum of PEG- <i>b</i> -PBCL.....	91
Figure 4.4. SEC trace of PEG- <i>b</i> -PBCL with THF as the eluent.....	91
Figure 4.5. CMC plots of PEG- <i>b</i> -PCL (left) and PEG- <i>b</i> -PBCL (right).	92
Figure 4.6. TEM images and DLS of empty micelles for PEG- <i>b</i> -PCL (a and c) and PEG- <i>b</i> -PBCL (b and d).	93
Figure 4.7. Absorbance spectra of drug loading variations (a) polymer variation, (b) DOX variation, and (c) RSV variation. Encapsulation efficiencies of drug loading variations (d) polymer variation, (e) DOX variation, and (f) RSV variation.....	96
Figure 4.8. DLS size comparison of empty and RSV and DOX combination loaded PEG- <i>b</i> -PCL micelles.	98
Figure 4.9. DLS size comparison of empty and RSV and DOX combination loaded PEG- <i>b</i> -PBCL micelles.	98
Figure 4.10. TEM images and DLS of combination loaded micelles for PEG- <i>b</i> -PCL (a and c) and PEG- <i>b</i> -PBCL (b and d).	99
Figure 4.11. <i>In vitro</i> drug release over time of DOX from PEG- <i>b</i> -PCL and PEG- <i>b</i> -PBCL micelles at 37 °C.	100
Figure 4.12. Cytotoxicity of PEG- <i>b</i> -PCL and PEG- <i>b</i> -PBCL empty micelles on HeLa cells after 24 hours.....	101
Figure 4.13. Cytotoxicity of DOX, RSV, and combination loaded PEG- <i>b</i> -PCL micelles on HeLa cells after 24 hours.	102
Figure 4.14. Cytotoxicity of DOX, RSV, and combination loaded PEG- <i>b</i> -PBCL micelles on HeLa cells after 24 hours.	102
Figure 4.15. Cellular uptake of combination loaded micelles into HeLa cells after 2 hours.....	103

LIST OF TABLES

Table 1.1. Properties of Commonly Used Polyesters	4
Table 1.2. Comparison of Ring-opening Polymerization Routes	6
Table 2.1. Properties and Mark-Houwink Parameters of Amphiphilic Block Copolymers	42
Table 2.2. Summary of CMC and Size Measurements.....	46
Table 2.3. Doxorubicin Loading of PCL- <i>b</i> -PMEEECL	47
Table 3.1. Summary of Polymer Compositions, Molecular Weights and Properties	65
Table 3.2. Summary of Polymeric Micelle Properties.....	67
Table 3.3. Summary of DOX Loaded Polymeric Micelle Properties	72
Table 4.1. Summary of Molecular Weights and Compositions of the Block Copolymers	89
Table 4.2. DLS and EE of Combination Loaded Micelles.	94
Table 4.3. Drug Loading Results with Varying Ratios of Polymer PEG- <i>b</i> -PBCL.....	97
Table 4.4. Drug Loading Results with Varying Ratios of RSV in PEG- <i>b</i> -PBCL.	97
Table 4.5. Drug Loading Results with Varying Ratios of DOX in PEG- <i>b</i> -PBCL.	97

LIST OF SCHEMES

Scheme 2.1. Ring-opening polymerization of MEEEECL and ϵ -caprolactone monomers using zinc undecylenate and either benzyl alcohol or pentaerythritol as initiators to form linear and star-like block copolymers.	34
Scheme 3.1. Synthesis of γ -ethoxy- ϵ -caprolactone and γ -2-[2-(2-methoxyethoxy)ethoxy]ethoxy- ϵ -caprolactone, functionalized ϵ -caprolactone monomers.	63
Scheme 3.2. Synthesis of 4-arm and 6-arm star-like PECL- <i>b</i> -PMEEEECL amphiphilic diblock copolymers.	64
Scheme 4.1. Synthesis of γ -benzyl- ϵ -caprolactone monomer.	88
Scheme 4.2. Synthesis of PEG- <i>b</i> -PCL and PEG- <i>b</i> -PBCL through coordination-insertion ring-opening polymerization.	88

CHAPTER 1
RECENT ADVANCES IN ALIPHATIC POLYESTERS FOR DRUG DELIVERY
APPLICATIONS

Authors: Katherine E. Washington, Ruvanthi N. Kularatne, Vasanthi Karmegam, Michael C.
Biewer, and Mihaela C. Stefan

The Department of Chemistry and Biochemistry, BE26

The University of Texas at Dallas

800 West Campbell Road

Richardson, Texas 75080-3021

Reprinted (Adapted) with permission from *WIREs Nanomedicine and Nanobiotechnology* **2016**,
DOI: 10.1002/wnan.1446. Copyright (2016) Wiley Periodicals, Inc.

1.1 Abstract

The use of aliphatic polyesters in drug delivery applications has been a field of significant interest spanning decades. Drug delivery strategies have made abundant use of polyesters in their structures owing to their biocompatibility and biodegradability. The properties afforded from these materials provide many avenues for the tunability of drug delivery systems to suit individual needs of diverse applications. Polyesters can be formed in several different ways, but the most prevalent is the ring-opening polymerization of cyclic esters. When used to form amphiphilic block copolymers, these materials can be utilized to form various drug carriers such as nanoparticles, micelles, and polymersomes. These drug delivery systems can be tailored through the addition of targeting moieties and the addition of stimuli-responsive groups into the polymer chains. There are also different types of polyesters that can be used to modify the degradation rates or mechanical properties. Here, we discuss the reasons that polyesters have become so popular, the current research focuses, and what the future holds for these materials in drug delivery applications.

1.2 Introduction

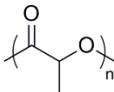
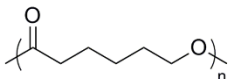
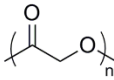
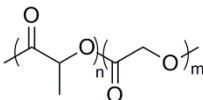
Aliphatic polyesters have been explored for several decades for use in biomedical applications owing to their biodegradability and biocompatibility.¹⁻⁶ It is important for materials in drug delivery to be able to achieve their purpose for a certain amount of time before being cleared from the body either by renal clearance or through degradation. There are several criteria that are important to consider when looking at biodegradable materials. The material itself, as well as the products produced, should be nontoxic. The mechanical properties should be suited to fulfill the task and the degradation time should align with completing the task.⁷ Polyesters also have an

advantage in their tunability; the crystallinity, thermal transitions, mechanical strength, and degradation can be altered based on molecular weight, composition (when used in block copolymers), or addition of substituents to the polymer backbones.⁷⁻¹⁰ The versatility provided by their tunability has enabled them to be used across a wide variety of biomedical applications such as drug delivery and tissue engineering.¹¹ However, the main focus here will be on aliphatic polyesters used for drug delivery.

Polyesters include poly(lactide)s (PLA), poly(caprolactone)s (PCL), poly(glycolide)s (PGA), poly(dioxanone)s (PDO), poly(butyrolactone)s (PBL), and poly(valerolactone)s (PVL) among others and combinations of these different polyesters as well. However, the most used materials are PLA, PCL, and PGA, whose properties are summarized in Table 1.1.¹²⁻¹⁴ These materials have good mechanical properties, hydrolytic degradation, and are biocompatible. PLA is one of the most popular polymers used for drug delivery, and is often used in copolymers with glycolide to form poly(lactide-*co*-glycolide) (PLGA). In the case of PLA homopolymers, there are two enantiomeric forms, poly(D-lactic acid) (PDLA) and poly(L-lactic acid) (PLLA) as well as racemic PLA.¹⁵ PLLA and PDLA are highly crystalline materials while racemic PLA is shown to be amorphous in nature. PLLA is often the most used because it is considered to be more biocompatible. PGA is a highly crystalline polymer that has a high melting point and low solubility in most solvents limiting its use in drug delivery applications,¹⁶ so it is commonly used as a copolymer with PLA to form PLGA. PLGA can be synthesized as either random or block copolymers, and there are several different types of PLGA that can be formed depending on the ratios used and the sequencing.^{7, 17} The crystallinity and glass transition temperature (T_g) can be tuned based on the type of PLGA, which is important as the glass transition temperature, in

addition to the melting point, has been shown to be influential on the release rate of encapsulated drugs.¹⁸ PLGA also has other advantages including faster hydrolysis than other polyesters due to the incorporation of GA, which can be used to tune the degradation rate depending on the composition of PGA and PLA.¹⁹ In addition, PLGA can be dissolved in a range of solvents when compared with PGA due to reduced crystallinity. PLGA has become very prevalent and has been used in a range of applications including the commercial use as a drug delivery device in Lupron Depot[®], which is used in the treatment of advanced prostate cancer.²⁰ PCL is a widely used polyester in drug delivery design owing to its good mechanical properties and slower degradation rates compared with other polyesters.²¹⁻²³ PCL is also easily tuned through addition of substituents

Table 1.1. Properties of Commonly Used Polyesters

	Structure	T_g (°C)	T_m (°C)	Degradation Time (months)
Poly(lactide) (PLA)		60-65	150-160	12-24
Poly(caprolactone) (PCL)		-60	60	> 24
Poly(glycolide) (PGA)		35-40	225-230	2-4
Poly(lactide-co-glycolide) (PLGA)		35-60	120-200	2-5

onto the monomer in typically either the α - or γ -position.^{10, 24} This allows tunability in the mechanical properties, thermal transitions, or even the hydrophilicity of the polymer.¹⁰ These substituents can also contain prodrugs or targeting moieties.²⁵⁻²⁷ Many of these polyesters are used in amphiphilic diblock copolymers where additional tuning from adjusting the compositions and block lengths can enable changes in size, drug loading capacities, and even drug release.²⁸ Here we focus on recent publications within the last 3 years including the above polymers and their derivatives.

1.3 Ring-Opening Polymerization

There are many different techniques used to synthesize polyesters including polycondensation or ring-opening polymerization (ROP) of cyclic esters. ROP is the most used method owing to higher molecular weights obtained with more control. Polycondensation requires high temperatures and long reaction times, which favors side reactions.³ The use of melt polycondensation has been shown to obtain higher molecular weights as well;²⁹⁻³⁰ however, ROP is still the most popular method for the preparation of polyesters and will be the main focus. There are many routes for ROP in the synthesis of polyesters including anionic, cationic, enzymatic, and coordination-insertion.^{3, 31-34} Cationic ROP has been shown to be hard to control and does not yield polymers with high molecular weight; therefore, it is not used as often. The advantages and disadvantages of some of the most popular types of ROP are summarized in Table 1.2.

1.3.1 Anionic ROP

Anionic ROP takes place through the nucleophilic attack of an initiator on the carbonyl carbon or on the carbon adjacent to the ester oxygen to open the ring and subsequently form a

Table 1.2. Comparison of Ring-opening Polymerization Routes

	Catalysts	Advantages	Disadvantages
Anionic ROP	alkoxides, organometals, amines, phosphines	High molecular weights achieved, some polymerizations are living	Sensitive to side reactions such as backbiting
Enzymatic ROP	Lipases	No toxic metals used, come from renewable resources	Lower yields, higher polydispersity
Coordination-Insertion ROP	Lewis acidic metal cations such as Sn(II) and an alcohol or amine initiator	High control, ability to produce high molecular weight polymers	Trace metals can be left behind which can be toxic in biological applications

linear polyester. The propagating species is balanced by a positive counter ion. Anionic ROP has been shown to provide polymers with high molecular weights and has shown to be *living* in some cases.³¹⁻³² However, anionic ROP has drawbacks as well including the presence of side reactions such as backbiting.³³

1.3.2 Enzymatic ROP

The use of enzymatic ROP has been explored as well and is attractive because it is important for polyesters used in biological applications to be free from toxic residue left from polymerization using metals. Some lipases have shown the ability to catalyze ROP of lactones. It has been shown that lipases are most active for larger lactones such as ϵ -caprolactone and have even been able to provide for polymers with high molecular weights.^{32, 35-36} However, the drawback to enzymatic ROP is that the reactions do not typically have high yield and are less controlled resulting in higher polydispersities.

1.3.3 Coordination-insertion ROP

Coordination-insertion ROP is another common way to make polyesters due to its control and ability to produce high molecular weight polymers. In this mechanism, the monomer is

coordinated to a metal center followed by the insertion into a metal-alkoxide species through the acyl-oxygen bond.³⁷ This polymerization requires a metal catalyst species and typically an alcohol initiator. Common metal catalysts for this polymerization are based on tin,³⁸ aluminum,³⁹⁻⁴⁰ and zinc.⁴¹⁻⁴³ The most employed catalyst for coordination-insertion polymerization of cyclic esters is tin(II) bis(2-ethylhexanoate). This catalyst is used most due to its approval by the Food and Drug Administration (FDA) as a food additive and ability to produce well-controlled high molecular weight polymers.^{38, 44} The largest concern with coordination-insertion ROP is that there can be traces of metal catalyst remaining after the polymerization which can be toxic when used in biological applications.

1.4 Polyester Nanocarriers for Drug Delivery

For drug delivery applications, there are many types of carriers used to deliver the drug *in vivo*. Polyesters have been used to form nanoparticles, polymeric micelles, dendrimers, and polymersomes. There are many other types of drug delivery vehicles that have been explored as well including carbon nanotubes and polymer-drug conjugates. However, since micelles, nanoparticles, and polymersomes are the most explored in recent years, here we will focus on those drug delivery vehicles (Figure 1.1).

1.4.1 Polymeric nanoparticles and micelles

Polymeric nanoparticles and micelles are formed from the self-assembly of amphiphilic block copolymer micelles. Nanoparticles have a wide range in sizes and can have a diameter ranging in size anywhere from 10-1000 nm.⁴⁵ Micelles are typically smaller, in the range of 5-

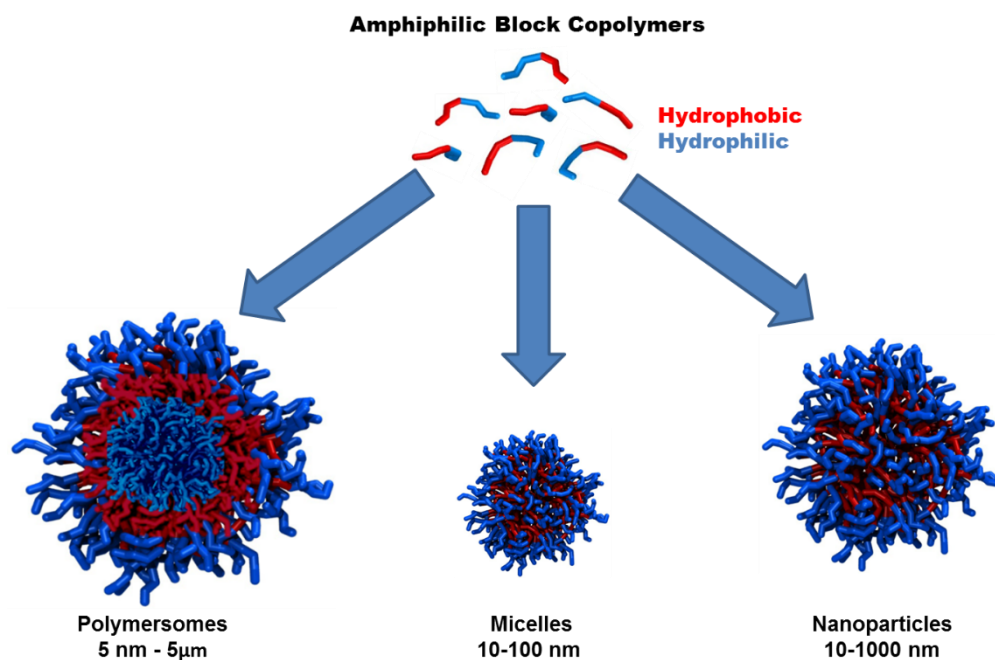


Figure 1.1. Types and sizes of common nanocarriers used for delivery of anti-cancer drugs.

100nm. The main difference between nanoparticles and micelles is the way that they are formed. Micellar formation is driven by thermodynamics where the aggregation of unimers only takes place above the critical micelle concentration (CMC), whereas the formation of nanoparticles is controlled by kinetic factors such as the temperature, pH, electrolytes, and solvents. During the formation of nanoparticles or micelles through self-assembly, hydrophobic drugs can migrate to the core with the hydrophobic block of the polymer to form the drug loaded carrier. These vehicles can then transport and deliver the drug to the intended site through bulk erosion or from stimuli triggered release.⁴⁶⁻⁴⁷ However, micelles and nanoparticles should fall within the range of 10-100 nm so that they are large enough to avoid renal clearance and at the same time are small enough to participate easily in the enhanced permeability and retention (EPR) effect.⁴⁸

1.4.2 Polymersomes

Polymersomes, or polymeric vesicles, are another popular form of drug transportation. Polymersomes are also formed from amphiphilic block copolymers and contain an aqueous solution in the core which is surrounded by the bi-layer membrane. The bi-layer membrane has a hydrophilic corona both inside and outside of the sphere and polymersomes have the ability to encapsulate not only hydrophobic drugs in the membrane, but also hydrophilic drugs, enzymes, proteins, peptides or DNA and RNA fragments in the hydrophilic core. Polymersomes have been shown to be very stable and have shown long circulation times in the blood.⁴⁹⁻⁵⁰ Polymersomes can be larger in size as well, sometimes larger than 200 nm, but it is important to control the size of the polymersomes for drug delivery use.⁵¹

1.4.3 Targeting of Drug Delivery Vehicles

Tumor sites can be targeted with polymeric nanocarriers: either through passive targeting with the EPR effect or by active targeting through the introduction of a targeting moiety to the polymer through end group variation or conjugation along the polymer backbone.⁵² In the case of passive targeting using the EPR effect, tumors have been found to have leaky vasculature allowing for the accumulation of particles ranging from 10 to in some cases 500 nm in size;⁵² however, most sources recommend that the size of particles should be between 10 and 100 nm to participate in the EPR effect.⁴⁸ At the same time, the tumors have also been shown to have poor clearance through the lymphatic system, which results in the retention of the particles in the tumor and allows for a chance to release the drug from the nanocarriers. Many of the drug delivery systems designed currently are aimed at taking advantage of this passive targeting mechanism. It is also possible to

have active targeting of these drug delivery systems through the use of antibodies, proteins, peptides, carbohydrates, vitamins, and nucleic acids.⁵²⁻⁵⁴ Carbohydrates such as glucose, mannose, galactose, and lactose have been used to functionalize for active targeting. Antibody targeting has also been used by attaching the antibodies to the end group of the micelle or nanoparticle forming polymer.⁵⁵ Another common method used for active targeting is the use of folates due to the overexpression of folate in many cancer cells. Peptides such as those containing the arginyl-glycyl-aspartic acid (RGD) sequence have also been used. In some cases, transferrin and aptamers have been used for targeting as well.⁵⁴

1.5 Nonstimuli-responsive Polyester Nanocarriers

There are several different types of polymers that have been synthesized for drug delivery that are based on polyesters. Some of these polymers have sophisticated designs where they can release the encapsulated drug depending on the surrounding stimuli, referred to as stimuli-responsive nanocarriers. However, the field of polyester nanocarriers includes many different types of designs including those that are not designed to release through external stimuli, but instead rely on erosion to release the encapsulated drug at the targeted site. Many studies in the last few years have focused on the encapsulation and delivery of drugs other than anticancer drugs or the delivery of genes or nucleic acids. Herein, the focus is on polyesters that are used for the delivery of anticancer drugs.

Some effort has been directed toward a combination drug loading using an anticancer drug with another therapeutic agent to improve cancer treatments. Qian and coworkers recently prepared PLA-*b*-polyethylene glycol (PEG) micelles for combination loading of the anticancer drug Paclitaxel (PTX) and β -lapachone, a cytotoxic agent that is bioactivated by

NADP(H):quinone oxidoreductase 1 (NQO1), which is an enzyme that has been known to be elevated in a number of tumors including pancreatic cancer, liver cancer, and breast cancer. Through coloadng, the encapsulation in PEG-*b*-PLA micelles was increased and the combination of the drugs showed strong synergistic cytotoxic effects in NQO1-overexpressing cancer cells.⁵⁶ Tu and coworkers reported coloadng of PTX and docetaxel (DTX) in PEG-*b*-PLA micelles to investigate the effect of the combination of the two drugs on the stability of methoxy PEG-*b*-poly(D,L-lactide) (mPEG-*b*-PLA) micelles compared to micelles loaded with a single drug. Their results showed that when the micelles were coloaded with the two drugs that the stability was increased and that there was also a complete and faster drug release compared with the single loaded micelles. There was also an increase in drug loading content shown for both of the drugs when loaded in combination.⁵⁷

Mixed micelles are another drug delivery method that has received attention as well. In 2015, Lo and coworkers reported mixed micelles for the delivery of doxorubicin (DOX) using a combination of α -tocopheryl succinate (vitamin E analogue) containing graft copolymers, poly(hydroxypropyl methacrylamide-*g*- α -tocopheryl succinate) (PHPMA-*g*- α -TOS), and diblock copolymers, mPEG-*b*-PLA. α -Tocopheryl succinate was used because it has been shown to have antitumor properties. The mixed micelles were shown to have greater stability and also presented low risk to L929 normal cells while exhibiting high toxicity toward HTC116 colon cancer cells.⁵⁸ Nanoparticles of mixed molecular weight PEG-*b*-PCL have also been reported by Burt and coworkers for the encapsulation of PTX and DTX and showed high incorporation of the drugs and controlled release over 14 days.⁵⁹

There have been many polyester nanocarriers that have been developed in recent years with targeting units as well. Zhai and coworkers reported daunorubicin delivery using cyclic RGD-decorated PEG-*b*-PLA micelles and Sun and coworkers reported the delivery of curcumin using RGD-functionalized PEG-*b*-PLA micelles.⁶⁰⁻⁶¹ Cheng and coworkers reported poly(Lac-OCA)-*b*-{poly[Tyr(alkynyl)-OCA]-*g*-mannose} micelles, prepared through the ROP of *O*-carboxyanhydrides (OCAs) that are derived from amino acids, for the targeted delivery of DOX. The mannose moiety allows for targeting of cancer cells that specifically express mannose receptors.⁶² Bikiaris and coworkers reported folate-pegylated polyester nanoparticles using folic acid (FA)-functionalized PEG-*b*-poly(propylene succinate) that are more selective in targeting tumors overexpressing the folate receptor such as those in breast cancer.⁶³

Different architectures have been used for polyester nanocarriers as well including star polymers, worm-like micelles, and polymersomes. Unimolecular star-like block copolymers synthesized from a cyclodextrin core were reported by Wang and coworkers. The hydrophobic PLA block was formed through the ROP of *rac*-lactide using 4-dimethylaminopyridine as the catalyst, and the hydrophilic PEG block was attached through atom-transfer radical polymerization (ATRP) after 2-bromoisobutyryl bromide was reacted with the terminal hydroxyl groups to form the ATRP macroinitiator. The 21-arm unimolecular micelles were then used for DOX encapsulation and were able to achieve a loading content of up to 10%.⁶⁴ Filomicelles, or worm-like micelles, were prepared by Marcinkowski and coworkers with diblock copolymers of PLA-*b*-PEG and the micelles were formed through a co-solvent evaporation method. The filomicelles were characterized with transmission electron microscopy and atomic-force microscopy and showed a highest drug loading content of 11.3%.⁶⁵ Polymersomes were formed by PCL-*b*-PEG

block copolymers by van Hest and coworkers through the new method of direct hydration of a highly concentrated block copolymer and oligo(ethylene glycol) solution.⁶⁶ The non-stimuli responsive polyesters discussed in this section are shown in Figure 1.2.

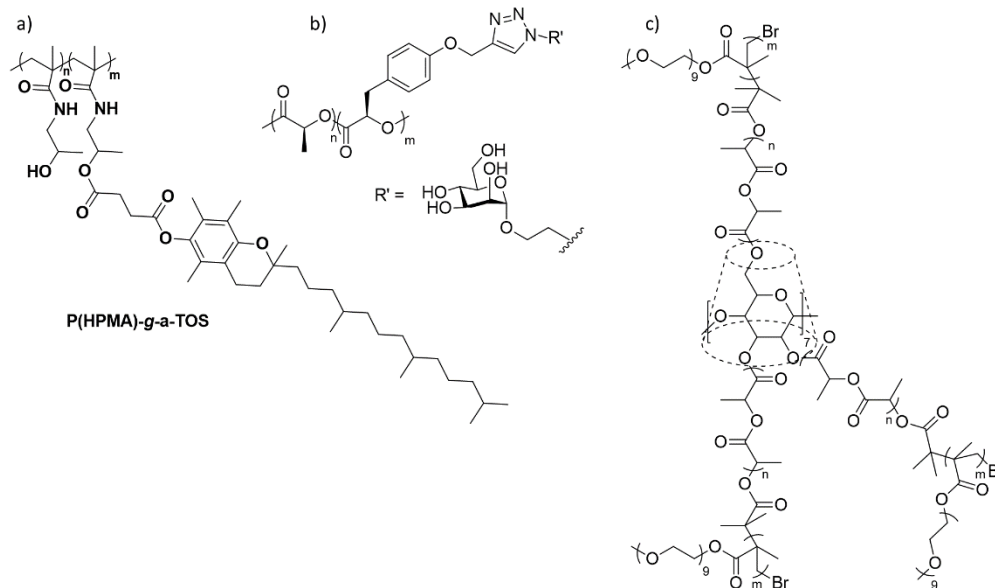


Figure 1.2. Non-stimuli responsive polyesters a) poly(hydroxypropyl methacrylamide)-g-α-tocopheryl succinate) b) poly(Lac-OCA)-b-poly(Tyr(alkynyl)-OCA-g-mannose c) β-CD-PLA-POEGMA 21-arm star-like polymer

There is still a lot of focus on nonstimuli-responsive nanocarriers in the field, although most of the research efforts are focused toward new loading methods, different architectures, or by trying to achieve delivery through more active targeting by attaching targeting moieties to the shell of the micelles or nanoparticles. The majority of the work in the field of polyester drug delivery vehicles, however, is focused on the stimuli-responsive nanocarriers.

1.6 Stimuli-responsive Polyester Nanocarriers

1.6.1 pH Responsive

pH-triggered drug release has become an important research direction due to the apparent change in pH in normal tissue versus cancer tissue. The physiological pH in normal/healthy tissue is ~7.4, while the extracellular environment of solid tumors is between 6.5 and 7.2.⁶⁷⁻⁶⁹ The main strategies for pH-responsive systems are to use polymers that have ionizable groups and undergo either changes in conformation, stability, or both or to use polymeric systems that have acid-sensitive bonds.

In order to utilize this change in pH as a trigger, pH-labile functional groups must either be present in the polymer backbone or they must be conjugated to the polymer backbone. Polymers containing amines, acetal/ketal groups, hydrazine/imide bonds, β -propiolate, and so forth are some of the acid-labile linkages used in pH-triggered release, which will undergo degradation or solubility changes with the pH gradient. Because of the presence of these acid-sensitive linkages, the anticancer drugs can be effectively delivered to the tumor site without any leakage of the cargo under physiological pH, thus sparing the healthy tissue from the adverse effects of the anticancer drugs. After endocytosis occurs in the cancer cells, the acid-labile linkages will undergo changes releasing the anticancer drug, which would lead to apoptosis and subsequent cell death.⁶⁷⁻⁶⁸

The use of poly(β -amino esters) (PAE) has been investigated for pH-sensitive drug delivery due to the change in solubility of PAE segments at different values of pH as a consequence of protonation and deprotonation of the amine groups, which results in a pH-sensitive polymer.^{67, 70} The amphiphilic triblock copolymer poly(β -amino ester)-*g*-PEG methyl ether-cholesterol (PAE-*g*-mPEG-Chol) reported by Zhang et al. had an increased cumulative release of the anticancer drug

up to ~85% after 24 h when the pH was 6 when compared to 33% at a pH of 7 during the same amount of time. When the tertiary amine groups in PAE segments protonate, they facilitate the transformation from hydrophobic to hydrophilic, which leads to a loose and swollen micelle structure. Also, the strong electrostatic repulsion between the PAE units after protonation increased the charge density on the micelle surface leading to the loose micelle structure. Hence, an increase in particle size with the decrease in pH has been observed, resulting in the release of the anticancer drug.⁷⁰ Wang and coworkers have observed similar phenomena with their poly(RGD-*co*- β -amino ester) copolymers where the drug release of ~80% was observed when the pH was 5.⁶⁷

It has been found that the charge on the surface of the micelle has a higher impact on blood circulation, nuclear localization functions, and membrane transduction. Having negatively charged corona in the micelles helps improve prolonged blood circulation time, while, as the cell membrane is negatively charged, cell internalization of the negatively charged micelles will be poor. Positively charged micelles will have a higher affinity to the cell membrane and thus will have rapid internalization; however, these micelles tend to aggregate and have rapid clearance after injection, as a result of nonspecific interactions with blood components. These concepts have been tested by Zhang and coworkers where they have synthesized copolymers of mPEG-*b*-poly(ϵ -caprolactone-*co*- γ -dimethyl maleamidic acid- ϵ -caprolactone) [mPEG-*b*-P(CL-*co*-DCL)] having varying amounts of acid-labile β -carboxylic amides. Because of the presence of β -carboxylic amides, the micelles will be negatively charged and they have obtained increased drug loading efficiency (DLE) with DOX ~84%. When the pH drops below 6, the hydrolysis of the β -carboxylic amides results in a positively charged micelle, which allows rapid internalization as well as

controlled drug release due to charge reversal-induced electrostatic repulsion between the micelle and DOX giving a cumulative release of >90% within 6 h.⁶⁸ Poly(ethylene oxide)-*b*-PCL-*b*-poly(acrylic acid) (PEO₁₁₃-*b*-PCL₁₃₂-*b*-PAA₁₅) triblock copolymer synthesized by Du and coworkers had a cumulative drug release of ~75% in 8 h. However, the DLE was only 38%. PAA was used for rapid endosomal escape as it enhances the loading and stabilization of DOX.⁷¹

A star quintopolymer comprising poly(ethylene glycol) (PEG, A), poly(ϵ -caprolactone) (PCL, B), polystyrene (PSt, C), poly(L-lactide) (PLLA, D), and poly(acrylic acid) (PAA, E) segments was reported by Zhao and coworkers where the ABCDE star quintopolymer exhibits a DLE of ~40% and a cumulative release of ~50% within 75 h with DOX. The PAA block is the pH-sensitive segment and the drug release occurs when the micelle is in an acidic medium.⁷²

Core-crosslinked, pH-responsive, polymeric micelles were fabricated by Lee and coworkers. The core crosslinks were obtained with catechol and Fe³⁺ ions. PEG-*b*-poly(1-3,4-dihydroxyphenylalanine) (PEG-*b*-PDOPA) were core-crosslinked after the formation of the micelles with Fe³⁺ ions at pH 7.4. At pH 5, the catechol-Fe³⁺ will be partially broken and the anticancer drug will be released. A cumulative release of ~60% DOX was obtained in a period of 24 h.⁷³ Figure 1.3 shows the pH responsive polyesters that have been discussed in this section.

1.6.2 Reduction Sensitive

Disulfide linkages are known to be bio-reducible, as they are reduced to thiols in intracellular environment in response to reductive reactions. Glutathione (GSH), a tripeptide containing cysteine with a thiol pendant group, is responsible for this reduction.⁷⁴ The concentration difference of the GSH between the normal cells and cancer cells has attracted much attention for the controlled release of the anticancer drugs into the tumor site. It has been found

et al. has the disulfide linkage between two PLA blocks, thus PEG-*b*-(PLA-ss-PLA)-*b*-PEG. This disulfide linkage in the presence of a reducing environment (GSH = 10 mM) will cleave; however, the polymer remains amphiphilic. Thus, the micelle will increase in size facilitating the release of the anticancer drug.⁷⁸

Shen and coworkers reported a core-crosslinked micelle with the use of PEG-*b*-poly[(ϵ -caprolactone)-*co*-(5,5-diazidomethyl trimethylene carbonate)] (mPEG-*b*-PDATCL). The reductive responsive drug delivery system was obtained by *in situ* core-crosslinking of the micelles with propargyl 3,3-dithiopropionate. Reductive cleavage (with DTT = 10 mM) of the disulfide linkages will lead to de-crosslinking and as such, the drug will be released.⁷⁹ Halila and coworkers synthesized a series of chitosan oligosaccharide-grafted PCL (PCL-*g*-COs) with pendant azide groups in the PCL backbone. These azide groups were crosslinked with bis[(propargyl carbamate)ethyl] disulfide (Cys-alkynyl) after micelle formation. The formed micelles were shown to degrade in the presence of GSH (10 mM).⁷⁶ An amphiphilic multiblock copolymer containing hydrophilic PEG and hydrophobic poly(butylene mercaptosuccinate) (PBMS) segments was synthesized by Zhu and coworkers. After formation of micelles with the amphiphilic multiblock copolymer (PEG-PBMS) the pendant thiol groups were crosslinked with H₂O₂. In the presence of a reductive environment (DTT = 10 mM), due to the cleavage of the core-crosslinks, the drug will be unloaded.⁸⁰

Farokhzad and coworkers synthesized a polyester with disulfide linkages in the hydrophobic block while PEG was used as the hydrophilic block. In response to reduction, the disulfide linkages in the hydrophobic block will break causing loss in hydrophobicity of the micelle and thus the micelle will break apart releasing the anticancer drug.⁷⁷

A core-shell-corona micelle was fabricated by Liu and coworkers using PEG-*b*-poly(acrylic acid-co-tert-butyl acrylate)-PCL [PEG43-*b*-P(AA30-co-tBA18)-*b*-PCL53] triblock copolymer. The acrylic acids are crosslinked with cystamine with the formed micelles, which result in a core-shell-corona micelle. The shell consisting of the disulfide linkages will be reduced with GSH, thus premature drug release during blood circulation will be lowered and a faster drug release within the cancer cell has been observed.⁸¹

Micelles with dual disulfide linkages were reported by Oh and coworkers. The dual disulfide linkages were located both in the hydrophobic PLA core and at the core/corona interface between PLA and polymethacrylate blocks containing pendant oligo(ethylene oxide) (POEOMA). The disulfide linkages in POEOMA-ss-(PLA-ss-PLA)-ss-POEOMA triblock copolymer (DL-ssABP) undergo reduction and the linkages were cleaved in response to GSH, shedding the POEOMA coronas from the PLA cores and degrading the PLA cores. This degradation of DL-ssABP micelles facilitates the rapid release of the drug at the tumor site.⁷⁴

A four-armed star-shaped micelle was fabricated by Zhou and coworkers using a PCL-PEG copolymer having the disulfide linkages between the two blocks. When the disulfide linkages undergo reduction in the presence of GSH, the two blocks will break apart disassembling the micelle, which facilitate the drug release. Targeting was achieved by using FA in the hydrophilic block.⁷⁵ The structures of the reduction responsive polyesters mentioned are shown in Figure 1.4.

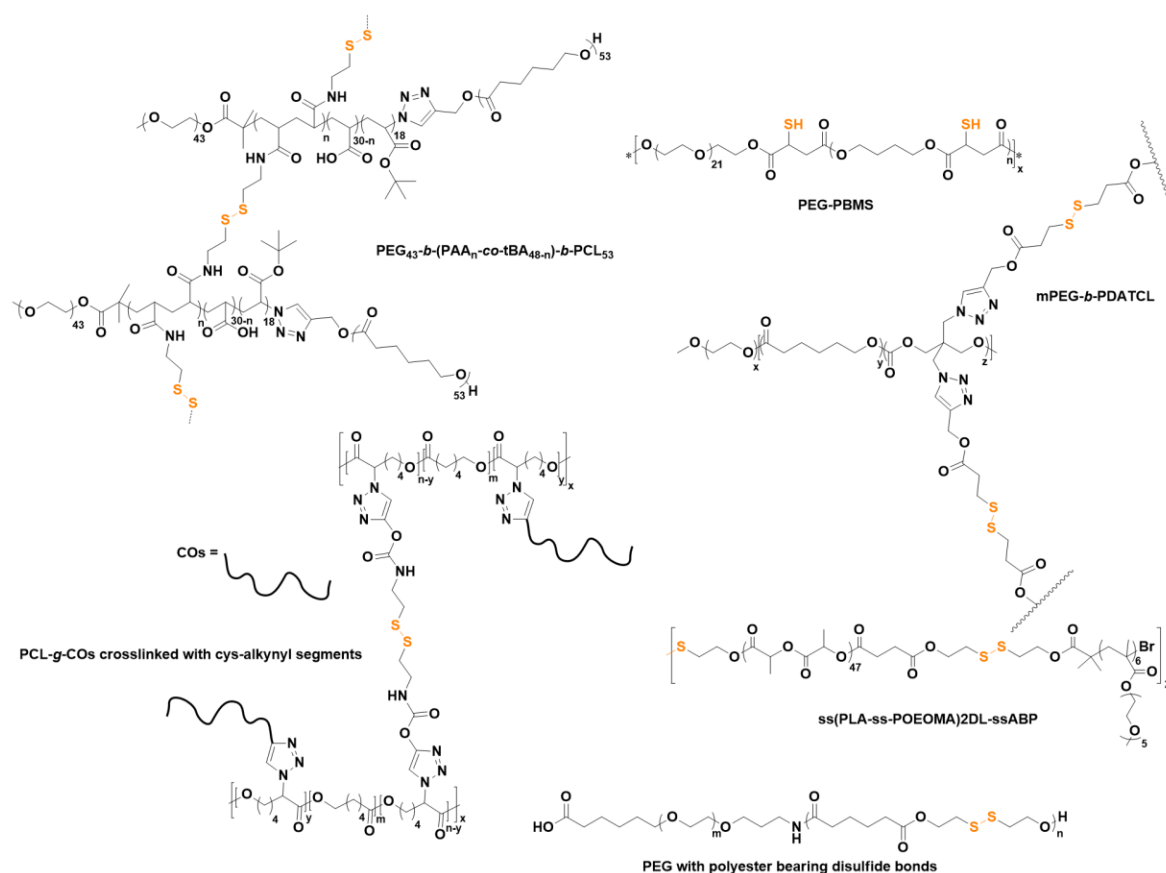


Figure 1.4. Reduction sensitive polyesters with reduction sensitive units in orange.

1.6.3 Temperature Responsive

Thermoresponsive systems in drug delivery have been widely investigated for stimuli-responsive systems. Thermosensitive nanocarriers ideally will retain their load at physiological temperature and release the drug within a tumor once external temperature is applied to induce local hyperthermia.⁶⁹ Polymers exhibiting lower critical solution temperature (LCST) or upper critical solution temperature (UCST) are used as polymers for thermoresponsive drug delivery systems. Polymers that exhibit LCST become insoluble in water above a certain temperature causing it to undergo a coil-to-globule transition. On the other hand, polymers exhibiting UCST

will undergo a globule-to-coil transition above the UCST and thus become soluble in water.^{24, 82} When this phenomenon is used in thermoresponsive drug delivery nanocarriers, due to either one of the two mechanisms, the anticancer drug will be released. There are other thermoresponsive systems that have been developed as well, including a polyester from Avgoustakis and coworkers,⁸³ in which the melting point of the polymer governs the drug release. However, the most studied out of these systems are the polymers exhibiting LCST, with poly(*N*-isopropylacrylamide) (PNIPAAm) as the most widely used thermoresponsive polymer in biomedical applications, which has an LCST of 32 °C.^{82, 84-85}

PCL-*g*-PNIPAAm synthesized by Bao and coworkers has an LCST of 35 °C for PCL₁₀-*g*-PNIPAAm_{7.6k} and 32.5 °C for PCL₂₀-*g*-PNIPAAm_{7.6k} and the polymers have shown to aggregate above the LCST.⁸⁴ Stefan and coworkers reported two thermoresponsive polymers containing poly{ γ -2-[2-(2-methoxyethoxy)ethoxy]ethoxy- ϵ -caprolactone} (PMEEECL) as the thermoresponsive segment. Block copolymers synthesized with γ -(2-methoxyethoxy)- ϵ -caprolactone as the hydrophobic block had LCSTs in the range of 31–43 °C.⁸⁵ The LCST of diblock terpolymers of PMEEECL-*b*-(PCL-*co*-PMECL) was in the range of 29–54 °C.²⁴ All these polymers were shown to aggregate above the LCST. An ABA-type triblock copolymer, P2, was synthesized by Ghosh and coworkers, where it showed an LCST of ~35 °C.⁸⁶

An amphiphilic poly(acrylamide-*co*-acrylonitrile)-*g*-PEG [poly(AAm-*co*-AN)-*g*-PEG] with a UCST of 43 °C was synthesized by Du and coworkers, where the polymer self-assembled into micelles and showed thermally sensitive drug release.⁸² The structures and transition temperatures of these thermoresponsive molecules are shown in Figure 1.5.

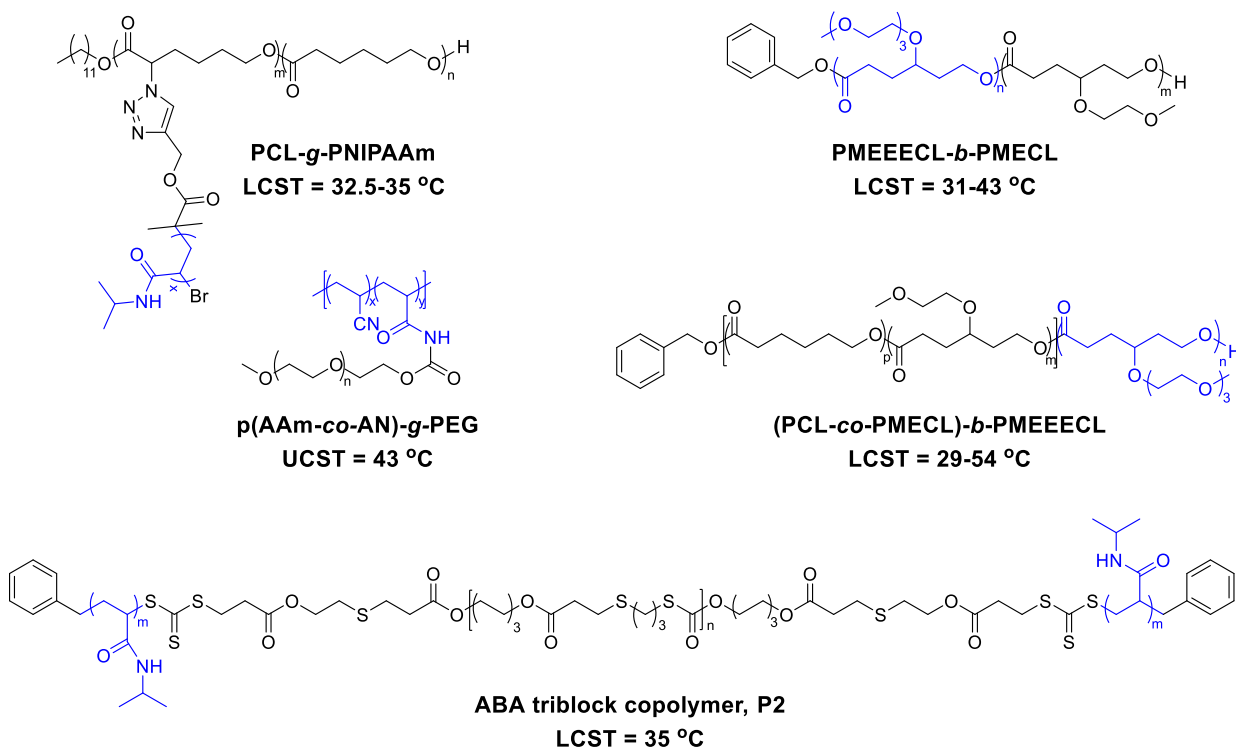


Figure 1.5. Thermoresponsive polyesters with thermoresponsive units highlighted in blue and their respective LCST or UCST values.

1.6.4 Light Sensitive

Light, being an external stimulus for stimuli-responsive nanoparticles, provides more control over the drug release at the specific site (spatial control) and at the correct time (temporal control). This remotely controlled process can be switched on and off as desired to release the payload. The irradiation is carried out by ultraviolet (UV), visible, or near infrared (NIR) light. Generally, light-responsive polymeric material that contains pendant groups undergoes a certain transformation in response to light. The type of photoresponsive group and its location in the nanoparticle is important. For instance, these groups can be in the micellar core, corona, or in the

core-corona interface, with the majority found in the corona. In response to light these nanoparticles can undergo irreversible or reversible changes.⁸⁷⁻⁸⁸

UV-sensitive polymeric nanoparticles were prepared by Wang and coworkers using photodegradable linkers, 5-hydroxy-2-nitrobenzyl alcohol (ONB), as junction points between hydrophilic dextran (Dex, or maltodextrin, MDex) and hydrophobic poly(4-substituted- ϵ -caprolactone) (PXCL) chains. The synthesized polymers are in the form of Dex-ONB-PXCL and MDex-ONB-PXCL. The photolabile ONB in the polymer backbone will be cleaved in response to UV irradiation disassembling the polymeric micelles and releasing the loaded drug.⁸⁷

Xu and coworkers reported an amphiphilic azobenzene-containing diblock copolymer AZO-mPEG-poly(5). When the azobenzene group undergoes a trans–cis isomerization in response to UV irradiation, the hydrophobicity of the micelle changes and thus releases the cargo. If visible light is shone afterward, the micelles would reassemble due to the cis–trans isomerization. This back and forth isomerization of the azobenzene group has been used for the drug release in a controlled manner. This phenomenon was demonstrated using scanning electron microscopy.⁸⁸ These light responsive polyesters are shown in Figure 1.6.

1.6.5 Multi-stimuli Responsive

Recently, polymeric nanoparticles that undergo changes in response to two or more stimuli have garnered much attention because they give unprecedented control over drug release. Among the combinations, pH/redox and pH/temperature are widely used.

A series of dual pH- and temperature-responsive block copolymer micelles were prepared

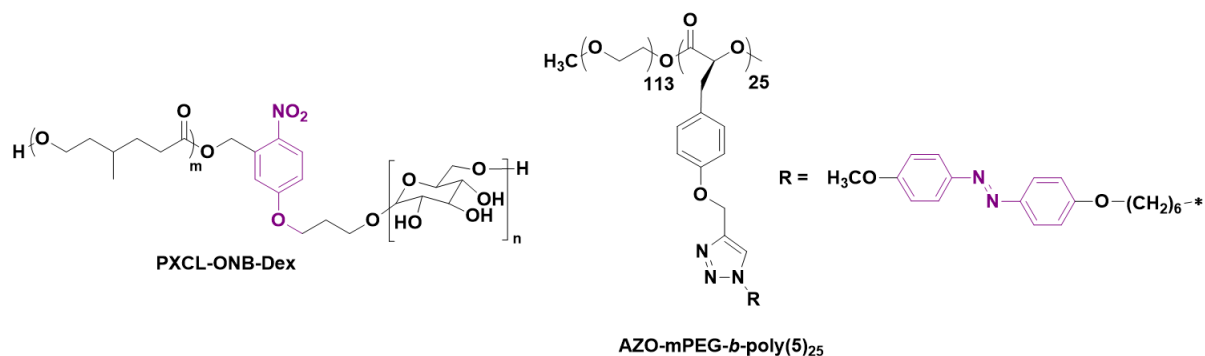


Figure 1.6. Light responsive polyesters with light sensitive units highlighted in purple.

with PCL and poly(triethylene glycol) as hydrophobic and hydrophilic blocks, respectively, by Jen and coworkers. The hydrophilic block was copolymerized with an amino acid-functionalized monomer to obtain pH sensitivity. When poly(triethylene glycol) was copolymerized with 6-aminocaproic acid (ACA) an LCST of 48.2 °C at pH 7.4 and an LCST of 35.6 °C at pH 5.3 were obtained. Thus, during circulation the micelles will be well dispersed and stable. Once cell internalization takes place the pH will be lowered (<6). As the LCST of the polymer is 35.6 °C at pH 5.3, the polymer chains will coil together inside the cell releasing the anticancer drug.⁸⁹ The block copolymer synthesized by Wang and coworkers exhibited dual responsiveness in a similar manner as mentioned above. The PCL-*b*-poly(methyl ethylene phosphate-*co*-ethyl ethylene phosphate) with a carboxyl end group [PCL₂₃-*b*-P(MEP₆₅-*co*-EEP₈₀)-COOH] showed an LCST of 40 °C at pH 7.4 and an LCST of 28 °C at pH 5.5.⁹⁰ A mixed-shell polymeric micelle was reported by Zhang and coworkers using diamino-triazine-terminated PCL (DAT-PCL), uracil-terminated mPEG (mPEG-U), and uracil-terminated poly(N-vinylcaprolactam) (PNVCL-U). In aqueous

media, these will form hydrogen bonding between DAT-PCL and mPEG-U or DAT-PCL and PNVCL-U and will form a mixed micelle. PNVCL-U has an LCST of 32 °C; thus, in the physiological pH, the PNVCL will collapse onto the PCL core protecting the drug inside the core. When at intracellular pH, due to the breakage of the hydrogen bonds, the micelles will disassemble and the drug will be released.⁹¹

PEG-PCL-PNIPAAm star terpolymer synthesized by Chen and coworkers self-assembles into vesicles in aqueous media and is dually responsive to pH and reduction environments. Because of the cleavable behavior of the star terpolymer in the presence of DTT, the polymer vesicle will undergo gradual dissociation releasing the drug.⁹² Zhou and coworkers reported a terpolymer with mPEG, PLA, and polyethylenimine (PEI). PEI and PLA were connected by redox-sensitive disulfide linkages. The mPEG-PLA-ss-PEI terpolymer was reacted with FA and 2,3-dimethylmaleic anhydride to obtain active targeting and pH responsivity, respectively. As explained previously, the micelles formed from this terpolymer will exhibit charge reversal in response to acidic environments due to the presence of the carboxylic groups in the PEI chains. After cell internalization due to charge reversal, the micelle will migrate into the cytoplasm from the lysosome via a proton-sponge effect and the PEI will shed in response to a higher concentration of GSH, releasing the anticancer drug.⁹³

A polyrotaxane-containing triblock copolymer was synthesized by Feng and coworkers using PCL, PNIPAAm, and α -cyclodextrins (α -CD). PNIPAAm acts as the thermoresponsive segment and an azobenzene group was attached to the polyrotaxane block by the hydroxyl group conjugated to α -CD to obtain light responsivity. This dual temperature and light-responsive triblock copolymer has a trans–cis isomerization of the azobenzene group in response to UV light

at 365 nm. An LCST of 32.8 °C was reported for this polymer and they have observed an increased drug release of ~90% above the LCST.⁹⁴

A multiresponsive polymer reported by Ren and coworkers consists of thermoresponsive poly{[2-(2-methoxyethoxy)ethyl methacrylate]-*co*-oligo(ethylene glycol) methacrylate} [poly(MEO2MA-*co*-OEGMA)], pH-responsive hydrogen bonding between PCL-adenine (PCL-A) and PEG-uracil (PEG-U), and redox-sensitive disulfide linkages between PCL and poly(MEO2MA-*co*-OEGMA). When the poly(MEO2MA-*co*-OEGMA)-ss-PCL-A: U-PEG micelles were in a pH 5 medium with a salt concentration of 0.12 M, they have observed a rapid release of Nile red due to the breakage of the hydrogen bonds, disassembling the micelle. In a reductive environment with DTT, a cumulative release of ~70% was obtained due to the reduction of disulfide linkages leading to deformation in the micelle, triggering drug release. When the micelle solution was heated to 45 °C, due to aggregation of thermoresponsive poly(MEO2MA-*co*-OEGMA), the micelle will be deformed and the drug is released.⁹⁵ The structures of the multiresponsive polyesters discussed are presented in Figure 1.7.

1.7 Conclusions

Although polyesters have been studied extensively, there are still many more avenues for improvement and new possibilities. The majority of the current research is focused on improving these materials by either increasing their uptake into tumor cells through the addition of targeting moieties, such as FA, RGD peptides, or carbohydrates. Additionally, there has been an effort to change the nature of the material itself to respond to external stimuli for the release of the drug. There are many types of stimuli that can be used for the release of the drug, including pH, temperature, reduction, and light. Attention is shifting to focus on materials that are either dual-

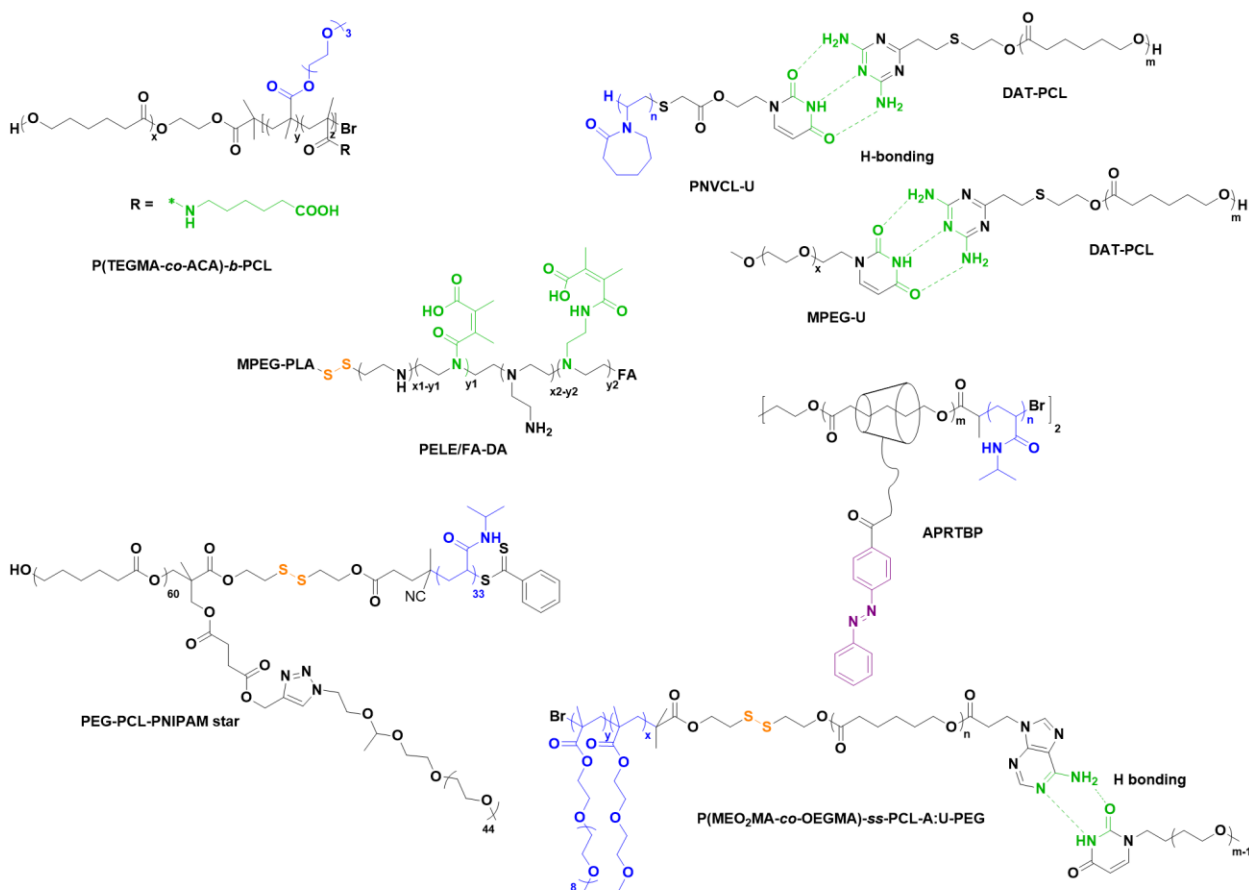


Figure 1.7. Multi-stimuli responsive polyesters for drug delivery applications, responsive units are highlighted in various colors to clarify their functionality (pH = green, light = purple, temperature = blue, and reduction = orange).

responsive or multiresponsive, due to the versatility that these new materials provide. Though there is also some motivation to use existing materials, such as the simple amphiphilic block copolymer PLA-*b*-PEG, for new applications such as in combination delivery of synergistic drugs as well as in combination with other polymers in mixed micelles.

There are still many directions that can be improved upon or explored in the field of aliphatic polyesters for drug delivery purposes. Yet, it is important to consider the limitations of these materials as well. New polymers that are developed as drug carrier systems should be easily

reproduced and should be feasible in the means of time and money for production if they are ever to make it through clinical trials and eventually to commercial use. Polymeric nanocarriers should also be stable *in vivo* and allow for enough drug loading to deliver an appropriate dose. With the addition of substituents to afford tunability to the polymer, it is important to consider not only the biocompatibility of the polymer itself but also of any products that might be formed during degradation. Even with all of the progress and research that has been done in this field, there is still more to be explored and improvements that can be made.

CHAPTER 2
**SYNTHESIS OF LINEAR AND STAR-LIKE POLY(E-CAPROLACTONE)-B-POLY{Γ-
2-[2-(2-METHOXY-ETHOXY)ETHOXY]ETHOXY-E-CAPROLACTONE}**
AMPHIPHILIC BLOCK COPOLYMERS USING ZINC UNDECYLENATE

Authors: Katherine E. Washington, Ruvanthi N. Kularatne, Jia Du, Matthew J. Gillings, Jack C.
Webb, Nicolette C. Doan, Michael C. Biewer, and Mihaela C. Stefan

The Department of Chemistry and Biochemistry, BE 26

The University of Texas at Dallas

800 W. Campbell Road

Richardson, Texas 75080-3021

Reprinted (Adapted) with permission *Journal of Polymer Chemistry Part A: Polymer Chemistry*
2016, 54,3601-3608. Copyright 2016 Wiley Periodicals, Inc.

2.1 Abstract

Linear and star-like amphiphilic diblock copolymers were synthesized by the ring-opening polymerization of ϵ -caprolactone and γ -2-[2-(2-methoxyethoxy)ethoxy]ethoxy- ϵ -caprolactone monomers using zinc undecylenate as a catalyst. These polymers have potential applications as micellar drug delivery vehicles, therefore the properties of the linear and 4-arm star-like structures were examined in terms of their molecular weight, viscosity, thermodynamic stability, size, morphology, and drug loading capacity. Both the star-like and linear block copolymers showed good thermodynamic stability and degradability. However, the star-like polymers were shown to have increased stability at lower concentrations with a critical micelle concentration (CMC) of $5.62 \times 10^{-4} \text{ g L}^{-1}$, which is less than half the concentration of linear polymer needed to form micelles. The star-like polymeric micelles showed smaller sizes when compared with their linear counterparts and a higher drug loading capacity of doxorubicin, making them better suited for drug delivery purposes.

2.2 Introduction

There have been many efforts on developing more efficient drug delivery systems to increase the efficacy of hydrophobic anticancer drugs. For this purpose, aliphatic polyesters, such as poly(caprolactone)s, poly(lactide)s, and poly(glycolide)s, have been studied extensively. These materials are attractive due to their biocompatibility and biodegradability.^{10, 23, 96-100} Among these, poly(caprolactone)s are one of the most attractive materials due to their tunability of properties through the addition of substituents in the γ -position.^{10, 25, 98} The modification of the polymer backbone by the introduction of various functionalities can alter the chemical and mechanical

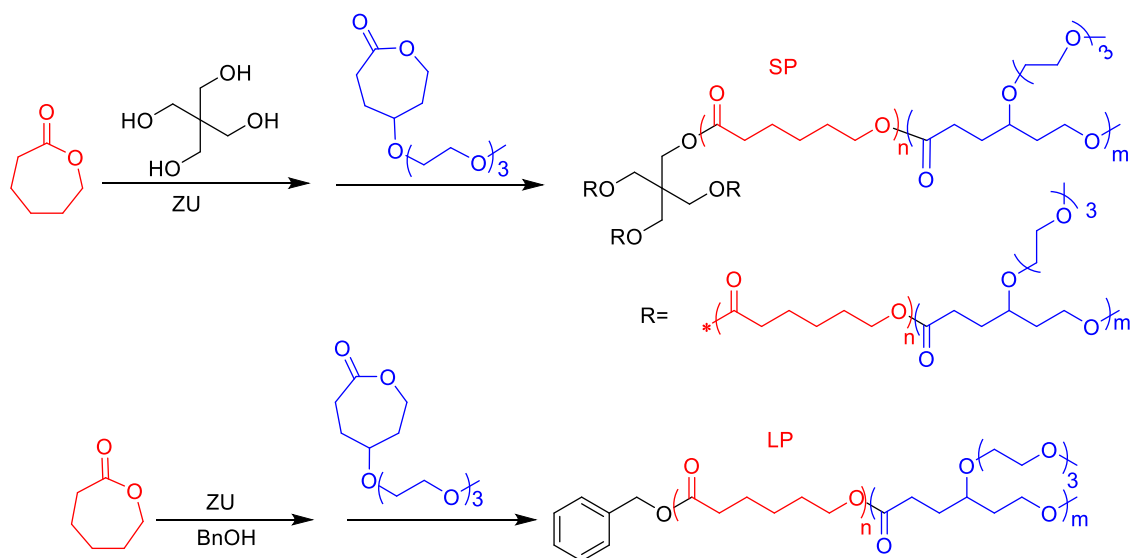
properties of the polymer, such as influencing the hydrophobicity or hydrophilicity of the polymer chain or imbuing the polymer with stimuli responsive properties. Poly(caprolactone)s are often used in amphiphilic block copolymers for use in micellar drug delivery systems. These polymeric micelles, if they are between the sizes of 10 and 100 nm, can participate in passive targeting for the delivery of anticancer drugs to tumor sites. Due to the leaky vasculature and poor clearance through the lymphatic system in some tumors, particles of this size tend to accumulate in tumor sites because of the enhanced permeability and retention (EPR) effect.^{48, 101} Polymeric micelles allow for a more efficient delivery of anticancer drugs which have poor water solubility and assist in protecting healthy cells against their toxic effects.

In the case of poly{ γ -2-[2-(2-methoxyethoxy)ethoxy]ethoxy- ϵ -caprolactone}, the addition of the oligo ethylene glycol substituent has been shown to afford hydrophilicity as well as thermoresponsivity.^{24, 85, 102-103} This biodegradable and biocompatible polymer can be used as the hydrophilic block in amphiphilic block copolymers that will self-assemble in aqueous environments to form micelles for drug delivery applications. Traditionally, poly(ethylene glycol) (PEG) is often used for the hydrophilic block in amphiphilic block copolymer systems.¹⁰⁴ However, although PEG is biocompatible, it is not biodegradable. Therefore, MEEECL offers the additional advantage of biodegradability through hydrolysis. Although MEEECL has been shown to have thermoresponsivity, the tunability of the lower critical solution temperature (LCST) is highly dependent on the hydrophobic portion of the block copolymer.^{102-103, 105} Depending on the polymer used for the hydrophobic portion of the amphiphilic block copolymer, the LCST is not always in an appropriate range for biological applications.

Another class of polymers that have garnered significant attention for drug delivery systems are star-like polymers, due to the different properties that they exhibit compared with their linear counterparts. Star-like polymers have been shown to have lower solution viscosity, higher density of functionalities, and unique topological structures when compared with their linear counterparts of similar molecular weights.¹⁰⁶⁻¹¹² Micelles generated from amphiphilic star-like polymers have also been shown in some cases to have higher drug loading capacities which are more efficient for drug delivery applications.^{106, 113} There are two classifications of star polymers, regular star polymers (homoarm) and miktoarm star polymers (heteroarm). Miktoarm star polymers have received significant attention recently for applications in biomedicine and nanotechnology.¹¹⁴ However, obtaining well defined miktoarm star polymers is challenging, due to complicated synthesis and purification procedures. There are several ways that star-like polymers can be synthesized including core-first, arm-first, and coupling-onto approaches.^{107, 115} The core-first approach involves growing the polymer chains from a multifunctional initiator core. This strategy can be used to synthesize block copolymers through a controlled coordination–insertion ring-opening polymerization using a multifunctional alcohol initiating species such as pentaerythritol and an organometallic catalyst such as zinc, tin, or aluminum alkoxides.⁴⁴ Usually amphiphilic star-like polymers involving ϵ -caprolactone have PEG as the hydrophilic block. In order to synthesize block copolymers in this way, either the arm-first method or a core-first approach is employed. In the arm-first method, the block copolymers would first be synthesized before coupling to a core to form the star-like polymer,¹¹⁶ while in the core-first method the hydrophobic block is synthesized through the ring-opening polymerization of ϵ -caprolactone followed by coupling PEG through end groups to the star-like PCL core.¹¹⁷⁻¹¹⁸

Tin(II) 2-ethylhexanoate is one of the most widely used catalysts for coordination–insertion ring-opening polymerizations which promotes a living polymerization with well-defined molecular weights. Moreover, tin(II) 2-ethylhexanoate is approved by the FDA as a food additive.¹¹⁹ However, another promising catalyst for coordination–insertion polymerization is zinc undecylenate (ZU). Zinc catalysts are typically less toxic than tin catalysts and zinc participates in human metabolism.¹²⁰ Additionally, zinc undecylenate has been shown to provide living polymerization of ϵ -caprolactone.⁴³ Typically, zinc undecylenate is used as an antifungal agent along with undecylenic acid. It has several advantages over tin(II) 2-ethylhexanoate in that it is relatively inexpensive, does not require further purification, and is easily removed after polymerization through precipitation of the polymer in hexane. Star-like block copolymers can be synthesized in a straightforward manner via coordination–insertion polymerization using zinc undecylenate as the catalyst with a multifunctional alcohol initiator through sequential monomer addition.

Herein, the synthesis of linear and star-like amphiphilic block copolymers based on poly(caprolactone)s using zinc undecylenate as a catalyst is reported. The amphiphilic block copolymers were synthesized as shown in Scheme 2.1. The properties of the two polymers were investigated for their applicability in drug delivery systems. The size, stability, and drug loading capabilities of polymeric micelles are critical when predicting their ability to function as a successful vehicle for the delivery of anticancer drugs *in vivo*. Star-like polymers of similar molecular weights to their linear counterparts have been reported to have improved stability and



Scheme 2.1. Ring-opening polymerization of MEEEECL and ϵ -caprolactone monomers using zinc undecylenate and either benzyl alcohol or pentaerythritol as initiators to form linear and star-like block copolymers.

drug loading, therefore it was predicted that 4-arm star-poly(ϵ -caprolactone)-*b*-poly{ γ -2-[2-(2-methoxy-ethoxy)ethoxy]ethoxy- ϵ -caprolactone} (PCL-*b*-PMEEEECL) would have improved properties compared to the linear PCL-*b*-PMEEEECL counterpart. The 4-arm star polymer was synthesized using a pentaerythritol initiator, while the linear equivalent was synthesized using a benzyl alcohol initiator. These polymers were compared using various parameters, including CMC, micellar size, and stability, and drug loading capacity, to determine their applicability as micellar drug carriers.

2.3 Experimental

2.3.1 Materials

All commercially available chemicals were purchased from Sigma-Aldrich or Fisher Scientific and used without further purification unless otherwise noted. Benzyl alcohol was

purified by vacuum distillation prior to use. ϵ -Caprolactone was purified by distilling over calcium hydride. All polymerization reactions were conducted under purified nitrogen. The polymerization glassware and syringes were dried at 120 °C for at least 24 h and cooled in a desiccator prior to use.

2.3.2 Analysis

^1H NMR spectra of the synthesized monomers and polymers were recorded on a Bruker AVANCE III 500 MHz NMR instrument at 25 °C in CDCl_3 . ^1H NMR data are reported in parts per million as chemical shifts relative to tetramethylsilane (TMS) as the internal standard. GC/MS was performed on an Agilent 6890-5973 GC/MS workstation. Molecular weight and polydispersity indices of the synthesized polymers were measured by size exclusion chromatography (SEC) analysis on an OMNISEC multi-detector system equipped with Viscotek columns (T6000M), connected to a refractive index (RI), low angle light scattering (LALS), right angle light scattering (RALS), and viscosity detectors with HPLC grade THF as the eluent, and triple point calibration based on polystyrene standards. Fluorescence spectra of the synthesized polymers were collected with a Perkin-Elmer LS 50 BL luminescence spectrometer at 25 °C with emission wavelength set at 390 nm. Dynamic light scattering (DLS) measurements were performed using a Malvern Zetasizer Nano ZS instrument equipped with a He–Ne laser (633 nm) and 173° backscatter detector. Transmission electron microscopy (TEM) imaging of the DOX-loaded micelles was performed on a Tecnai G2 Spirit Biotwin microscope by FEI and images were analyzed using Image J software. Samples were prepared by treating copper mesh grid with 1 mg mL⁻¹ aqueous polymer micelle solution for 2 min, followed by staining with 1% phosphotungstic acid for 30 s.

Absorbance spectra for DOX loading determination was recorded using an Agilent UV/Vis spectrophotometer.

2.3.3 Synthetic Procedures

The synthesis of the monomer γ -2-[2-(2-methoxyethoxy)ethoxy]ethoxy- ϵ -caprolactone (MEEECL) was carried out according to previously reported procedures.¹⁰²

Synthesis of Linear Poly(ϵ -caprolactone)-b-poly{ γ -2-[2-(2-methoxyethoxy)ethoxy]ethoxy- ϵ -caprolactone}

ϵ -Caprolactone (0.20 g, 0.0018 mol) was added directly into a Schlenk flask and left stirring under vacuum for 1 h. Benzyl alcohol (0.0025 g, 2.3×10^{-5} mol) in toluene (0.1 mL) was added under nitrogen atmosphere with zinc undecylenate (0.01 g, 2.3×10^{-5} mol) in toluene (0.2 mL). The reaction flask was left stirring and introduced to a thermostatted oil bath at 110 °C for 4.5 h until the monomer was consumed as determined by GC/MS. At that time, γ -2-[2-(2-methoxyethoxy)ethoxy] ethoxy- ϵ -caprolactone (0.5 g, 0.0018 mol) was added to the Schlenk flask under a nitrogen atmosphere and the reaction was left stirring at 110 °C overnight. The reaction mixture was dissolved in a small amount of THF and then the polymer was recovered by precipitation in hexane followed by re-precipitation in methanol.

¹H NMR (500 MHz, CDCl₃, δ): 1.382 (m, 10H), 1.561 (m, 17H), 1.642 (m, 19H), 1.805 (m, 4H), 2.305 (t, 9H), 2.380 (m, 2H), 3.377 (s, 3H), 3.491 (m, 1H), 3.635 (m, 12H), 4.059 (t, 9H), 4.163 (m, 2H); M_n (SEC): 9300, PDI = 1.225.

*Synthesis of 4-Arm Star-like Poly(ϵ -caprolactone)-*b*-poly{ γ -2-[2-(2-methoxyethoxy)ethoxy]ethoxy- ϵ -caprolactone}*

ϵ -Caprolactone (0.41 g, 0.0036 mol) was added directly into a Schlenk flask and left stirring under vacuum for 1 h. Pentaerythritol (0.006 g, 4.5×10^{-5} mol) was added under nitrogen atmosphere and allowed to stir for 10 min to fully dissolve before adding zinc undecylenate (0.077 g, 1.8×10^{-4} mol) in toluene (0.5 mL). The reaction flask was introduced to a thermostatted oil bath at 110 °C for 4.5 h until the monomer was consumed as determined by GC/MS. At that time, γ -2-[2-(2-methoxyethoxy)ethoxy]ethoxy- ϵ -caprolactone (1.0 g, 0.0036 mol) was added to the Schlenk flask under a nitrogen atmosphere and the reaction was left stirring at 110 °C overnight. The reaction mixture was dissolved in a small amount of THF and then the polymer was recovered by precipitation in hexane followed by reprecipitation in methanol.

^1H NMR (500 MHz, CDCl_3 , δ): 1.380 (m, 5H), 1.641 (m, 15H), 1.818 (m, 4H), 2.303 (t, 5H), 2.383 (m, 2H), 3.372 (s, 3H), 3.460 (m, 1H), 3.589 (m, 12H), 4.056 (t, 5H), 4.159 (m, 2H). M_n (SEC) = 12400, PDI = 4.324.

2.3.4 Characterization

Preparation of Micelles

Polymeric micelles were formed through nanoprecipitation and dialysis. The polymer (5 mg) was dissolved in THF (0.4 mL) and added dropwise to 5 mL of water under sonication. The resulting micelle suspension was transferred to SnakeSkin® dialysis tubing (MWCO 3500 Da) and dialyzed against a minimum of 1500 mL deionized water over a 24-h period. The final contents of the dialysis tubing were filtered through a Nylon syringe filter (0.22 μm) to obtain a polymeric micelle solution with a concentration of 1 mg mL^{-1} .

Preparation of DOX Loaded Micelles

DOX-loaded micelles were prepared in a manner similar to the empty micelles. DOX·HCl was first neutralized by adding three equivalents of triethylamine in DMSO. An aliquot of the neutralized DOX solution containing 0.5 mg of DOX was added to a polymer solution (5 mg in 0.4 mL DMSO). The DOX-polymer solution was then added dropwise into 5 mL of deionized water under sonication. The resulting suspension was transferred to dialysis tubing and dialyzed against a minimum of 1500 mL of deionized water over a 24 h period. The contents of the dialysis tube were finally filtered using a Nylon syringe filter (0.22 μm) to obtain a 1 mg mL⁻¹ solution of DOX loaded micelles. To determine the drug loading capacity (DLC) and encapsulation efficiency (EE), the drug loaded micelle solutions were lyophilized and redissolved in DMSO. The absorbance of the solution at 495 nm was fitted to a pre-established standard curve of DOX in DMSO.

Determination of CMC

The CMC was determined using pyrene, a hydrophobic fluorescent molecule, as a probe. Various concentrations of polymer samples were combined with a small amount of pyrene (6.0×10^{-5} M in THF) in 0.2 mL THF. The polymer/pyrene samples were added dropwise into 10 mL of deionized water. The resulting solutions were stirred for 4 h to allow micelle assembly and complete evaporation of THF. The resulting solutions contained concentrations from 1×10^{-5} to 1 g L⁻¹ of polymer and a constant concentration of pyrene. Fluorescence spectra of the polymer/pyrene solutions were collected at 25 °C with emission wavelength of 390 nm. The ratio of intensities of the pyrene excitation peaks at 337.5 nm and 334.5 nm were recorded and plotted against the logarithm of the polymer concentration (c). The x coordinate at the intersection of the

two trend lines before and after the abrupt increase in the $I_{337.5}/I_{334.5}$ versus $\log(c)$ curve was taken to be the critical micelle concentration.

Dynamic Light Scattering (DLS) Analysis

Aqueous suspensions of micelles were prepared as stated above at a concentration above the determined CMC, at 1 mg mL^{-1} . The micelles were analyzed to determine their hydrodynamic diameters (D_h) using dynamic light scattering. Prior to measurement, the polymer micelle solutions were filtered with a $0.22 \text{ }\mu\text{m}$ nylon syringe filter. Size measurements were recorded at $25 \text{ }^\circ\text{C}$ in triplicate.

Demonstration of Polymer Degradation

A sample of polymer (10 mg) was dissolved in 50 mL of PBS (pH 7.4, DNase-, RNase-, and Protease-Free) and was stirred in a closed system in a thermostatted oil bath at $37 \text{ }^\circ\text{C}$ over a period of 7 days. Samples were taken periodically and analyzed by SEC to monitor the change in M_n from $t = 0$ to $t = 7$ days. The resulting change in molecular weight is plotted as % of initial M_n versus days spent in PBS solution at $37 \text{ }^\circ\text{C}$.

2.4 Results and Discussion

A new fully degradable polymer was designed using MEEEECL and ϵ -caprolactone (ϵ -CL) for potential use in drug delivery applications. Zinc undecylenate was used as the catalyst for the ring-opening polymerizations due to the advantages it provides such as living polymerization and easy removal by precipitation of the polymers in hexane. In an effort to compare the micellar properties and drug delivery capabilities of different polymer architectures, linear and 4-arm star-like PCL-*b*-PMEEEECL polymers of similar compositions and molecular weights were synthesized. It was hypothesized that the 4-arm star-like polymer would have improved properties

when compared with the linear polymer including higher stability, lower viscosity, and improved drug loading capabilities. The polymer properties, CMC, size, degradation, and drug loading capacity (DLC), and encapsulation efficiency (EE) for DOX were examined for both polymers to determine if there was any significant improvement in the properties of the 4-arm star-like polymer over the linear polymer.

2.4.1 Synthesis and Characterization of Linear and Star-Like Polymers

A linear polymer (LP) was synthesized using benzyl alcohol as the initiator, and the star-like polymer (SP) was synthesized using multifunctional pentaerythritol as the initiator. The ratios used in polymerization of the linear and 4-arm star-like block copolymers were catalyst:initiator: ϵ -CL:MEEECL of 1:1:80:80 and catalyst:initiator: ϵ -CL:MEEECL of 4:1:80:80, respectively. ϵ -CL was added initially for polymerization to form the hydrophobic segment, and after full consumption of the monomer as determined by GC/MS, MEEECL was subsequently added and allowed to polymerize to form the hydrophilic segment for each polymer. The polymerization of the hydrophobic ϵ -CL is performed first so that the initiator end group will be incorporated into the hydrophobic core of the micelle in order to facilitate self-assembly of stable micelles. The ratios were targeted to form similar molecular weights and compositions for each polymer for accurate comparison.

The ^1H NMR spectra for LP and SP are shown in Figures 2.1 and 2.2 respectively, and the polymer compositions and molecular weights as determined through ^1H NMR and size exclusion chromatography (SEC) are summarized in Table 2.1. The molecular weights (M_n) that were acquired from SEC and determined through ^1H NMR are within 1000 g mol^{-1} . The PDI for the

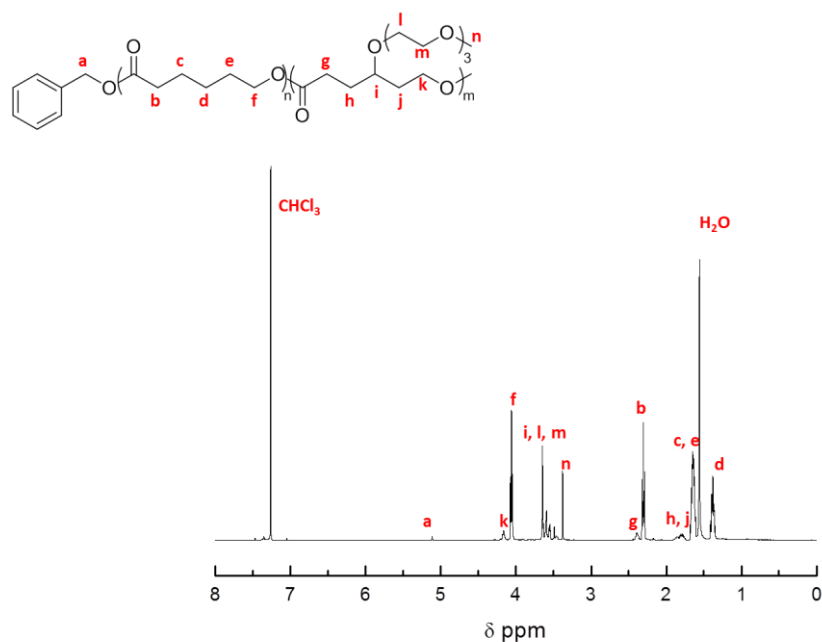


Figure 2.1. ^1H NMR spectrum of linear poly(ϵ -caprolactone)-*b*-poly{ γ -2-[2-(2-methoxyethoxy)ethoxy]ethoxy- ϵ -caprolactone}

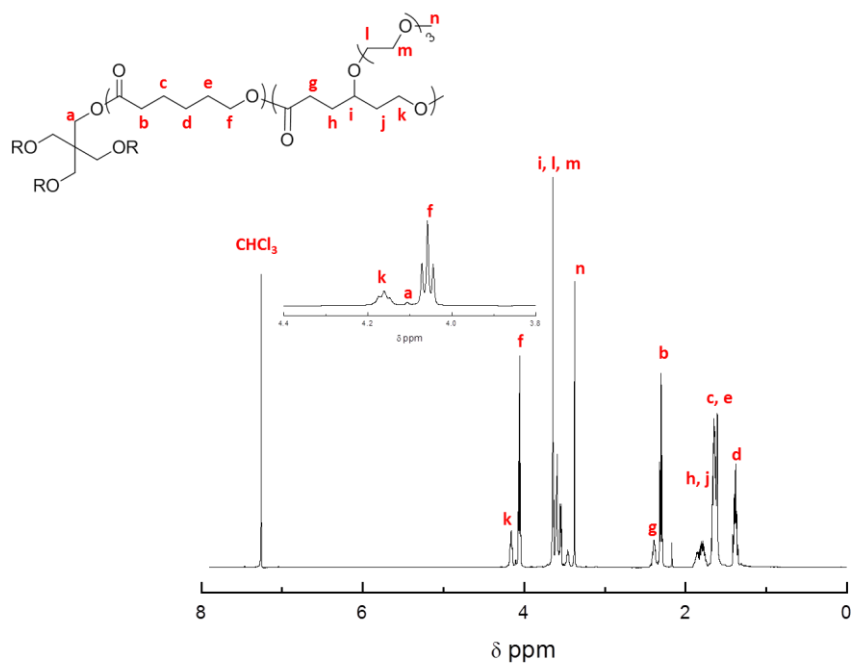


Figure 2.2. ^1H NMR spectrum of 4-arm star-like poly(ϵ -caprolactone)-*b*-poly{ γ -2-[2-(2-methoxyethoxy)ethoxy]ethoxy- ϵ -caprolactone}

linear polymer is 1.225 indicating fairly uniform chain lengths, while the PDI for the star polymer is broader at 4.324. This could indicate uneven chain growth among the different branches of the star polymer. However, the SEC traces for the linear and star-like polymers both show monomodal distributions after addition of the second monomer which indicate that the polymers formed are block copolymers (Figures 2.3 and 2.4). The M_n determined for the linear block copolymer through ^1H NMR was calculated by comparing the integration of the benzylic protons of the end group from the benzyl alcohol initiator (5.1 ppm) to the protons closest to the oxygen in the repeat units of the caprolactone backbone for each block of the polymer (4.059 ppm for ϵ -CL and 4.163 ppm for MEEECL). The M_n determined for the 4-arm star-like block copolymer was calculated by comparing the integration of the protons near oxygen on the pentaerythritol core (4.12 ppm) of the polymer to the protons closest to oxygen in the repeat units of the caprolactone backbone for each block of the polymer (4.056 ppm for ϵ -CL and 4.159 ppm for MEEECL).

Table 2.1. Properties and Mark-Houwink Parameters of Amphiphilic Block Copolymers

	M_n^{NMR} (g mol ⁻¹) ^a	M_n^{SEC} (g mol ⁻¹) ^b	PDI ^b	R_h^c	IV ^d	dn/dc	α^e	Log K ^e	B_m^f	mol % ϵ -CL ^a	mol % MEEECL ^a
LP	9020	9300	1.225	2.942	0.159	0.05	0.730	-3.754	-	80	20
SP	11700	12400	4.324	4.324	0.149	0.04	0.241	-1.745	4.39	72	28

^a Determined through ^1H NMR spectroscopy. ^b Determined by size exclusion chromatography equipped with RI, viscosity, RALS, and LALS detectors using polystyrene as a standard. ^c Hydrodynamic radius of polymer in THF as determined by SEC. ^d Intrinsic viscosity in THF as determined through SEC. ^e Mark-Houwink parameters determined by SEC. ^f Average number of branches determined through SEC using Mark-Houwink parameters of linear PCL-*b*-PMEEECL as a reference.

The SEC measurements were taken with an instrument equipped with RI, light scattering, and viscosity detectors to determine molecular weight of the star polymer more accurately. When it comes to star polymers, it is important to have more than just the concentration detectors, such as RI, to be able to determine a more accurate molecular weight.¹²¹⁻¹²² The dn/dc was determined for each polymer and allowed for the determination of absolute molecular weight using

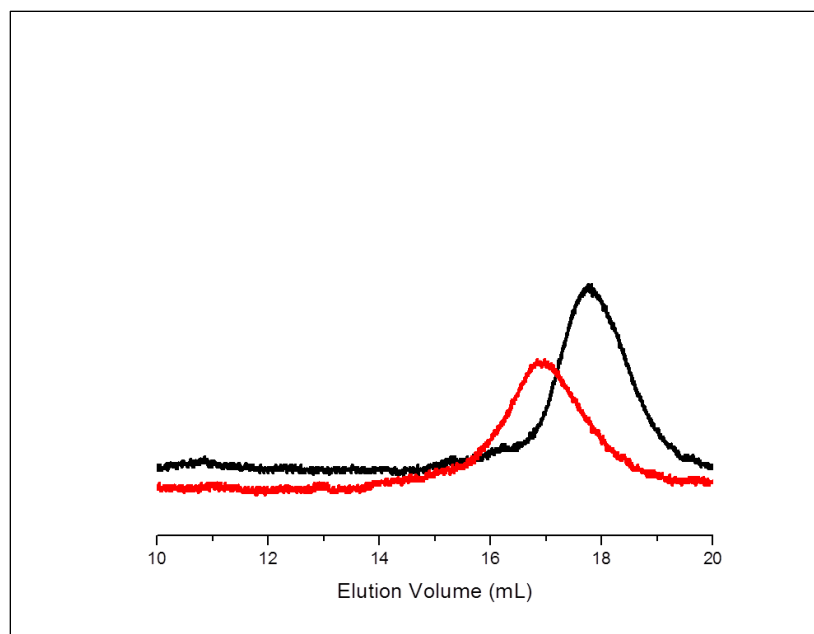


Figure 2.3. SEC for linear PCL precursor (black trace) and for the linear poly(ϵ -caprolactone)-*b*-poly{ γ -2-[2-(2-methoxy-ethoxy)ethoxy]ethoxy- ϵ -caprolactone} diblock copolymer (red trace)

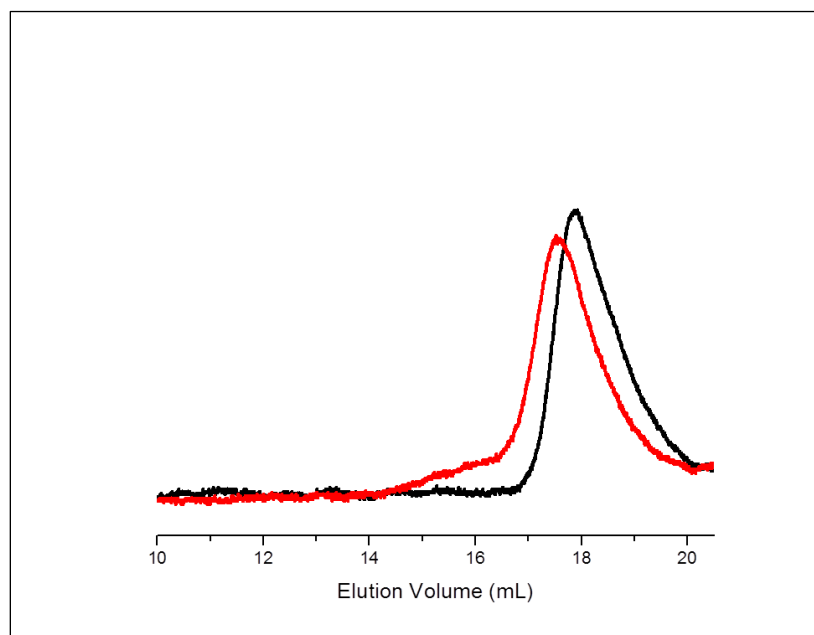


Figure 2.4. SEC for 4-arm star-like PCL precursor (black trace) and for the 4-arm star-like poly(ϵ -caprolactone)-*b*-poly{ γ -2-[2-(2-methoxy-ethoxy)ethoxy]ethoxy- ϵ -caprolactone} diblock copolymer (red trace)

the triple detection system in SEC. The intrinsic viscosity (IV) was measured with the instrument as well, showing the star polymer had a lower intrinsic viscosity which is expected due to the increase in density from the branching of the polymer arms. The Mark–Houwink parameters of the polymers were also examined using SEC to determine the amount of branching within the star polymer. The values of the Mark–Houwink parameters for both polymers are shown in Table 2.1. The resulting Mark–Houwink plot (Figure 2.5) shows the lower IV due to the increased density from the branching in the star polymer. The number of branches was determined according to the following equations:

$$g'_m = \frac{[\eta]_{M,branched}}{[\eta]_{M,linear}}$$

$$g'_m = \frac{6B_m}{(B_m + 1)(B_m + 2)}$$

where g'_m is the branching ratio that is determined through the ratio of the IV of the branched to the linear polymer and B_m is the average number of branches. Using the linear polymer as a reference, the 4-arm star-like block copolymer was determined to have an average number of branches of 4.39 which is close to the expected value of 4.

2.4.2 Evidence of Self-Assembly

The CMC was determined using pyrene as a probe. LP showed a CMC of 1.20×10^{-3} g L⁻¹, while SP showed a CMC of 5.62×10^{-4} g L⁻¹ (Figure 2.6; Table 2.2). In this case, the CMC of LP is more than twice that of SP, indicating that SP has higher thermodynamic stability when

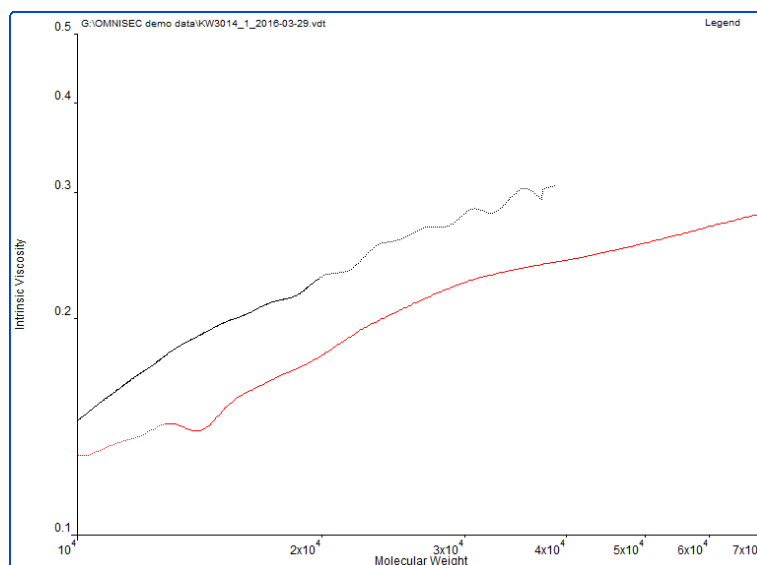


Figure 2.5. Mark-Houwink plot for linear poly(ϵ -caprolactone)-*b*-poly{ γ -2-[2-(2-methoxyethoxy)ethoxy]ethoxy- ϵ -caprolactone} (black trace) and 4-arm star-like poly(ϵ -caprolactone)-*b*-poly{ γ -2-[2-(2-methoxyethoxy)ethoxy]ethoxy- ϵ -caprolactone} (red trace)

compared with LP in aqueous medium which is important when considering stability of the micelles for *in vivo* applications.

The hydrodynamic diameters (D_h) of the micelles were estimated using dynamic light scattering (DLS). The D_h determined for the empty micelles was found to be 96.4 nm for LP with a dispersity of 0.101 and 66.9 nm for SP with a dispersity of 0.148 (Table 2.2). The size from TEM was found to be comparable to the sizes determined from DLS, however there may be more dispersity in the sizes than indicated through DLS. The TEM also showed the morphology of the micelles to be spherical in nature. There is a size difference between the linear and star-like polymer micelles of approximately 30 nm, however the sizes obtained for LP and SP empty micelles are within the desired range of 10–100 nm to participate in the EPR effect.

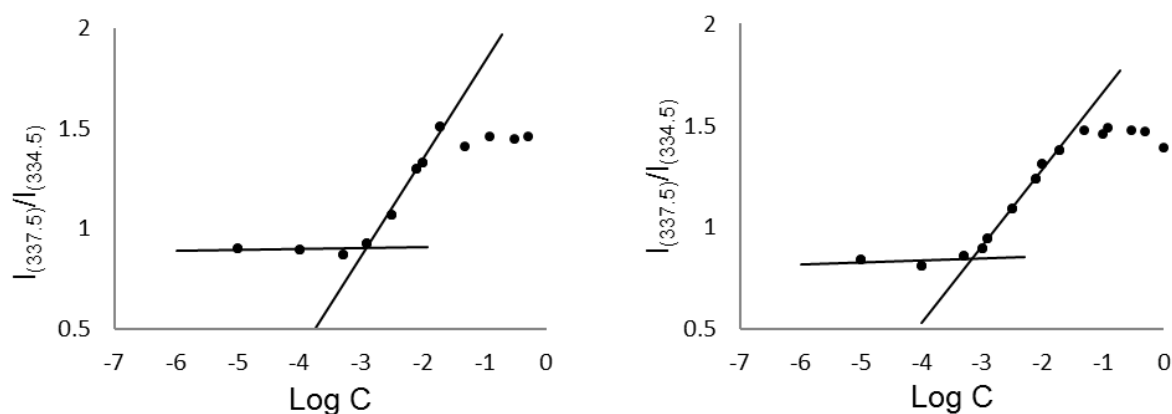


Figure 2.6. Determination of CMC of (left) linear and (right) star-like PCL-*b*-PMEEEECL

Table 2.2. Summary of CMC and Size Measurements

	CMC (g L ⁻¹) ^a	<i>D_h</i> (nm) ^b	Micelle Dispersity ^b
LP	1.20 × 10 ⁻³	96.4 ± 0.5	0.101
SP	5.62 × 10 ⁻⁴	66.9 ± 0.6	0.148

^aDetermined through fluorescence spectroscopy using pyrene as a probe. ^bHydrodynamic diameter and dispersity determined with dynamic light scattering, n=3.

2.4.3 Drug Loading with Doxorubicin

The drug loading capacity of the polymer micelles was investigated using the anticancer drug, doxorubicin. Doxorubicin is a commonly used chemotherapeutic drug for the treatment of many different cancers including breast, lung, ovarian, thyroid, and non-Hodgkin's and Hodgkin's lymphoma, among others.¹²³ Doxorubicin also has limited aqueous solubility, therefore it would benefit from encapsulation in micelles for drug delivery applications. The loading capacities of the linear and star-like polymers were compared, with the star-like architecture expected to have better loading capabilities. Doxorubicin was loaded in a feed weight ratio of 10:1, polymer to drug, using a dialysis method to compare their loading capacities. The DLC and EE were calculated using the following formulas:

$$DLC = \frac{\text{wt. of drug encapsulated}}{\text{wt. of polymer}} \times 100\%$$

$$EE = \frac{\text{wt. of DOX encapsulated}}{\text{initial wt. of DOX added}} \times 100\%$$

The absorbance at 495 nm was used to calculate the concentration of DOX encapsulated into the micelles. The star-like polymers showed a higher drug loading capacity and encapsulation efficiency than the linear counterpart with a DLC of 1.14% and EE of 11.4%. The linear polymers had a lower encapsulation of DOX with a DLC of 0.77% and EE of 7.7%. The size and morphology of the micelles after drug loading was investigated using DLS (Figure 2.7) and TEM (Figure 2.8) and compared to the empty micelles. The average size of the micelles increased in both the linear and the star-like block copolymers after the encapsulation of doxorubicin, indicating that doxorubicin was incorporated into the core of the micelles. LP showed a size of 113 nm after DOX encapsulation, which is larger than the desired size range for the EPR effect indicating that SP, which stays within the desired range of 10–100 nm after loading, might be a better suited for drug delivery (Table 2.3).

Table 2.3. Doxorubicin Loading of PCL-*b*-PMEEECL

	<i>D_h</i> (nm) ^a	Micelle Dispersity ^a	DLC (wt %) ^b	EE (wt %) ^b
LP	113.1 ± 0.3	0.107	0.77	7.7
SP	91.2 ± 0.5	0.076	1.14	11.4

^aDetermined through dynamic light scattering ^bDetermine by UV-Vis using absorption wavelength of 495 nm.

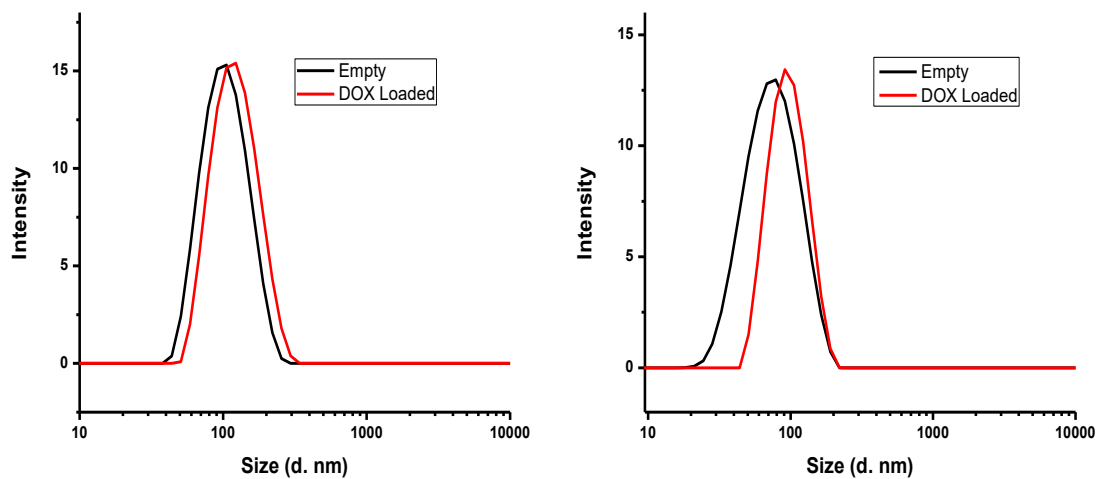


Figure 2.7. DLS of (left) linear and (right) star-like PCL-*b*-PMEEECL showing size differences between the empty and DOX loaded micelles.

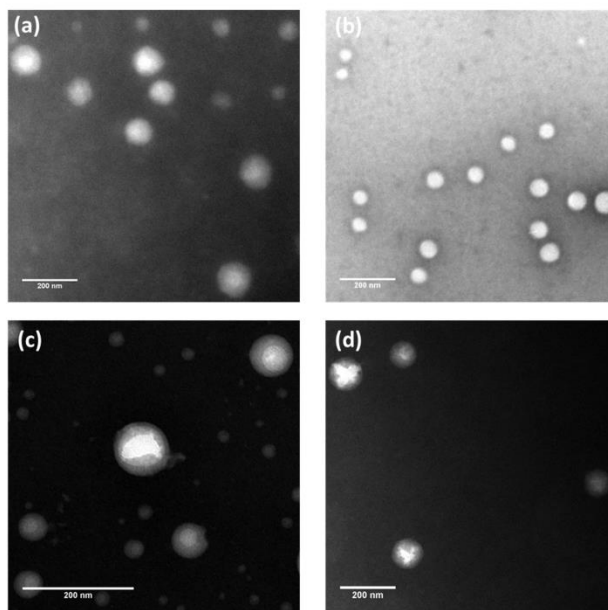


Figure 2.8. TEM images of empty (a) linear and (b) star-like PCL-*b*-PMEEECL and DOX loaded (c) linear and (d) star-like PCL-*b*-PMEEECL, scale bars are 200 nm.

The drug loading for these polymers is relatively low when compared with that shown of PEG-*b*-PCL micelles.¹²⁴⁻¹²⁵ The drug loading of amphiphilic block copolymer micelles is highly dependent on the composition of block copolymers and the molecular weight and crystallinity of the hydrophobic segment.¹²⁴ The longer PCL segment in these block copolymers could have increased crystallinity which limits the drug loading. However, there is potential for fine tuning the polymers to increase the drug loading through altering the chain lengths of the hydrophobic or hydrophilic blocks or through the addition of substituents on the hydrophobic portion of the block copolymer that will favorably interact with the hydrophobic drug to increase the loading.

2.4.4 Polymer Degradation

The biodegradability of LP and SP was measured to determine the amount of molecular weight lost over time under physiological conditions through SEC. The polymers were dissolved in PBS buffer solution (pH 7.4) and kept at 37 °C for several days. Samples were taken periodically over 7 days and examined for their change in molecular weight. Both polymers showed comparable degradation over time as shown in Figure 2.9 with both polymers degrading to around 10% of their initial molecular weight within 7 days. This degradation should allow for drug release over time.

2.5 Conclusions

The synthesis and characterization of 4-arm star-like poly(ϵ -caprolactone)-*b*-poly{ γ -2-[2-(2-methoxy-ethoxy)ethoxy]ethoxy- ϵ -caprolactone} and its linear counterpart are reported. The properties including critical micelle concentration, hydrodynamic diameter, degradation, and drug loading capacity and efficiency were compared to find that the star-like block copolymers

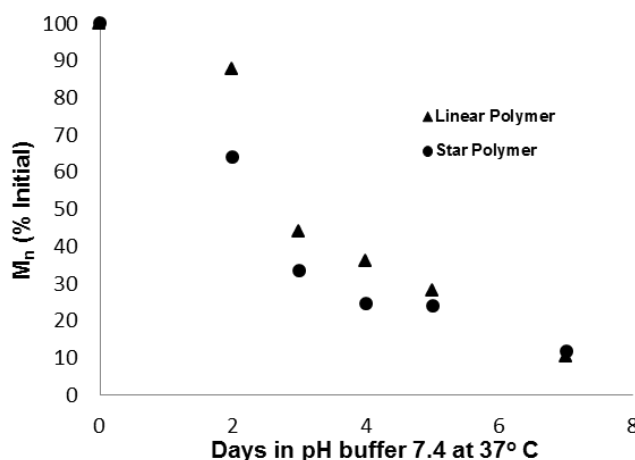


Figure 2.9. Degradation of linear and star-like PCL-*b*-PMEEEECL in PBS (pH 7.4) over 7 days. demonstrated not only higher thermodynamic stability, but also had lower intrinsic viscosity, and smaller sizes. SP showed higher drug loading capacity and encapsulation efficiency as well compared to LP, and also was within the desired range of 10–100 nm for the EPR effect after DOX loading. Both of the polymers were shown to degrade significantly over 7 days under physiological conditions showing their biodegradability. These results show that the 4-arm star-like polymer was a more efficient vehicle for drug delivery. However, it is worth exploring other γ -substituted ϵ -caprolactone monomers for the hydrophobic portion of the block copolymer in an effort to increase the drug loading capacity and encapsulation efficiency.

2.6 Acknowledgments

Katherine carried out all of the synthesis of the monomers and polymers with assistance from Ruvanthi, Matthew, Nicolette and Jack. The characterization including ^1H NMR, SEC, TEM and DLS measurements were completed by Katherine with some assistance from Jia. This work was supported by funding from NIH (1R21EB019175-01A1), Welch Foundation (AT-1740), and NSF

(DMR-1505950). Additionally, we would also like to thank Dr. Carrie Schindler from Malvern Instruments for assistance in SEC measurements.

CHAPTER 3
THERMORESPONSIVE STAR-LIKE Γ -SUBSTITUTED POLY(CAPROLACTONE)S
FOR MICELLAR DRUG DELIVERY

Authors: Katherine E. Washington, Ruvanthi N. Kularatne, Jia Du, Yixin Ren, Matthew J.
Gillings, Calvin X. Geng, Michael C. Biewer, and Mihaela C. Stefan

The Department of Chemistry and Biochemistry, BE 26

The University of Texas at Dallas

800 W. Campbell Road

Richardson, Texas 75080-3021

Manuscript titled “Thermoresponsive star-like γ -substituted poly(caprolactone)s for micellar drug delivery” submitted to Journal of Materials Chemistry B.

3.1 Abstract

Temperature responsive drug carriers are attractive due to their ability to provide controlled release of the encapsulated cargo based on the use of external stimuli. In this work, 4- and 6-arm thermoresponsive star-like block copolymers were synthesized through the ring-opening polymerization of γ -substituted ϵ -caprolactone monomers γ -2-[2-(2-methoxyethoxy)ethoxy]ethoxy- ϵ -caprolactone (MEEECL) and γ -ethoxy- ϵ -caprolactone (ECL) using pentaerythritol and *myo*-inositol as multifunctional initiators. These amphiphilic block copolymers self-assembled into micelles and were characterized in terms of their feasibility as drug carriers. Both polymers were shown to be thermodynamically stable and demonstrated temperature responsivity in a desirable range for drug delivery, 39.4 °C and 39.8 °C for the 4- and 6-arm polymers respectively. It was shown that the 6-arm star polymer had a higher drug loading capability allowing it to function as a better vehicle for drug delivery in cytotoxicity experiments. These star polymers show promise as drug carriers due to their biocompatibility, biodegradability, and temperature controlled release of Doxorubicin.

3.2 Introduction

Considerable efforts in recent years have aimed to develop smart drug carriers for improved delivery of anticancer drugs to tumor sites with increased efficiency and decreased side effects.^{54, 126-131} In particular, there is interest in developing systems that can release their cargo in a triggered response either from the application of external stimuli or from a change in environment.^{69, 132-134} These systems allow for an increased control over where and when the encapsulated cargo is delivered and can be used to preferentially release drugs at tumor sites. Types of stimuli responsive

polymers can include those that are sensitive to pH, temperature, reduction conditions, light, or they can be sensitive to multiple stimuli.

In the case of polymeric micellar drug delivery systems, polymers made from aliphatic polyesters such as poly(glycolide)s, poly(lactide)s, and poly(caprolactone)s have been studied extensively.^{33, 135} Polyesters are attractive due to their biocompatibility and biodegradability through hydrolysis of the esters in the backbone. Among these, poly(caprolactone)s have been one of the most interesting materials due to the ease of property tunability through addition of substituents to the backbone.^{10, 98} In this manner, substituents can affect the hydrophilicity or hydrophobicity of the polymer, provide stimuli responsiveness, and can play a role in subsequent micellar properties such as stability, size, degradation rate, and drug loading capabilities. The stability of these systems is of great importance. In order to function as drug carriers, it is important that they can stay intact upon dilution in the bloodstream.¹³⁶ In addition, the size can be used to passively target tumors through the enhanced permeability and retention (EPR) effect. Ideally, the particles should be in the size range of 10-100 nm so that they are large enough to avoid clearance and small enough to bypass filtration in the spleen.^{101, 137-139} In these ways, polymeric micelles show promise as means to deliver poorly water soluble anticancer drugs more efficiently while protecting healthy cells from their toxic effects.

Temperature responsive polymers can be advantageous in polymeric micellar drug delivery systems, as they allow control over the release of the drug based on the application of localized heating or mild hyperthermia.¹⁴⁰ Polymers that display a lower critical solution temperature (LCST), provide a release mechanism of drug based on a solubility transition of the polymer in aqueous medium upon heating above the LCST. Previously in our group, poly{ γ -2-[2-(2-

methoxyethoxy)ethoxy]ethoxy- ϵ -caprolactone} (PMEEEECL) was synthesized through the ring-opening polymerization of a tri(ethylene glycol) substituted ϵ -caprolactone monomer.¹⁰² This polymer was shown to be water soluble and in addition exhibited thermoresponsive properties. When part of an amphiphilic block copolymer, it was shown that the LCST can be tuned depending on the hydrophobic block.^{85, 98, 103, 105} Although these systems showed promising values for the LCST and showed thermodynamic stability, the drug loading was relatively low.

In an effort to improve on these systems, star-like block copolymers containing PMEEEECL as the hydrophilic block and poly(γ -ethoxy- ϵ -caprolactone) (PECL) as the hydrophobic block were synthesized. Star-like polymers were chosen because they have been shown to have increased drug loading over their linear counterparts.^{107, 141} The resulting polymeric micelles were examined for their thermoresponsive properties, thermodynamic stability, biocompatibility and biodegradability, drug loading capabilities, and cytotoxicity, and are reported herein.

3.3 Experimental

3.3.1 Materials

All commercially available chemicals were purchased from Sigma Aldrich or Fisher Scientific and used without further purification unless otherwise noted. Benzyl alcohol and Sn(Oct)₂ were purified through vacuum distillation prior to use. All polymerization reactions were conducted under purified nitrogen in glassware that was dried at 120 °C for at least 24 hours and cooled in a desiccator prior to use.

3.3.2 Analysis

^1H NMR spectra of the synthesized monomers and polymers were recorded on a Bruker AVANCE III 500 MHz NMR instrument at 25 °C in CDCl_3 . ^1H NMR data are reported in parts per million as chemical shifts relative to tetramethylsilane (TMS) as the internal standard. GC/MS was performed on an Agilent 6890-5973 GC/MS workstation. Molecular weight and polydispersity indices of the synthesized polymers were measured by SEC analysis on an OMNISEC multi-detector system equipped with Viscotek columns (T6000M), connected to a refractive index (RI), low angle light scattering (LALS), right angle light scattering (RALS), and viscosity detectors with HPLC grade THF as the eluent, and triple point calibration based on polystyrene standards. Fluorescence spectra of the synthesized polymers were collected with a Perkin-Elmer LS 50 BL luminescence spectrometer at 25 °C with emission wavelength set at 390 nm. LCST measurements were performed using a temperature controlled Cary5000 UV-Vis spectrometer. Dynamic light scattering (DLS) measurements were performed using a Malvern Zetasizer Nano ZS instrument equipped with a He–Ne laser (633 nm) and 173° backscatter detector. Transmission electron microscopy (TEM) imaging of the DOX-loaded micelles was performed on a Tecnai G2 Spirit Biotwin microscope by FEI and images were analyzed using Image J software. Samples were prepared by treating copper mesh grid with 1 mg mL⁻¹ aqueous polymer micelle solution for 2 minutes, followed by staining with 2% phosphotungstic acid for 30 seconds. TMAFM images were obtained by depositing the DOX loaded micelles on freshly cleaved mica substrate and allowing to air dry and using a VEECO-dimension 5000 Scanning Probe Microscope with silicon cantilever with spring constant 42 nm⁻¹. Images were acquired at 1 Hz scan frequency and analyzed with Nanoscope 7.30 software to generate the 3D renderings.

Absorbance spectra for DOX loading determination was recorded using an Agilent UV/Vis spectrophotometer. Cytotoxicity and cellular uptake measurements were performed with a Biotek Cytation 3 imaging reader.

3.3.3 Synthetic Procedures

The synthesis of monomers MEEEECL and ECL were performed according to previously published procedures and are shown in Scheme 1.¹⁰³

Synthesis of 4-arm star-like PMEEEECL-b-PECL

ECL (0.387 g, 0.00245 mol) was added into a Schlenk flask and stirred under vacuum for one hour. At that time, pentaerythritol (4.17 mg, 3.1×10^{-5} mol) and $\text{Sn}(\text{Oct})_2$ (53 mg, 1.2×10^{-5} mol) were added in 0.3 mL toluene under a nitrogen atmosphere to the reaction flask. The reaction was introduced into a thermostatted oil bath at 110 °C. The consumption of monomer was monitored using GC/MS. After ECL was consumed, previously dried MEEEECL (0.7 g, 0.00245 mol) was added in 0.2 mL of toluene to the reaction flask under nitrogen. The polymerization was allowed to continue over night and after the MEEEECL was consumed, the reaction was quenched by precipitation in hexane, yielding 0.8 g of clear gel-like polymer.

^1H NMR (500 MHz, CDCl_3 , δ): 1.163 (t, 3H), 1.772 (m, 6H), 1.856 (m, 3H), 2.380 (t, 4H), 3.373 (s, 3H), 3.469 (m, 4H), 3.546 (m, 2H), 3.597 (m, 4H), 3.644 (m, 7H), 4.161 (m, 4H)

Synthesis of 6-arm star-like PMEEEECL-b-PECL

ECL (0.224 g, 0.0014 mol) was added into a Schlenk flask and stirred under vacuum for one hour. At that time, myo-inositol (3.2 mg, 1.8×10^{-5} mol) and $\text{Sn}(\text{Oct})_2$ (45 mg, 1.1×10^{-5} mol) were added in 0.3 mL toluene under a nitrogen atmosphere to the reaction flask. The reaction was introduced into a thermostatted oil bath at 110 °C. The consumption of monomer was monitored

using GC/MS. After ECL was consumed, previously dried MEEECL (0.4 g, 0.0014 mol) was added in 0.2 mL of toluene to the reaction flask under nitrogen. The polymerization was allowed to continue over night and after the MEEECL was consumed, the reaction was quenched by precipitation in hexane, yielding 0.5 g of clear gel-like polymer.

^1H NMR (500 MHz, CDCl_3 , δ): 1.165 (t, 3H), 1.785 (m, 6H), 1.857 (m, 3H), 2.382 (t, 4H), 3.375 (s, 3H), 3.471 (m, 4H), 3.547 (m, 2H), 3.599 (m, 4H), 3.646 (m, 7H), 4.1632 (m, 4H)

3.3.4 Determination of LCST

In order to determine the LCST, 2 mg of polymer was dissolved in 10 mL of water to make a 0.2 wt. % solution. The % transmittance at 600 nm was recorded at temperatures ranging from 25 °C to 55 °C. The LCST or cloud point was taken at the point of 50% drop in transmittance for each sample.

3.3.5 Determination of CMC

The CMC was determined using pyrene, a hydrophobic fluorescent molecule, as a probe. Various concentrations of polymer samples were combined with a small amount of pyrene (6.0×10^{-5} M in THF) in 0.2 mL THF. The polymer/pyrene samples were added dropwise into 10 mL of deionized water. The resulting solutions were stirred for 4h to allow micelle assembly and complete evaporation of THF. The resulting solutions contained concentrations from 1×10^{-5} to 1 g L^{-1} of polymer and a constant concentration of pyrene. Fluorescence spectra of the polymer/pyrene solutions were collected at 25 °C with emission wavelength of 390 nm. The ratio of intensities of the pyrene excitation peaks at 337.5 nm and 334.5 nm were recorded and plotted against the logarithm of the polymer concentration (C). The x coordinate at the intersection of the

two trend lines before and after the abrupt increase in the $I_{337.5}/I_{334.5}$ vs. Log (C) curve was taken to be the critical micelle concentration.

3.3.6 Preparation of Micelles

Polymeric micelles were formed through nanoprecipitation and dialysis. The polymer (5 mg) was dissolved in THF (0.4 mL) and added dropwise to 5 mL of water under sonication. The resulting micelle suspension was transferred to SnakeSkin[®] dialysis tubing (MWCO 3500 Da) and dialyzed against a minimum of 1500 mL deionized water over a 24-hour period. The final contents of the dialysis tubing were filtered through a Nylon syringe filter (0.22 μm) to obtain a polymeric micelle solution with a concentration of 1 mg mL⁻¹.

3.3.7 Preparation of DOX Loaded Micelles

DOX-loaded micelles were prepared in a manner similar to the empty micelles. DOX·HCl was first neutralized by adding 3 equivalents of triethylamine in DMSO. An aliquot of the neutralized DOX solution containing 0.5 mg of DOX was added to a polymer solution (5 mg in 0.4 mL DMSO). The DOX-polymer solution was then added dropwise into 5 mL of deionized water under sonication. The resulting suspension was transferred to dialysis tubing and dialyzed against a minimum of 1500 mL of deionized water over a 24 hour period. The contents of the dialysis tube were finally filtered using a Nylon syringe filter (0.22 μm) to obtain a 1 mg mL⁻¹ solution of DOX loaded micelles. To determine the DLC and EE, the drug loaded micelle solutions were diluted with DMSO in a 1:1 ratio in order to release the drug from the micelles. The absorbance of the solution at 485 nm was fitted to a pre-established standard curve of DOX in DMSO/ DI H₂O.

3.3.8 DLS Analysis

Aqueous suspensions of micelles were prepared as stated above at a concentration above the determined CMC, at 1 mg mL^{-1} . The micelles were analyzed to determine their hydrodynamic diameters (D_h) using dynamic light scattering. Prior to measurement, the polymer micelle solutions were filtered with a $0.22 \text{ }\mu\text{m}$ nylon syringe filter. Size measurements were recorded at $25 \text{ }^\circ\text{C}$ in triplicate.

3.3.9 Demonstration of Polymer Degradation

A sample of 6-arm PMEEECL-*b*-PECL (15 mg) was dissolved in 3 mL of PBS (pH 7.4, DNase-, RNase-, and Protease-Free) and was stirred in a closed system in a thermostatted oil bath at $37 \text{ }^\circ\text{C}$ over a period of 6 days. Samples were taken periodically and analyzed by SEC to monitor the change in M_n from $t=0$ to $t=6$ days. The resulting change in molecular weight is plotted as % of initial M_n vs. days spent in PBS solution at $37 \text{ }^\circ\text{C}$.

3.3.10 Biological Studies

Unless otherwise indicated, all cell culture experiments were performed using RPMI-1640 medium with L-glutamine and sodium bicarbonate supplemented with 10% fetal bovine serum and 1% penicillin-streptomycin. Cells were grown in a humidified environment at $37 \text{ }^\circ\text{C}$, 5% CO_2 . Cell viability studies were performed using the CellTiter-Blue[®] assay (Promega) according to the manufacturer's recommended protocol.

3.3.11 Empty Micelle Cytotoxicity Studies

HeLa cells were seeded in transparent flat-bottom 96-well plates at a cell density of 5,000

cells per well in 100 μL growth medium. After 24h to allow cell adhesion, the medium was removed, the cells were washed with 100 μL PBS, and 100 μL fresh growth medium was added to each well. Empty micelles (1 mg mL^{-1} in PBS) were diluted to concentrations ranging from 0.06 mg mL^{-1} to 0.5 mg mL^{-1} . Micelle dilutions (100 μL) were added to the cells via multichannel micropipette. The micelles were incubated for 24 hours with the cells. At this time, the cell viability was evaluated by the CellTiter-Blue[®] assay, N=4.

3.3.12 DOX Loaded Micelle Cytotoxicity Studies

HeLa cells were seeded in transparent flat-bottom 96-well plates at a cell density of 5,000 cells per well in 100 μL growth medium. After 24h to allow cell adhesion, the medium was removed, the cells were washed with 100 μL PBS, and 100 μL of fresh growth medium was added to the cells. DOX-loaded micelles (1 mg mL^{-1} in PBS) were diluted in PBS to concentrations ranging from 0.06 mg mL^{-1} to 0.5 mg mL^{-1} . DOX-loaded micelle dilutions (100 μL) were added to the cells via multichannel micropipette. Free DOX dosing was given assuming the dose from the predetermined drug loading. The cells were then incubated at either 37 °C or 40 °C for 24 hours with the DOX-loaded micelles. After this time, the cell viability was evaluated using the CellTiter-Blue[®] assay, N=4.

3.3.13 Cellular Uptake

HeLa cells were seeded in a 35-mm glass bottom dish at a density of 250,000 cells per well and allowed to adhere for 24 h in 2 mL of growth media. At that time, the medium was removed, the cells were washed with 2mL of PBS, and 2 mL of fresh growth medium was added along with 1 mL of DOX-loaded micelles (0.2 mg mL^{-1} in PBS). The cells dosed with DOX-loaded micelles

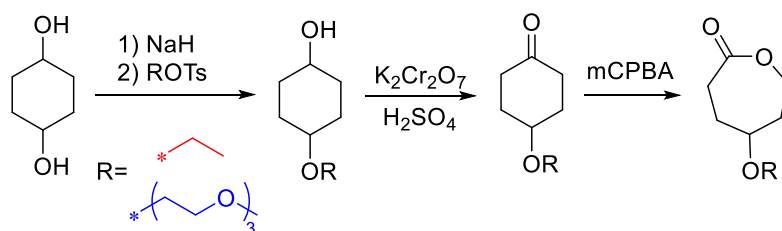
were allowed to incubate for 4 hours. After the uptake period, the cells were washed 3 times with 2 mL of PBS, fixed with 4% paraformaldehyde (room temperature, 10 minutes), washed 3 times with 2 mL of PBS, and the nuclei were counterstained with DAPI. Images were obtained using a BioTek Cytation 3 Cell Imaging Multi-Mode Reader.

3.4 Results and Discussion

3.4.1 Polymer Synthesis

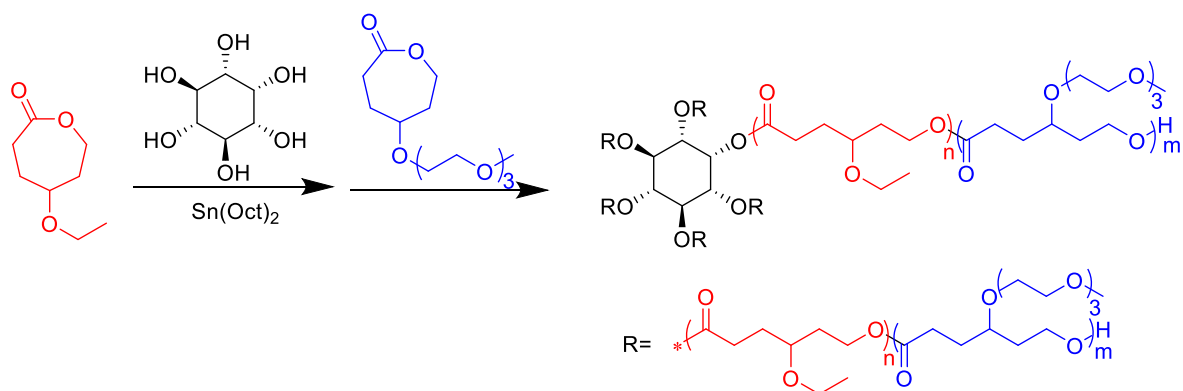
In previous reports, a linear polymer consisting of ECL and MEEECL was examined for its thermoresponsivity, thermodynamic stability, and drug loading capabilities.¹⁰³ The linear polymer was synthesized through the ring-opening polymerization of the ECL and MEEECL monomers using stannous (II) 2-ethylhexanoate ($\text{Sn}(\text{Oct})_2$) as a catalyst and benzyl alcohol as the initiator. This polymer showed promise in terms of temperature responsivity and thermodynamic stability, however it was shown to have limited drug loading capabilities (2.05 wt. %). In an attempt to increase the drug loading as well as the stability, while still maintaining the attractive thermoresponsive properties, two functionalized star-like diblock polycaprolactones were synthesized. The ECL and MEEECL monomers were synthesized according to previous published procedures (Scheme 3.1) and were used for the hydrophobic and hydrophilic block respectively.¹⁰²⁻
¹⁰³ The star polymers were synthesized with $\text{Sn}(\text{Oct})_2$ as the catalyst with two different multifunctional alcohol initiators to form the 4-arm (from pentaerythritol initiator) and 6-arm (from *myo*-inositol initiator) block copolymers (Scheme 3.2). The polymerizations were carried out at 110 °C with sequential monomer addition, starting with the hydrophobic ECL monomer. The polymerizations were carried out using the following molar ratios in order to target a 50:50

molar composition of hydrophilic to hydrophobic block: [Initiator]: [Sn(Oct)2]: [ECL]: [MEEECL]: [1]: [4]: [50]: [50] for the 4-arm polymer (**4A**) and [1]: [6]: [50]: [50] for the 6-arm polymer (**6A**). This particular composition was targeted in an effort to be comparable to the previously published linear polymer.¹⁰³



Scheme 3.1. Synthesis of γ -ethoxy- ϵ -caprolactone and γ -2-[2-(2-methoxyethoxy)ethoxy]ethoxy- ϵ -caprolactone, functionalized ϵ -caprolactone monomers.

The ^1H NMR spectra are shown in Figures 3.1 and 3.2, and a summary of the molecular weights and composition of the polymers is shown in Table 3.1. The compositions were determined from the integration of the peaks of the substituents of the block copolymers, the methoxy group on the oligo ethylene glycol substituent at ~ 3.37 ppm was integrated versus the methyl group of the ethoxy substituent at ~ 1.17 ppm. The molecular weights of the two polymers were determined using size exclusion chromatography (SEC) equipped with a triple detection system, allowing for the determination of the absolute molecular weight. The hydrodynamic radius (R_h) of the polymers in THF and the intrinsic viscosity (IV) were determined as well and are listed in Table 3.1, the SEC traces can be seen in Figures 3.3 and 3.4.



Scheme 3.2. Synthesis of 4-arm and 6-arm star-like PECL-*b*-PMEEEECL amphiphilic diblock copolymers

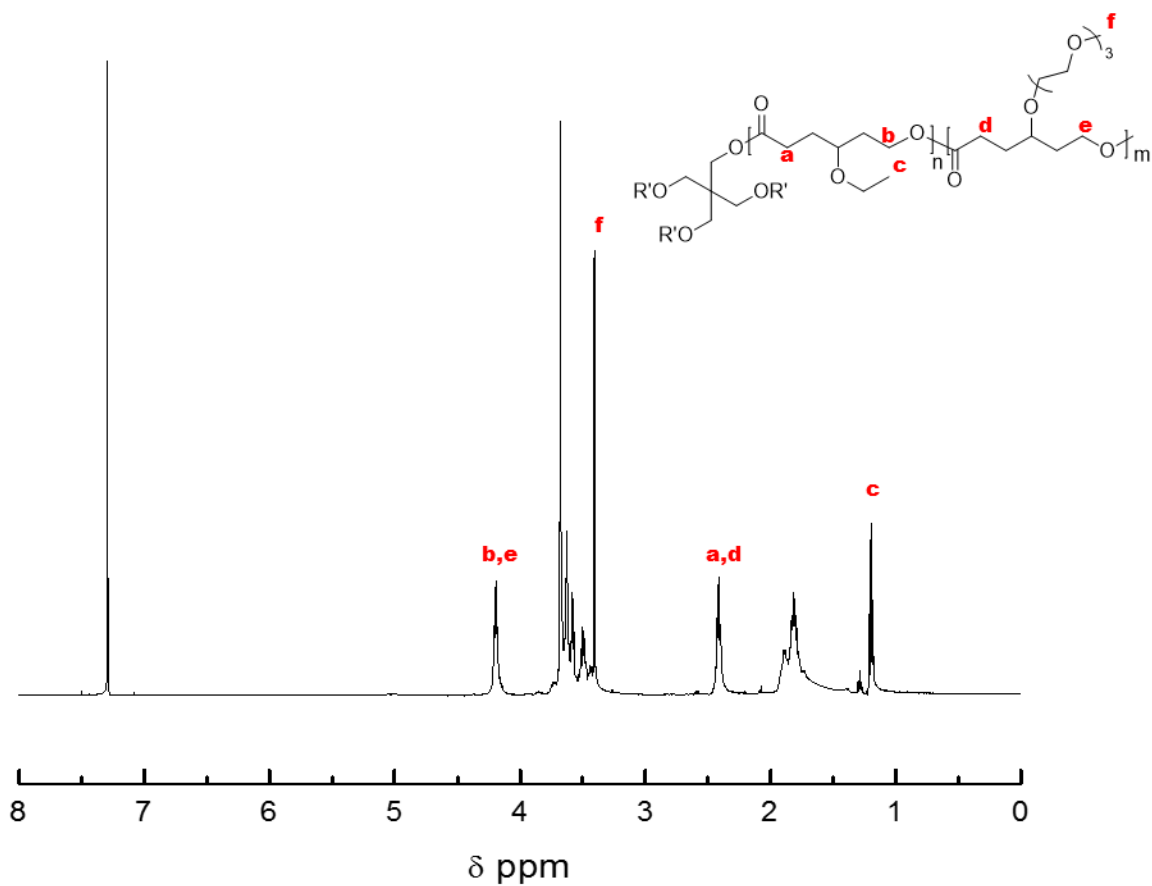


Figure 3.1. ^1H NMR spectrum of 4-arm star-like PECL-*b*-PMEEEECL.

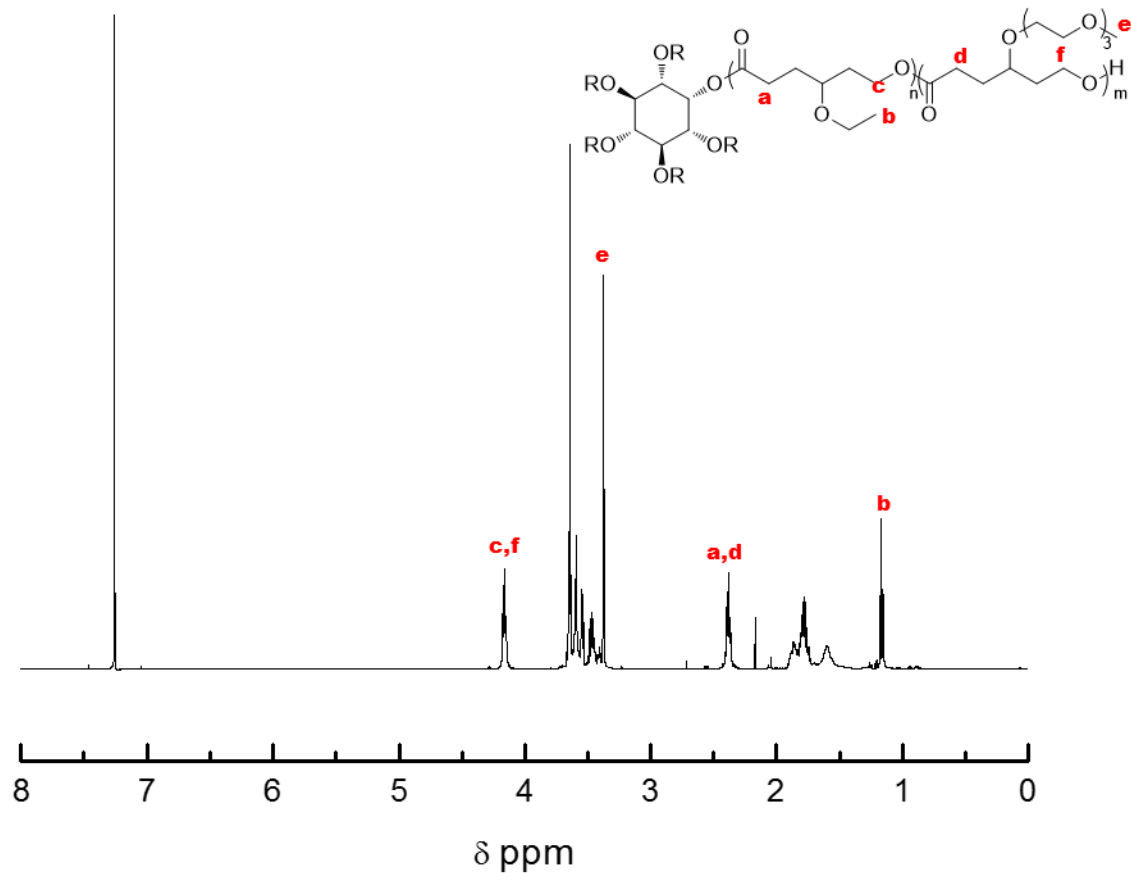


Figure 3.2. ^1H NMR spectrum of 6-arm star-like PECL-*b*-PMEEEECL.

Table 3.1. Summary of Polymer Compositions, Molecular Weights and Properties

	M_n (g mol $^{-1}$) ^a	PDI ^a	R_h ^a	IV ^a	mol % ECL	mol % MEEEECL
4A	20,400	1.1	2.762	0.0706	49.7	50.3
6A	28,800	1.4	3.720	0.0956	47.2	52.8

^aDetermined by SEC equipped with triple detection and THF as the eluent ^bDetermined by ^1H NMR spectroscopy

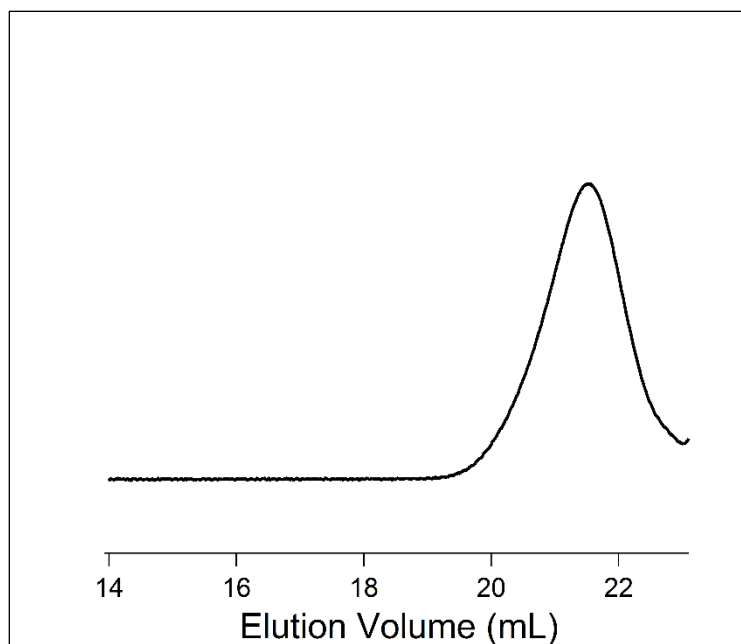


Figure 3.3. SEC trace of 4-arm star-like PECL-*b*-PMEEECL.

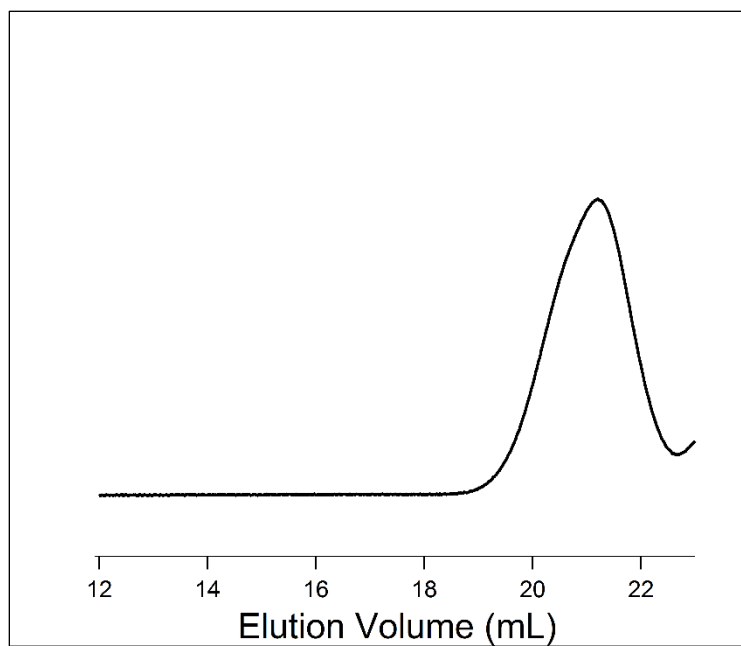


Figure 3.4. SEC trace of 6-arm star-like PECL-*b*-PMEEECL.

3.4.2 Self-Assembly and Thermoresponsivity

The LCST of the polymers was determined by measuring the change in transmittance with increasing temperature. The transmittance decreases above the LCST due to the dehydration and precipitation of the polymer from the aqueous solution. The transmittance was measured with a UV-vis spectrophotometer at 600 nm. The LCST was taken as the temperature where there is a 50% drop in the transmittance during heating (Figure 3.5 A and C). The LCST of 4A and 6A were comparable, with 4A showing LCST of 39.4 °C and 6A exhibiting LCST of 39.8 °C (Table 3.2).

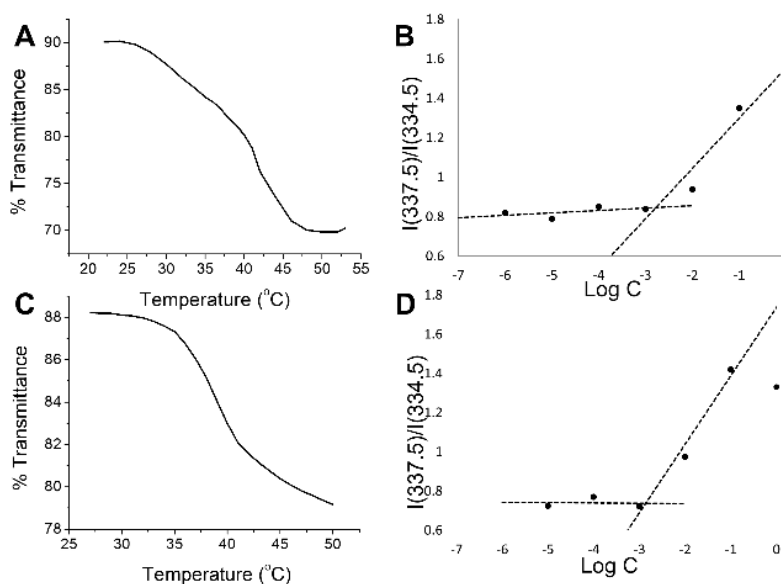


Figure 3.5. Transmittance and CMC plots showing thermoresponsiveness and thermodynamic stability of 4A (A and B) and 6A (C and D) respectively.

Table 3.2. Summary of Polymeric Micelle Properties

	CMC (g L ⁻¹) ^a	LCST (°C) ^b	D _h ^c (nm)	Size Dispersity ^c
4A	1.68 × 10 ⁻³	39.8	80.85	0.085
6A	1.37 × 10 ⁻³	39.4	50.98	0.131

^aDetermined by fluorescence spectroscopy with pyrene as a fluorescent probe ^bDetermined by 50% drop in transmittance at 600 nm upon heating aqueous polymer solution ^cHydrodynamic diameter of micelles at 25 °C from dynamic light scattering.

These LCST values are very useful for drug delivery applications since they are higher than physiological temperature (37 °C), meaning the micelles will be stable as they circulate in the bloodstream, and below 40 °C allowing the application of external temperature to release the encapsulated cargo. The transmittance plots of 4A and 6A are shown on the left in Figure 3.7.

The critical micelle concentration (CMC) was determined by fluorescence spectroscopy using pyrene as a probe.¹⁴² The pyrene excitation spectrum shows a peak shift from 334.5 nm to 337.5 nm as pyrene goes from a hydrophilic environment into the hydrophobic core of the micelle. The intensity ratio ($I_{337.5}/I_{334.5}$) was plotted against the logarithm of the polymer concentration, where the intersection of the two slopes is estimated as the CMC (Figure 3.5, B and D). The estimated CMC value for 4A was found to be $1.68 \times 10^{-3} \text{ g L}^{-1}$ and for 6A it was $1.37 \times 10^{-3} \text{ g L}^{-1}$ (Table 3.2). The CMCs for these polymers are fairly similar, however in comparison with the previously synthesized linear polymer ($8.95 \times 10^{-3} \text{ g L}^{-1}$), the values are almost a magnitude lower indicating that the star polymers are more thermodynamically stable.¹⁰³ This could be due to the increased density of the functional groups in the star polymer allowing increased hydrophobic interactions.

3.4.3 Size and Morphology

The size and morphology of the empty polymeric micelles were investigated by dynamic light scattering (DLS) and transmission electron microscopy (TEM). Empty micelles were prepared through a dialysis method at a concentration of 1 mg mL^{-1} . The micelles were examined first by DLS to determine the size of the hydrodynamic diameter (D_h) and the dispersity of the sample. The micelles exhibited sizes of 80.85 nm and 50.98 nm for 4A and 6A respectively (Table 3.2, Figure 3.6). The micelles formed from polymer 6A were observed to be much smaller in size when compared to those formed from 4A.

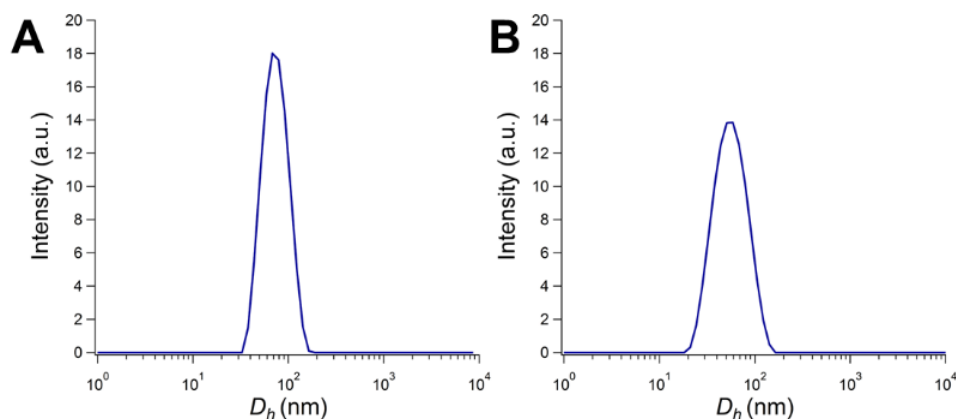


Figure 3.6. Size distribution (D_h) for 4A (A) and 6A (B) polymeric micelles at 25 °C obtained from DLS.

In order to observe the morphology, TEM was performed using phosphotungstic acid for negative staining. Amphiphilic block copolymers can assemble into various structures such as spherical micelles, vesicles, or cylindrical micelles depending on several factors including the composition of the block copolymer, the molecular weight, the solvent system, or the surrounding environment.¹⁴³ The polymer was shown to form spherical micelles in aqueous solution which can be visualized from the TEM (Figure 3.7). This could be expected based on our previous results considering star polymers formed from substituted polycaprolactones with PMEEECL as the hydrophilic block.¹⁴⁴ The size measured with TEM was in correlation with the values obtained from DLS. However, unlike the distribution observed with DLS, there appears to be more variation in the size observed through TEM which is evidenced by the appearance of additional smaller micelles.

3.4.4 Doxorubicin Encapsulation

In order to determine the feasibility of the star polymers as drug carriers, doxorubicin

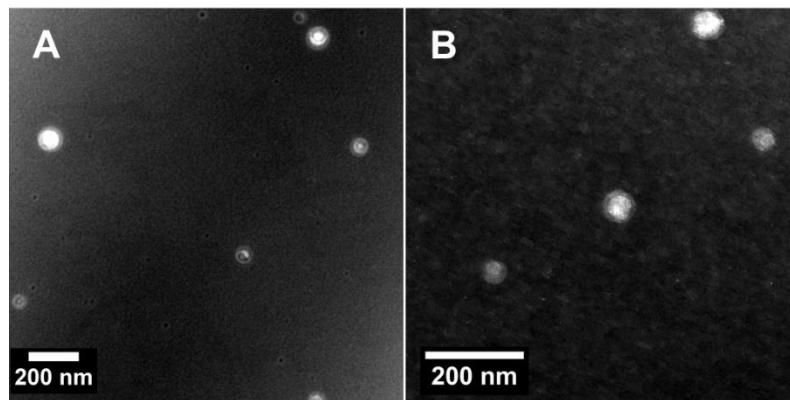


Figure 3.7. TEM images of empty polymeric micelles (A) 4A and (B) 6A.

(DOX) was loaded into the micelles through a dialysis method. The absorbance of the DOX loaded micelles measured at 485 nm was fitted against a pre-established calibration curve in order to determine the concentration of the loaded drug. (Figure 3.8) The drug loading content (DLC) and encapsulation efficiency (EE) were determined according to the following equations:

$$DLC = \frac{\text{weight of encapsulated DOX}}{\text{weight of polymer}} \times 100$$

$$EE = \frac{\text{weight of encapsulated DOX}}{\text{weight of total DOX}} \times 100$$

We speculated that the 6-arm polymer (6A) would have a higher drug loading than the 4-arm polymer (4A) due to increased density of functional units in the core of the micelle. Also, based on previous knowledge that star polymers have increased loading over linear polymers, we speculated that both of the star polymers would have a higher loading than the previously synthesized linear polymer (2.05 wt.%).^{103, 144} The DOX loading was performed in the same

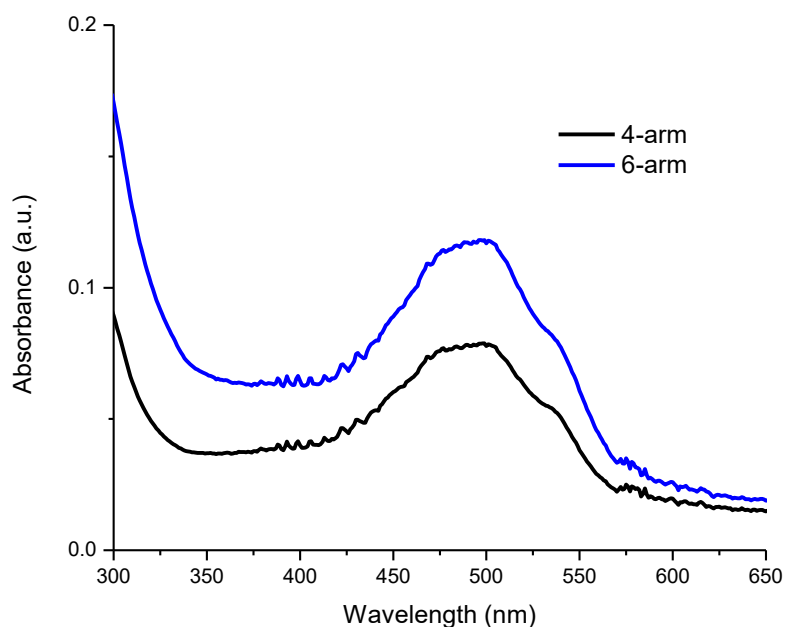


Figure 3.8. Absorbance spectra of DOX loaded star polymers.

method as the earlier published linear polymer, and in the same ratio (10:1 polymer: drug) in order to allow for an accurate comparison of the loading. Polymer 4A has been shown to have a DLC of 2.06 wt.%, while polymer 6A had a DLC of 2.63 wt.%. Polymer 4A had a drug loading comparable to that of the reported value of the linear polymer, while polymer 6A was shown to have the highest DLC and encapsulation efficiency as hypothesized. A summary of the drug loading is shown in Table 3.3. The change in size and the morphology was investigated after loading as well using DLS, tapping mode atomic force microscopy (TMAFM), and TEM. The micelles retained their spherical shape after loading as well and both polymers showed an increase in size after loading (Figure 3.9). As before, the sizes measured from TEM showed good correlation with those measured from DLS. Even after loading, the micelles retained a size ideal for passive targeting

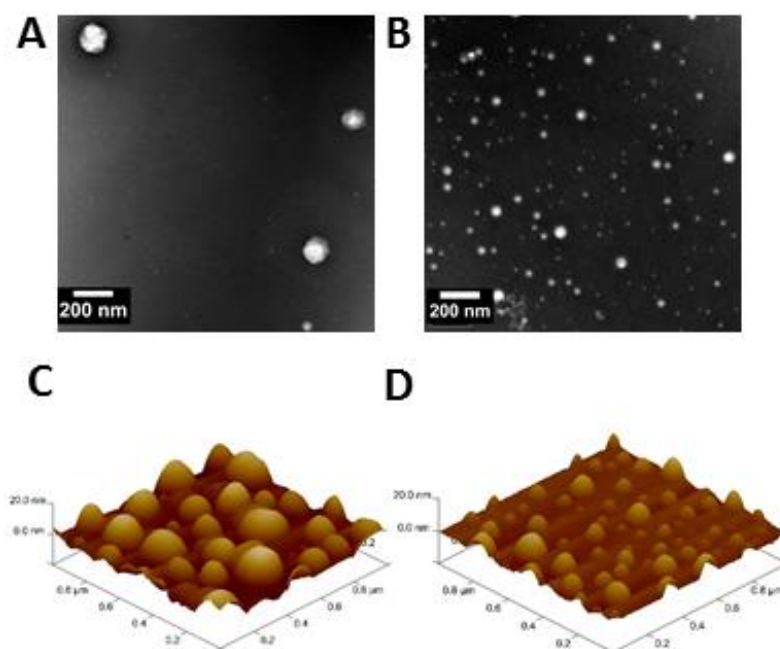


Figure 3.9. TEM images of DOX loaded micelles (A) 4A and (B) 6A, scale bar = 200 nm. TMAFM images of DOX loaded polymeric micelles (C) 4A and (D) 6A deposited on mica-substrate, scan size: 1 μ m.

Table 3.3. Summary of DOX Loaded Polymeric Micelle Properties

	DLC (wt. %) ^a	EE (wt. %) ^a	D_h^{DOX} (nm) ^b	Size Dispersity ^b
4A	2.06	20.6	102.8	0.155
6A	2.63	26.3	64.5	0.159

^aDetermined with UV-Vis spectroscopy, absorbance measured at 485 nm ^bDetermined through dynamic light scattering at 25 °C

using the EPR effect, with 4A having the largest size just slightly over 100 nm at 102.8 nm. (Figure 3.10)

3.4.5 Biocompatibility and Degradation

The biodegradability of the synthesized block copolymer was examined by dissolving the 6A polymer in PBS (pH =7.4) and stirring the polymer solution at 37 °C for six days. The degradation was measured by determining the % change in molecular weight (M_n) over time

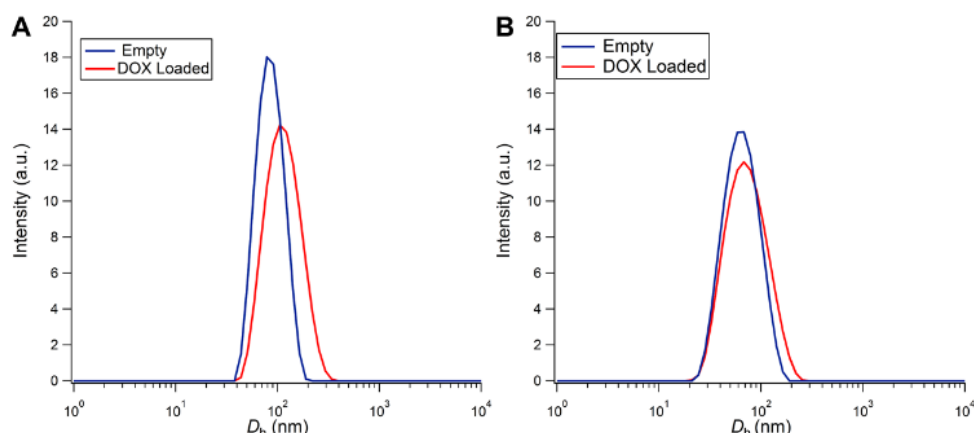


Figure 3.10. Size distribution (D_h) obtained through DLS for (A) 4A and (B) 6A comparing the sizes of empty and DOX loaded micelles.

(Figure 3.11). The polymer showed significant degradation over several days, to about 30 % of the initial molecular weight, indicating the polymer was biodegradable under physiological conditions. It can be assumed that polymer 4A would be degradable over time as well since it has a similar structure and composition. It has been shown recently that although star-like polyesters degrade at a slower rate than linear polymers, the number of arms does not affect the rate of degradation as significantly.¹⁴⁵ In order to evaluate the biocompatibility of these polymers, cytotoxicity measurements were performed using various concentrations of the empty polymers on HeLa cells. CellTiter-Blue[®] cytotoxicity kit was used to examine the cell viability after the cells had been exposed to the polymer solutions for 24 hours. The polymers were not shown to exhibit significant toxicity to the cells even up to 0.5 mg mL^{-1} (Figure 3.12). According to these measurements, the polymers display excellent biocompatibility as well as biodegradability under physiological conditions.

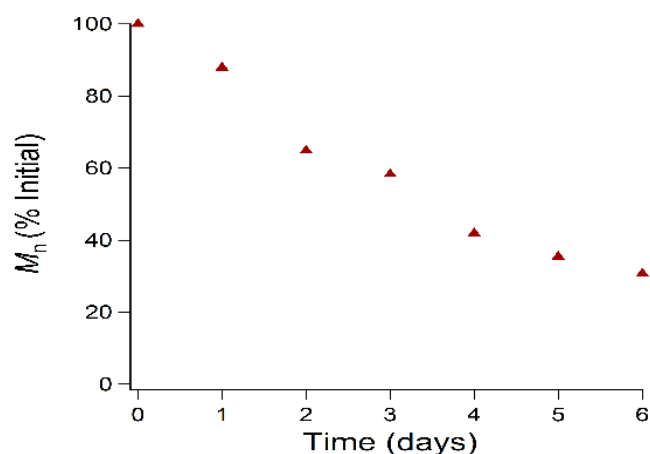


Figure 3.11. Degradation measurements of polymer 6A under physiological conditions (37 °C, pH 7.4), the % change in molecular weight (M_n) is plotted versus time.

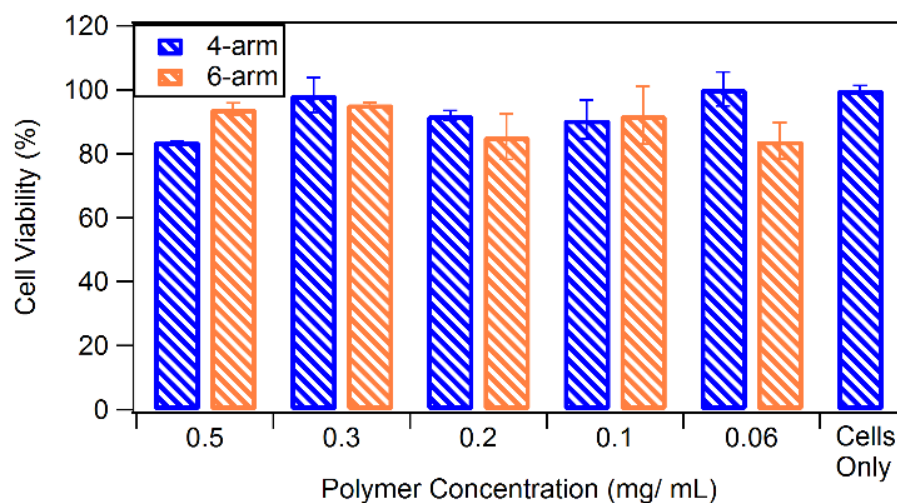


Figure 3.12. Cell viability measurements of varying concentrations of empty polymeric micelles in PBS using HeLa cells and CellTiter Blue[®] cytotoxicity kit.

3.4.6 Cytotoxicity and Cellular Uptake of DOX Loaded Micelles

The cytotoxicity of the DOX loaded micelles was examined using HeLa cells at various concentrations. In the interest of determining the temperature controlled release of DOX in cells, the cells were incubated at either physiological temperature (37 °C) or at a temperature above the LCST of the polymers (40 °C). HeLa cells were dosed with DOX loaded micelles and allowed to

incubate for at either temperature. After 24 hours, the cell viability was measured using CellTiter-Blue[®] assay. It was shown at all concentrations that the release of DOX was more substantial at temperatures above the LCST causing less cells to be viable. Free DOX was administered to HeLa cells as well in concentrations coinciding with the amount loaded into the star polymer micelles based on the DLC determined. In all cases, the free DOX showed higher cytotoxicity to the cells, however the cells exposed to DOX loaded micelles at temperatures higher than the LCST exhibited cytotoxicity closer to that of the free DOX dosages (Figure 3.13). The DOX loaded 6A micelles exhibited higher toxicity than the DOX loaded 4A micelles, which can be attributed to the higher loading capabilities of the 6A micelles.

The ability of the micelles to be taken into the cancer cell was observed through cellular uptake experiments using HeLa cells. The DOX loaded micelles were added to HeLa cells and incubated for 4 hours. At that time, the cells were washed and the nuclei were counterstained with DAPI to visualize the cell nuclei through fluorescence microscopy, shown in Figure 3.14. The red signal, attributed to DOX can be seen within the cell nuclei, indicating the endocytosis of the micelles into the cell and the internalization of DOX into the nucleus of the cell.

3.5 Conclusions

Temperature responsive 4- and 6-arm star-like polymers were successfully synthesized by living ring-opening polymerization of functionalized ϵ -caprolactone monomers ECL and MEEECL. These polymers were shown to be thermodynamically stable with CMCs $\sim 10^{-3}$ g L⁻¹. Additionally, they were shown to have advantageous LCST values slightly above physiological temperature, beneficial for use in drug delivery systems. These polymers were also shown to be biocompatible, exhibiting relatively low toxicity to HeLa cells at doses up to 0.5 mg mL⁻¹, and

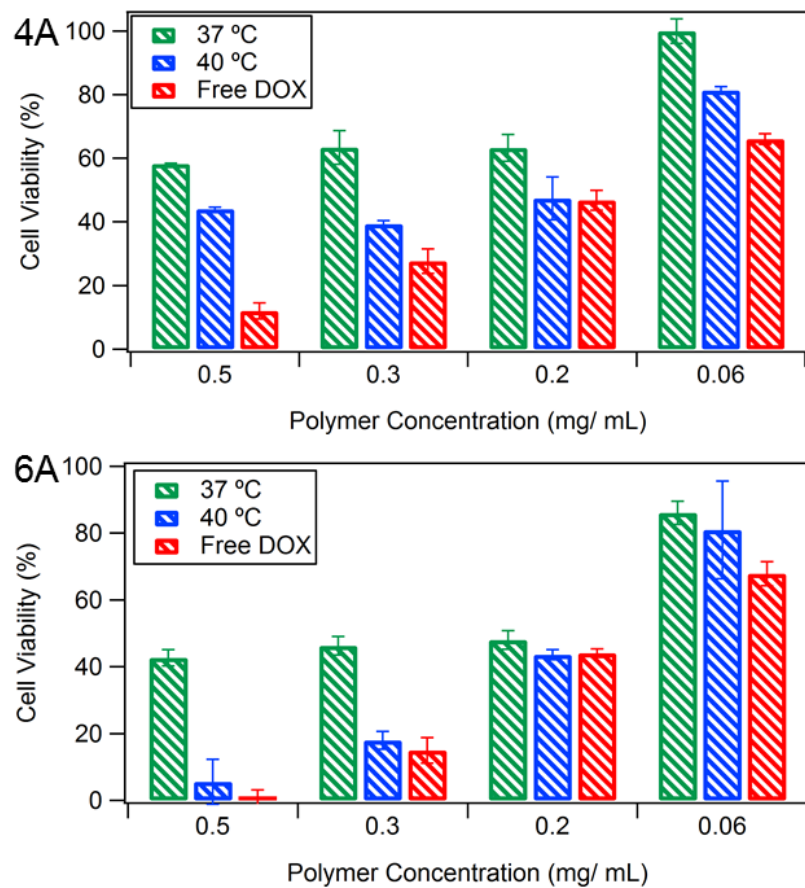


Figure 3.13. Cell viability of HeLa cells after dosing with DOX loaded micelles above and below the LCST.

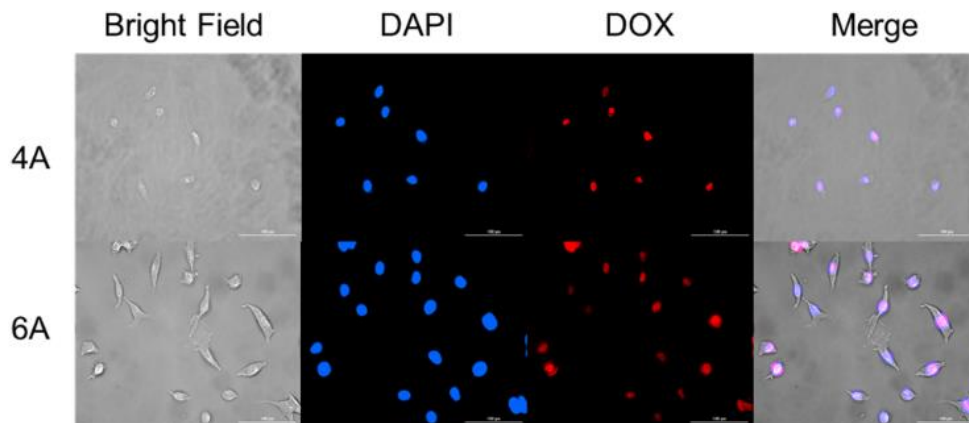


Figure 3.14. Uptake of 4A and 6A DOX loaded micelles in HeLa cells after incubating for 4 hours. Cell nuclei were stained with DAPI.

biodegradable over time under physiological conditions. However, the DOX loaded micelles showed significant cytotoxicity to cancer cells when they were incubated at temperatures higher than the LCST of the polymers indicating that the polymers provide thermally controlled release. Future optimization of these drug delivery systems should focus on improving the drug loading capabilities either through changes in the substituents of the hydrophobic block or through different loading methods.

3.6 Acknowledgments

The synthesis of monomers and polymers in this project was completed by Katherine with assistance from Matthew, Calvin, and Yixin. The characterization in this project was completed by Katherine, with the exception of AFM which was completed by Jia. Ruvanthi and Katherine completed the cell study experiments together. We gratefully acknowledge the support for this work from NSF (CHE-1609880) and Welch Foundation (AT-1740).

CHAPTER 4

**COMBINATION LOADING OF DOXORUBICIN AND RESVERATROL IN
POLYMERIC MICELLES TO INCREASE LOADING EFFICIENCY AND EFFICACY**

Authors: Katherine E. Washington, Ruvanthi N. Kularatne, Michael C. Biewer, and
Mihaela C. Stefan

The Department of Chemistry and Biochemistry, BE 26

The University of Texas at Dallas

800 W. Campbell Road

Richardson, Texas 75080-3021

Manuscript titled “Combinatorial Loading of Doxorubicin and Resveratrol in Polymeric Micelles to Increase Loading Efficiency and Efficacy” in preparation.

4.1 Abstract

The combined administration of doxorubicin (DOX) and resveratrol (RSV) is a promising new direction for cancer treatment on account of the therapeutic benefits provided from RSV. Combination loading of these drugs in polymeric micelles composed of either poly(ethylene glycol)-*b*-poly(ϵ -caprolactone) (PEG-*b*-PCL) or poly(ethylene glycol)-*b*-poly(γ -benzyl- ϵ -caprolactone) (PEG-*b*-PBCL) was explored to increase the loading efficiency and the therapeutic efficacy of micellar drug delivery systems. The combined loading of RSV and DOX not only shows potential for improved cytotoxic effects to cancer cells, but also the addition of RSV allows improved drug loading of DOX into polymeric micelles due to interactions between DOX and RSV. Herein, we report the combination loading of DOX and RSV into polymeric micelles using PEG-*b*-PCL and PEG-*b*-PBCL polymers with the highest encapsulation efficiencies (EE) of DOX and RSV in PEG-*b*-PBCL found to be 87.7% and 18.7%, respectively. In the case of PEG-*b*-PCL, EE was 10.8% and 0.6% for DOX and RSV, indicating that the π -stacking capabilities of the benzyl substituents in PEG-*b*-PBCL with the drug molecules enables increased loading capacity. The size and morphology of the resulting combination loaded micelles, as well as their cytotoxicity and cellular uptake into HeLa cells are reported herein.

4.2 Introduction

Doxorubicin (DOX) is often used for the treatment of several different types of cancer including breast cancer, ovarian cancer, and lymphoma. It has been regarded as one of the most potent chemotherapeutic drugs approved by the Food and Drug Administration (FDA). However, DOX is generally known to have toxic side effects to noncancerous cells and its use is limited by

its cardiotoxicity.¹⁴⁶⁻¹⁴⁷ In addition, DOX can induce drug resistance in cancer cells due to high dosage and repeated treatment. In an effort to combat these drawbacks, attention has been focused toward developing a treatment with reduced side-effects from DOX. Recently, studies have shown that the adverse reactions of DOX can potentially be mitigated with the co-administration of antioxidants such as polyphenolic compounds.

One such polyphenolic compound, resveratrol (RSV), has received attention due to its cardioprotective properties.¹⁴⁸⁻¹⁴⁹ RSV is derived from natural sources such as grapes, peanuts, and blueberries among others, with *trans*-RSV as the biologically active form.¹⁴⁸ The “French Paradox” in which cardiovascular disorders in France are low even though their diet has a high content of fat, has been attributed to the consumption of red wine which contains a significant amount of RSV.¹⁴⁸ RSV has received attention in research as it has shown health benefits in addition to its antioxidant nature, including anti-inflammatory and anti-tumorigenic properties.¹⁵⁰⁻¹⁵¹ DOX, paclitaxel, curcumin, and cis-platin are several different anti-cancer drugs that have been used in combination with RSV, in order to mitigate their toxic side effects and overcome the effects of multi-drug resistance.¹⁵²⁻¹⁵⁴ The combined administration of RSV with DOX has been shown to reduce cardiotoxicity and act as a chemosensitizer, providing a synergistic effect against cancer cells both *in vitro* and *in vivo*.¹⁵⁵⁻¹⁶⁰ The cardioprotective effects of RSV are largely attributed to reduced oxidative stress, the inhibition of apoptosis, and modulated autophagy process.¹⁶¹ Research has been moving toward the combined loading of DOX and RSV into nanoparticles for controlled delivery to mitigate toxic side effects as well as cancer cell resistance to DOX.¹⁶²⁻¹⁶³ Combination therapy using DOX and RSV shows an encouraging new path towards more efficient cancer treatment.

Developing a drug delivery system for the combined delivery of DOX and RSV through polymeric micelles is a way to deliver the drugs in a controlled and less toxic manner. Amphiphilic block copolymers containing a hydrophilic poly(ethylene glycol) (PEG) segment and a hydrophobic polyester segment are commonly used for drug encapsulation.^{135, 164} Biodegradable and biocompatible polyesters, in particular poly(caprolactone)s, are often used as the hydrophobic segment due to their tunability through the addition of substituents to the polyester backbone.^{10, 24, 98, 144} In this report, the combined drug loading of RSV and DOX is investigated in polymeric micelles using PEG-*b*-PCL and PEG-*b*-PBCL. These two polymers were compared for their drug loading potential, based on different interactions they may have with the drugs for loading. An increased drug loading capacity is achievable for PEG-*b*-PBCL than for PEG-*b*-PCL due to the π -stacking abilities of the drug molecules with the benzyl substituents. In addition, differing ratios of polymer, DOX, and RSV are examined in order to optimize the encapsulation efficiency of the polymeric drug delivery systems.

4.3 Experimental

4.3.1 Materials

All commercially available chemicals were purchased from Sigma Aldrich or Fisher Scientific and used without further purification unless otherwise noted. Sn(Oct)₂ was purified through vacuum distillation prior to use. All polymerization reactions were conducted under purified nitrogen in glassware that was dried at 120 °C for at least 24 hours and cooled in a desiccator prior to use.

4.3.2 Analysis

^1H NMR spectra of the synthesized monomers and polymers were recorded on a Bruker AVANCE III 500 MHz NMR instrument at 25 °C in CDCl_3 . ^1H NMR data are reported in parts per million as chemical shifts relative to tetramethylsilane (TMS) as the internal standard. Molecular weight and polydispersity indices of the synthesized polymers were measured by SEC analysis on an OMNISEC multi-detector system equipped with Viscotek columns (T6000M), equipped with refractive index (RI) detector with HPLC grade THF as eluent and calibration was based on polystyrene standards. Fluorescence spectra of the synthesized polymers were collected with a Perkin-Elmer LS 50 BL luminescence spectrometer at 25 °C with emission wavelength set at 390 nm. Dynamic light scattering (DLS) measurements were performed using a Malvern Zetasizer Nano ZS instrument equipped with a He–Ne laser (633 nm) and 173° backscatter detector. Transmission electron microscopy (TEM) imaging of the empty and combination loaded micelles was performed on a Tecnai G2 Spirit Biotwin microscope by FEI and images were analyzed using Gatan Digital Micrograph software. Samples were prepared by treating copper mesh grid with 1 mg mL⁻¹ aqueous polymer micelle solution for 2 minutes, followed by staining with 2% phosphotungstic acid for 30 seconds. Absorbance spectra for DOX and RSV loading determination was recorded using an Agilent UV/Vis spectrophotometer. Cytotoxicity and cellular uptake measurements were performed with a Biotek Cytation 3 imaging reader.

4.3.3 Synthetic Procedures

The synthesis of monomer γ -benzyl- ϵ -caprolactone (BCL) was performed according to a previously published procedure.¹⁰³

Synthesis of PEG-b-PCL

PEG ($M_n = \sim 2000 \text{ g mol}^{-1}$, 0.35 g, $1.75 \times 10^{-4} \text{ mol}$) and ϵ -caprolactone (1.0 g, 0.0088 mol) were added into a Schlenk flask and stirred under vacuum for one hour. At that time, $\text{Sn}(\text{Oct})_2$ (71 mg, $1.75 \times 10^{-4} \text{ mol}$) was added in 0.2 mL of toluene under a nitrogen atmosphere to the reaction flask. The reaction was introduced into a thermostat oil bath at 110°C . The polymerization was allowed to continue overnight and the reaction was quenched by precipitation in hexane after the complete consumption of ϵ -caprolactone, yielding solid white polymer (yield = 1.23 g).

^1H NMR (CDCl_3 , 500 MHz) δ : 1.378 (m, 2H), 1.638 (m, 4H), 2.301 (t, 2H), 3.375 (s, 0.06H), 3.638 (s, 4H), 4.055 (t, 2H); $M_n = 10,500 \text{ g mol}^{-1}$; PDI = 1.3

Synthesis of PEG-b-PBCL

PEG ($M_n = \sim 2000 \text{ g mol}^{-1}$, 0.14 g, $7.0 \times 10^{-5} \text{ mol}$) and BCL (0.76 g, 0.0035 mol) were added into a Schlenk flask and stirred under vacuum for one hour. At that time, $\text{Sn}(\text{Oct})_2$ (28 mg, $7.0 \times 10^{-5} \text{ mol}$) was added in 0.2 mL toluene under a nitrogen atmosphere to the reaction flask. The reaction was introduced into a thermostat oil bath at 110°C . The polymerization was allowed to continue over night and the reaction was quenched by precipitation in hexane after the complete consumption of BCL, yielding a clear gel-like polymer (yield = 0.84 g).

^1H NMR (CDCl_3 , 500 MHz) δ : 1.812 (m, 4H), 2.348 (t, 2H), 3.380 (s, 0.06H), 3.548 (m, 1H), 3.644 (s, 3.7H), 4.143 (t, 2H), 4.468 (m, 2H), 7.301 (m, 4H); $M_n = 16,900 \text{ g mol}^{-1}$; PDI = 1.5

4.3.4 Preparation of Micelles

Polymeric micelles were formed through a solvent evaporation method. The polymer (4 mg) was dissolved in THF (2 mL) and added dropwise to 4 mL of water under rapid stirring and

the THF was allowed to evaporate. The resulting micelle suspension was filtered through a Nylon syringe filter (0.22 μm) to obtain a polymeric micelle solution with a concentration of 1 mg mL⁻¹.

4.3.5 Preparation of DOX Loaded Micelles

DOX loaded, RSV loaded, and combination loaded micelles were prepared in a manner similar to the empty micelles. DOX·HCl was first neutralized by adding 3 equivalents of triethylamine in THF. An aliquot of the neutralized DOX or RSV solution containing the appropriate ratio of DOX, RSV, or a combination of the two was added to a polymer solution. The drug-polymer solution was then added dropwise into deionized water under rapid stirring. The resulting suspension was filtered with a Nylon syringe filter (0.22 μm) to obtain a 1 mg mL⁻¹ solution of loaded micelles. To determine the drug loading content (DLC) and encapsulation (EE), the drug loaded micelle solutions were diluted with DMSO in a 1:1 ratio. The absorbance of the solution at 485 nm was fitted to a pre-established standard curve of DOX in DMSO/DI H₂O and at 320 nm to a pre-established standard curve of RSV in DMSO/DI H₂O.

4.3.6 Determination of Critical Micelle Concentration (CMC)

The CMC was determined using pyrene, a hydrophobic fluorescent molecule, as a probe. Various concentrations of polymer samples were combined with a small amount of pyrene (6.0 x 10⁻⁵ M in THF) in 0.2 mL THF. The polymer/pyrene samples were added dropwise into 10 mL of deionized water. The resulting solutions were stirred for 4 h to allow micelle assembly and complete evaporation of THF. The resulting solutions contained concentrations ranging from 1 x 10⁻⁵ to 1 g L⁻¹ of polymer and a constant concentration of pyrene. Fluorescence spectra of the polymer/pyrene solutions were collected at 25 °C with emission wavelength of 390 nm. The ratio

of intensities of the pyrene excitation peaks at 337.5 nm and 334.5 nm were recorded and plotted against the logarithm of the polymer concentration (C). The x coordinate at the intersection of the two trend lines before and after the abrupt increase in the $I_{337.5}/I_{334.5}$ vs. Log (C) curve was taken to be the critical micelle concentration.

4.3.7 DLS Analysis

Aqueous suspensions of micelles were prepared as stated above at a concentration above the determined CMC, at 1 mg mL^{-1} . The micelles were analyzed to determine their hydrodynamic diameters (D_h) using dynamic light scattering. Size measurements were recorded at 25°C in triplicate.

4.3.8 Determination of *In vitro* Drug Release

A 1 mg mL^{-1} solution of combination loaded micelles of PEG-*b*-PCL and PEG-*b*-PBCL (4 mL) were prepared. The solution was transferred to a dialysis tube with molecular weight cut-off of 3500 Da. The solutions were then dialyzed against 15 mL of buffer solution (pH 7.4 or pH 5.0) at 37°C over 50 h, with samples taken at specific time intervals to determine the amount of DOX released over time. At each time interval, 2 mL of external buffer solution was removed and replaced with fresh buffer. The samples were diluted with DMSO (2 mL) and the absorbance of the solution was measured to calculate the amount of drug released based on pre-established calibration curves.

4.3.9 Biological Studies

Unless otherwise indicated, all cell culture experiments were performed using RPMI-1640

medium with L-glutamine and sodium bicarbonate supplemented with 10% fetal bovine serum and 1% penicillin-streptomycin. Cells were grown in a humidified environment at 37 °C with 5% CO₂. Cell viability studies were performed using the CellTiter-Blue[®] assay (Promega) according to the manufacturer's recommended protocol.

4.3.10 Empty Micelle Cytotoxicity Studies

HeLa cells were seeded in transparent flat-bottom 96-well plates at a cell density of 5,000 cells per well in 100 µL growth medium. After 24 h to allow cell adhesion, the medium was removed, the cells were washed with 100 µL PBS, and 100 µL fresh growth medium was added to each well. Empty micelles (1 mg mL⁻¹ in PBS) were diluted to concentrations ranging from 0.02 mg mL⁻¹ to 0.2 mg mL⁻¹. Micelle dilutions (100 µL) were added to the cells via a multichannel micropipette. The cells were incubated for 24 h with the micelles. At this time, the cell viability was evaluated by the CellTiter-Blue[®] assay, N=4.

4.3.11 Loaded Micelle Cytotoxicity Studies

HeLa cells were seeded in transparent flat-bottom 96-well plates at a cell density of 5,000 cells per well in 100 µL growth medium. After 24 h to allow cell adhesion, the medium was removed, the cells were washed with 100 µL PBS, and 100 µL of fresh growth medium was added to the cells. DOX loaded micelles (1 mg mL⁻¹ in PBS), RSV loaded micelles (1 mg mL⁻¹), and combination loaded micelles (1 mg mL⁻¹ in PBS) were diluted in PBS to concentrations ranging from 0.02 mg mL⁻¹ to 0.2 mg mL⁻¹. Loaded micelle dilutions (100 µL) were added to the cells via a multichannel micropipette. Free DOX and free RSV dosing were given assuming the dose from

the predetermined drug loading. The cells were then incubated for 24 h with the loaded micelles. After this time, the cell viability was evaluated using the CellTiter-Blue[®] assay, N=4.

4.3.12 Cellular Uptake

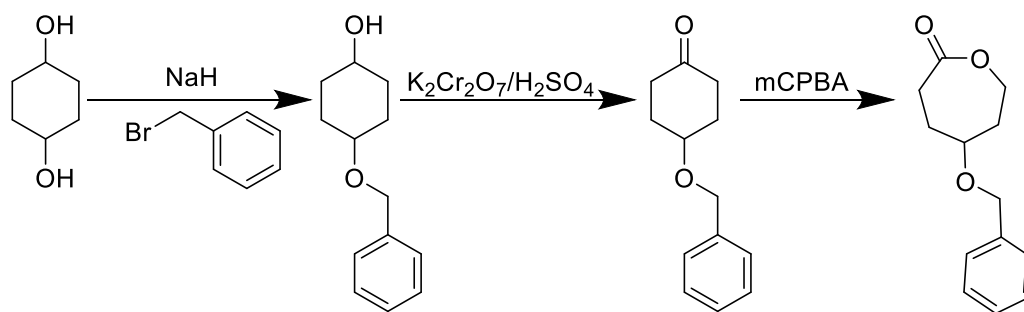
HeLa cells were seeded in a 35-mm glass bottom dish at a density of 250,000 cells per well and allowed to adhere for 24 h in 2 mL of growth media. At that time, the medium was removed, the cells were washed with 2 mL of PBS, and 2 mL of fresh growth medium was added along with 1 mL of combination loaded micelles (0.2 mg mL⁻¹ in PBS). The cells dosed with combination loaded micelles were allowed to incubate for 2 hours. After the uptake period, the cells were washed 3 times with 2 mL of PBS, fixed with 4% paraformaldehyde (incubated at room temperature for 10 minutes), washed 3 times with 2 mL of PBS, and the nuclei were counterstained with DAPI. Images were obtained using a BioTek Cytation 3 Cell Imaging Multi-Mode Reader.

4.4 Results and Discussion

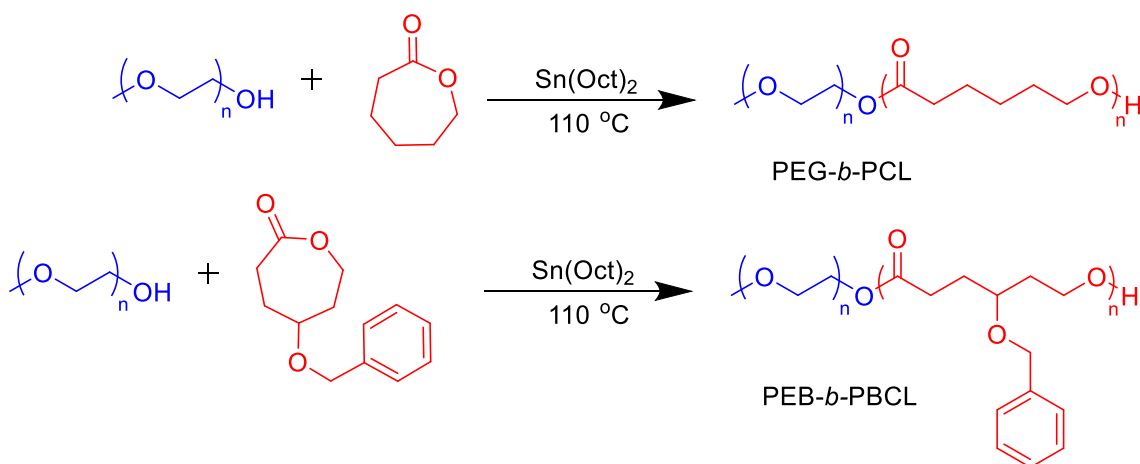
4.4.1 Polymer Design and Synthesis

In an effort to understand the effects on loading from the perspective of the choice of polymer, two different polymers were synthesized in this project, PEG-*b*-PCL and PEG-*b*-PBCL. It was presumed that the addition of a benzyl substituent in the γ -position to the hydrophobic block of the polymer would aid in an increased loading due to its ability to interact with DOX and RSV through π stacking interactions. The γ -benzyl- ϵ -caprolactone was synthesized according to previously reported procedures and is shown in Scheme 4.1. To synthesize the polymers, a coordination-insertion ring-opening polymerization was performed using tin(II) 2-ethylhexanoate

(Sn(Oct)₂) as the catalyst and PEG ($M_n \sim 2000 \text{ g mol}^{-1}$) as the macroinitiator (Scheme 4.2). PEG forms the hydrophilic portion of the polymer with PCL or PBCL functioning as the hydrophobic segment. A ratio of 50:50 hydrophilic: hydrophobic was targeted in order for consistency between the two polymers. These polymers were characterized with ¹H NMR spectroscopy and size exclusion chromatography (SEC). The compositions of the two polymers were shown to be comparable, with PEG-*b*-PBCL having a higher molecular weight due to the benzyl substituent. A summary of the polymer composition and molecular weights is shown in Table 4.1.



Scheme 4.1. Synthesis of γ -benzyl- ϵ -caprolactone monomer.



Scheme 4.2. Synthesis of PEG-*b*-PCL and PEG-*b*-PBCL through coordination-insertion ring-opening polymerization.

Table 4.1. Summary of Molecular Weights and Compositions of the Block Copolymers

	M_n^{NMR} (g mol ⁻¹) ^a	M_n^{SEC} (g mol ⁻¹) ^b	PDI ^b	mol% hydrophilic ^a	mol% hydrophobic ^a	CMC (g L ⁻¹) ^c
PEG-<i>b</i>-PCL	7700	10500	1.3	47	53	9.66 x 10 ⁻⁴
PEG-<i>b</i>-PBCL	13100	16900	1.5	48	52	7.94 x 10 ⁻⁴

^aDetermined by ¹H NMR spectroscopy ^bDetermined through SEC with triple detection and THF as the eluent ^cDetermined by fluorescence spectroscopy using pyrene as a probe

To determine the composition of the polymers, the protons corresponding to PEG at 3.51 ppm were integrated against the protons from the caprolactone unit at either 4.06 ppm for PEG-*b*-PCL (Figure 4.1) or 4.14 ppm for PEG-*b*-PBCL (Figure 4.3) in the ¹H NMR spectrum. The molecular weight was determined by ¹H NMR by the integration of the peak at 4.06 ppm for PEG-*b*-PCL and 4.14 ppm for PEG-*b*-PBCL versus the protons corresponding to methyl end group of PEG at 3.37 ppm. The molecular weights obtained from SEC are shown to be higher than those determined through ¹H NMR, which could be due to differences in the hydrodynamic volume of the polymers versus that of the polystyrene standards used for calibration. The SEC traces can be found in Figures 4.2 and 4.4 for PEG-*b*-PCL and PEG-*b*-PBCL, respectively.

4.4.2 Self-assembly and Morphology

The CMC of each polymer was determined by fluorescence spectroscopy using pyrene as a probe. When pyrene migrates from a hydrophilic to hydrophobic environment there is a shift in the excitation peak from ~334.5 nm to ~337.5 nm. The intensity ratio ($I_{337.5}/I_{334.5}$) was plotted against the logarithm of the concentration, where the intersection of the different slopes is estimated to be the CMC (Figure 4.5). In this case, the CMCs of the polymers were fairly similar, with the PEG-*b*-PBCL having a slightly lower CMC at 7.94 x 10⁻⁴ g L⁻¹ (Table 4.1). This can be

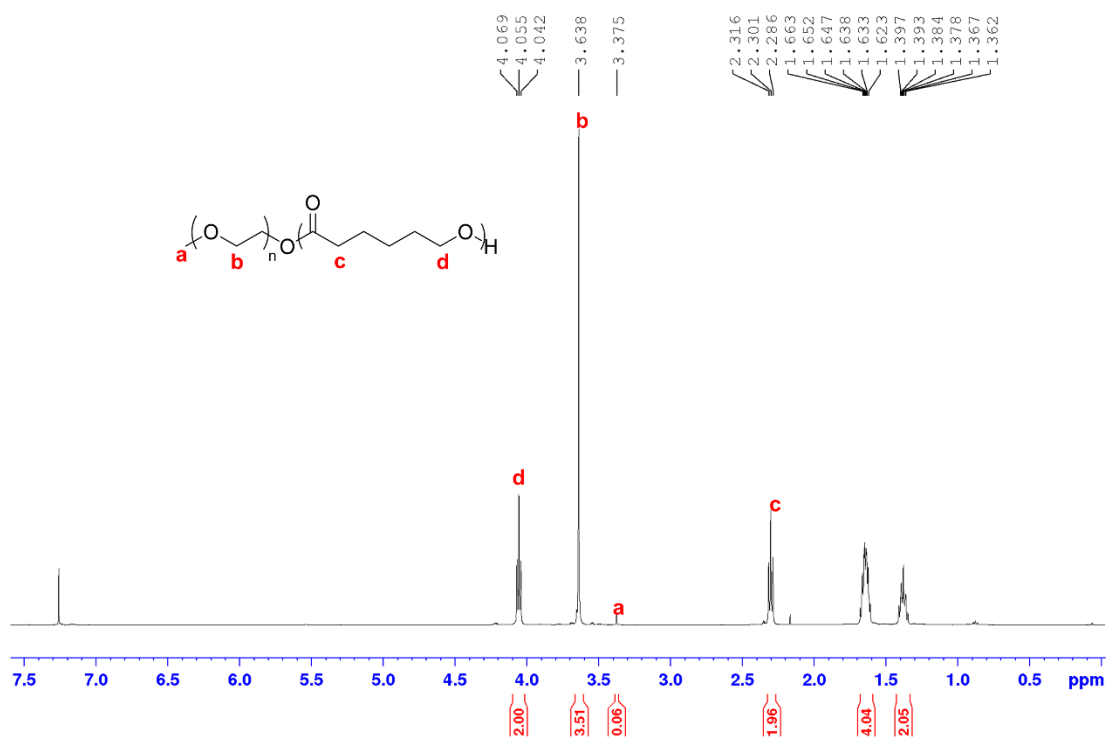


Figure 4.1. ^1H NMR spectrum of PEG-*b*-PCL.

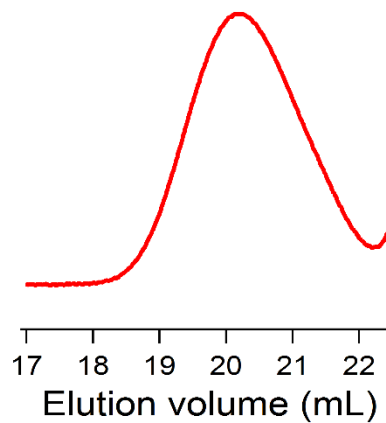


Figure 4.2. SEC trace of PEG-*b*-PCL with THF as the eluent.

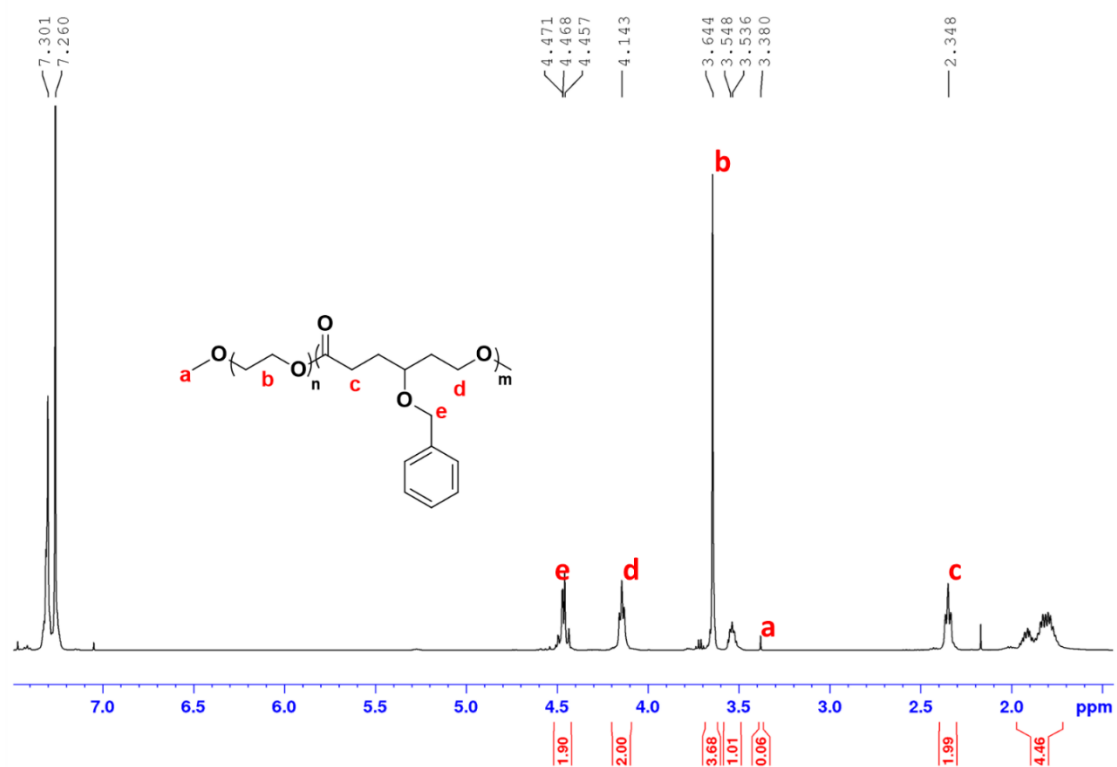


Figure 4.3. ^1H NMR spectrum of PEG-*b*-PBCL.

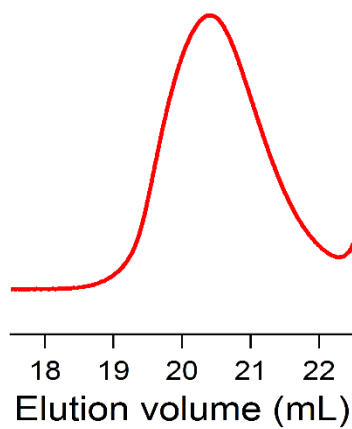


Figure 4.4. SEC trace of PEG-*b*-PBCL with THF as the eluent.

attributed to the benzyl substituent on the PEG-*b*-PBCL polymer increasing the hydrophobicity of the PCL segment which can provide more stable micelles.¹⁶⁵

The size of the empty micelles was determined by DLS and the morphology was determined by TEM. The micelles were formed through a solvent evaporation method where the polymer was dissolved in THF and added dropwise to DI H₂O under rapid stirring. After allowing the solvent to evaporate, the resulting micelle solution was filtered using 0.22 μ m Nylon syringe

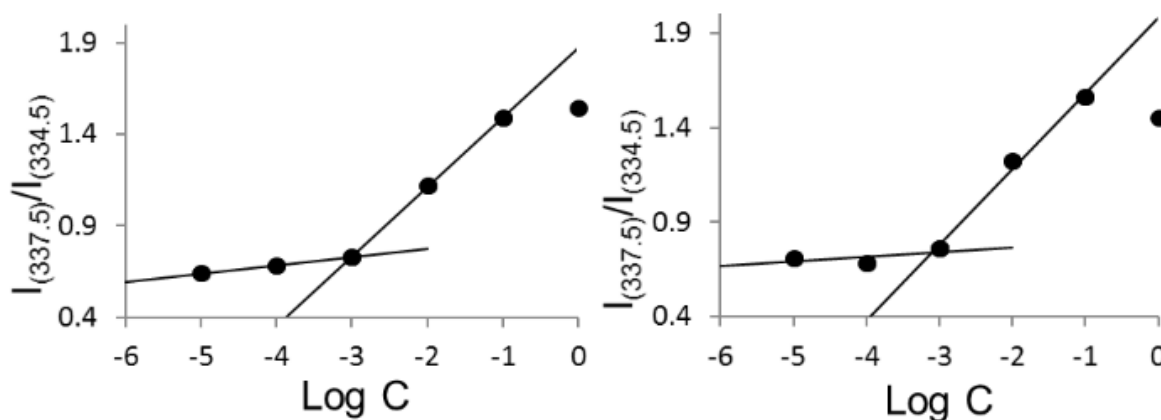


Figure 4.5. CMC plots of PEG-*b*-PCL (left) and PEG-*b*-PBCL (right).

filters. The PEG-*b*-PCL formed smaller micelles with an average size of 44.3 nm compared to 71.5 nm for PEG-*b*-PBCL. Both of the polymers were shown to form spherical micelles with fairly narrow dispersity as observed through the DLS and TEM images (Figure 4.6). The PEG-*b*-PCL had a slightly lower dispersity, but tended to aggregate more as seen by the TEM.

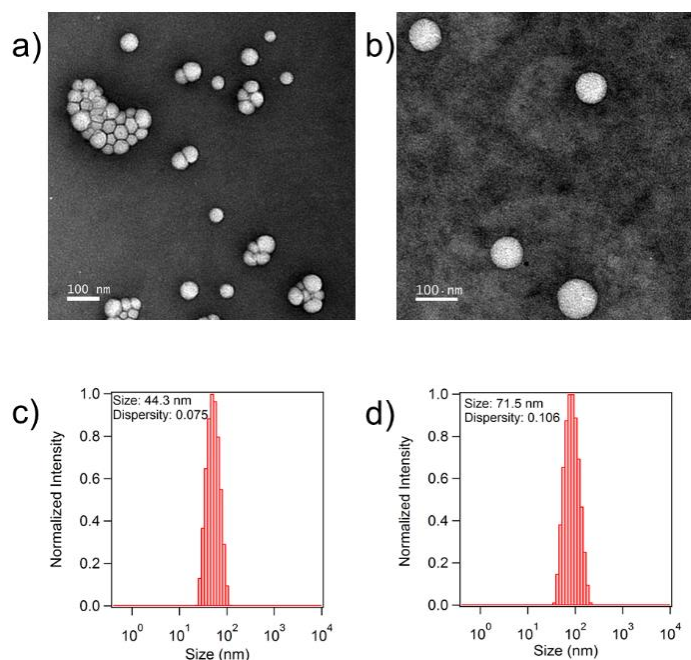


Figure 4.6. TEM images and DLS of empty micelles for PEG-*b*-PCL (a and c) and PEG-*b*-PBCL (b and d).

4.4.3 Drug Loading Capabilities

The DLC and EE of PEG-*b*-PCL and PEG-*b*-PBCL were examined by loading DOX, RSV, and a combination of the two drugs in a ratio of [polymer]:[RSV]:[DOX] at 10:1:1. The micelles were loaded through a solvent evaporation method using THF as the solvent. The DLC and EE were determined by measuring the absorbance at 320 nm for RSV and 485 nm for DOX and fitted against a pre-established calibration curve. The DLC and EE were calculated according to the following equations:

$$DLC = \frac{\text{amount of drug loaded}}{\text{amount of polymer}} \times 100$$

$$EE = \frac{\text{amount of drug loaded}}{\text{theoretical amount of drug}} \times 100$$

The combination loaded micelles were shown to have the highest loading for DOX in both PEG-*b*-PCL and PEG-*b*-PBCL (Table 4.2, entries 3 and 6), showing that by combining the two drugs, more DOX could be encapsulated than when loading DOX alone. This could be due to interactions between the two drugs such as hydrogen bonding, π -stacking, or both. Finding ways to increase loading efficiencies of these drug carriers is beneficial, since polymeric micelles suffer from low DLC and EE,¹⁶⁵⁻¹⁶⁶ which will improve the effectiveness of these systems. The loading of RSV continued to be low even when loading in combination, but was shown to increase significantly in the case of PEG-*b*-PBCL (Table 4.2, entry 4). PEG-*b*-PBCL exhibited the highest drug loading overall due to the presence of benzyl substituents on the hydrophobic segment which enable π -stacking between the polymer and the drugs.

Table 4.2. DLS and EE of Combination Loaded Micelles.

Entry	Polymer	Ratio [Polymer]:[RSV]:[DOX]	DLC ^{RSV} (%) ^a	EE ^{RSV} (%) ^a	DLC ^{DOX} (%) ^b	EE ^{DOX} (%) ^b
1	PEG- <i>b</i> -PCL	10:1:0	0.24	2.4	-	-
2		10:0:1	-	-	0.96	9.6
3		10:1:1	0.06	0.6	1.08	10.8
4	PEG- <i>b</i> -PBCL	10:1:0	0.22	2.2	-	-
5		10:0:1	-	-	3.10	31.0
6		10:1:1	1.87	18.7	8.77	87.7

^aDetermined by fitting to a pre-established calibration curve at 320 nm ^bDetermined by fitting to a pre-established calibration curve at 485 nm

To further explore the effect of combined loading of the two drugs, various ratios of polymer, RSV, and DOX were examined using PEG-*b*-PBCL, since it showed a higher loading capability than that of PEG-*b*-PCL. First, the amount of polymer used for loading was varied in the following ratios [PEG-*b*-PBCL]:[RSV]:[DOX]: 20:1:1, 10:1:1, and 5:1:1. It was shown that 5:1:1 had the highest EE of DOX at 91.1%, however it was only slightly higher than that of the 10:1:1 ratio at 87.7%. The 20:1:1 had the lowest DLC and EE for DOX at 1.72% and 34.3% respectively. For the loading of RSV, 10:1:1 had the highest EE at 18.7% compared with 11.9% for 5:1:1 and 5.16% for 20:1:1 (Figure 4.7, a and d). Since the 10:1:1 had the highest EE for RSV and a comparable EE for DOX, the polymer:drug ratio was kept constant at 10:1 and further studies for RSV and DOX variations were carried out.

For further optimization of the ratio of RSV to DOX, the [PEG-*b*-PBCL]:[RSV]:[DOX] ratio was varied from 10:1:1 to 10:5:1, with the amount of polymer and DOX kept constant. It was shown that with increasing ratio of RSV there was a higher DLC of RSV up to the ratio of 10:3:1. The highest RSV loading was achieved at 10:3:1 with a DLC of 4.44% and EE of 14.8%. At the ratio of 10:5:1, a considerable amount of RSV precipitated out causing the lowest loading for RSV with a DLC and EE for the set at 1.02% and 2.0% respectively. However, in terms of DOX loading, as the ratio of RSV to DOX increased, the DLC and EE of DOX decreased indicating that a lower ratio of RSV was preferred in terms of DOX loading (Figure 4.7, b and e).

Finally, the amount of DOX was varied with respect to polymer and RSV. The [PEG-*b*-PBCL]:[RSV]:[DOX] ratios were varied from 10:1:1 to 10:1:5. As the ratio of DOX increased, the DLC increased up to 34.25%. However, although the DLC increased, the EE decreased as the ratio of DOX increased. In respect to RSV, the amount of RSV loaded in the micelles remained low

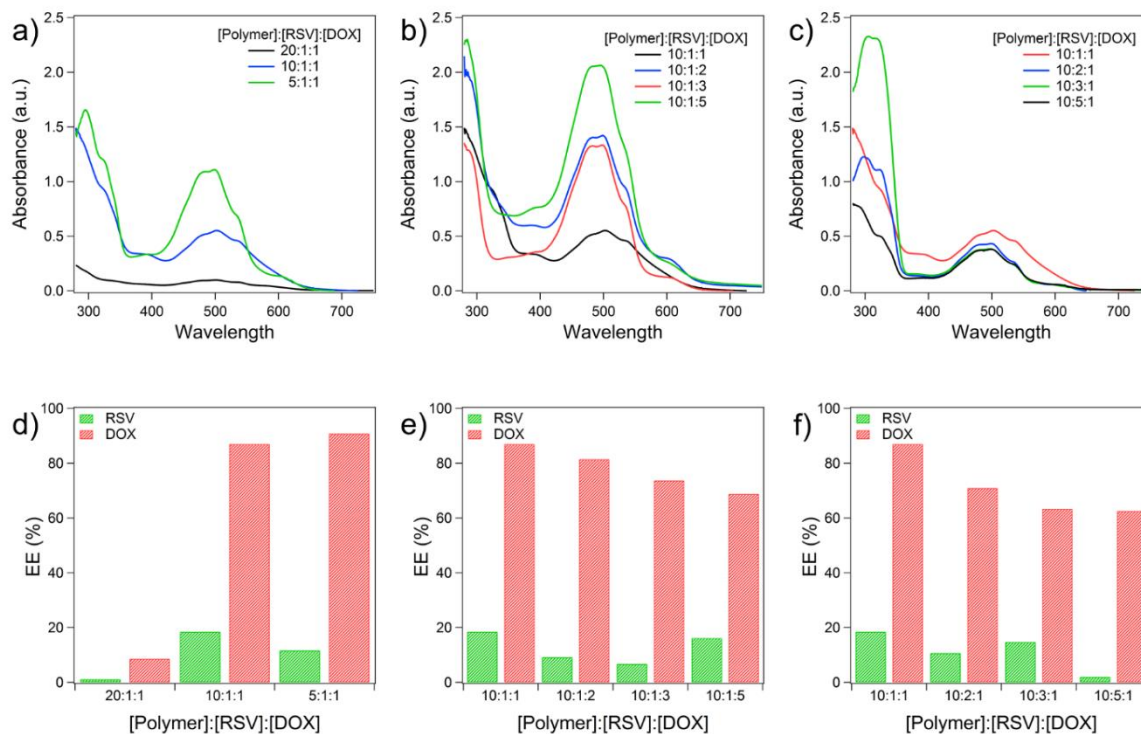


Figure 4.7. Absorbance spectra of drug loading variations (a) polymer variation, (b) DOX variation, and (c) RSV variation. Encapsulation efficiencies of drug loading variations (d) polymer variation, (e) DOX variation, and (f) RSV variation

(Figure 4.7, c and f). Based on the EE throughout all of the variations, the best ratio for DOX and RSV loading remained at 10:1:1. Hence, the ratio of [polymer]:[RSV]:[DOX] = 10:1:1 was chosen to observe changes in size and morphology measurements, as well as cellular studies. A full comparison of DLC and EE is available in Tables 4.3-4.5.

4.4.4 Size and Morphology of Combination Loaded Micelles

The size of the combination loaded PEG-*b*-PCL and PEG-*b*-PBCL micelles was investigated using DLS. It was shown that there was a relatively small size increase from the empty

Table 4.3. Drug Loading Results with Varying Ratios of Polymer PEG-*b*-PBCL.

Ratio [Polymer]:[RSV]:[DOX]	DLC ^{RSV} (%) ^a	EE ^{RSV} (%) ^a	DLC ^{DOX} (%) ^b	EE ^{DOX} (%) ^b
20: 1: 1	0.26	5.16	1.72	34.3
10: 1: 1	10: 1: 1	1.87	18.7	8.77
5: 1: 1	2.37	11.9	18.23	91.1

^aDetermined from pre-established calibration curve at 320 nm ^bDetermined from pre-established calibration curve at 485 nm

Table 4.4. Drug Loading Results with Varying Ratios of RSV in PEG-*b*-PBCL.

Ratio [Polymer]:[RSV]:[DOX]	DLC ^{RSV} (%) ^a	EE ^{RSV} (%) ^a	DLC ^{DOX} (%) ^b	EE ^{DOX} (%) ^b
10: 1: 1	1.87	18.7	8.77	87.7
10: 2: 1	2.17	10.9	7.17	71.7
10: 3: 1	4.44	14.8	6.34	63.4
10: 5: 1	1.02	2.0	6.33	63.3

^aDetermined from pre-established calibration curve at 320 nm ^bDetermined from pre-established calibration curve at 485 nm

Table 4.5. Drug Loading Results with Varying Ratios of DOX in PEG-*b*-PBCL.

Ratio [Polymer]:[RSV]:[DOX]	DLC ^{RSV} (%) ^a	EE ^{RSV} (%) ^a	DLC ^{DOX} (%) ^b	EE ^{DOX} (%) ^b
10: 1: 1	1.87	18.7	8.77	87.7
10: 1: 2	0.95	9.48	16.37	81.9
10: 1: 3	0.70	7.02	22.18	73.9
10: 1: 5	1.64	16.4	34.25	68.5

^aDetermined from pre-established calibration curve at 320 nm ^bDetermined from pre-established calibration curve at 485 nm

micelles for PEG-*b*-PCL to an average of 47.6 nm from 44.3 nm and PEG-*b*-PBCL to 84.4 nm from 71.5 nm. The smaller size increase for PEG-*b*-PCL is possibly due to the low loading capacity of these polymeric micelles. DLS spectra featuring a comparison of the size change between the

empty and loaded micelles is available in Figures 4.8 and 4.9. The DLS spectra and TEM images of the combination loaded micelles for both polymers are shown in Figure 4.10. The size determined from TEM is in agreement with the values that were obtained for DLS measurements as well. The TEM shows that the micelles retain their spherical shape and the micelles have a narrow dispersity. The sizes of the combination loaded micelles are in a range appropriate for participation in the enhanced permeability and retention (EPR) effect, which should allow for permeation and accumulation of the micelles in tumor tissue.¹⁶⁷

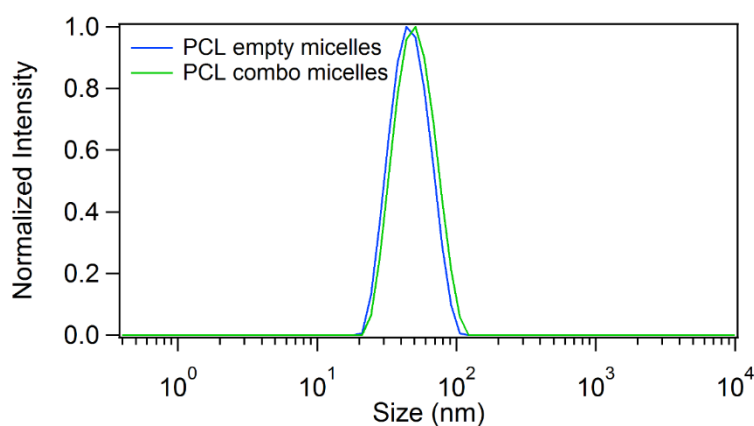


Figure 4.8. DLS size comparison of empty and RSV and DOX combination loaded PEG-*b*-PCL micelles.

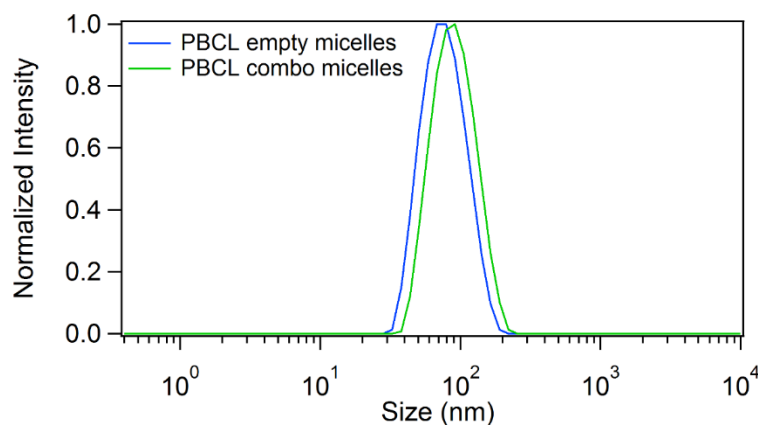


Figure 4.9. DLS size comparison of empty and RSV and DOX combination loaded PEG-*b*-PBCL micelles.

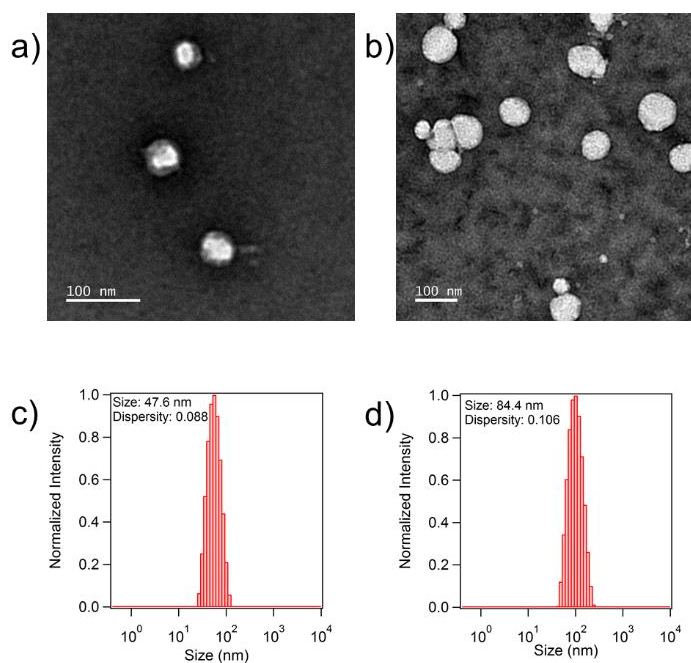


Figure 4.10. TEM images and DLS of combination loaded micelles for PEG-*b*-PCL (a and c) and PEG-*b*-PBCL (b and d).

4.4.5 *In vitro* Drug Release

The DOX release profiles were evaluated for combination loaded PEG-*b*-PCL and PEG-*b*-PBCL in buffer solutions at pH 7.4 and pH 5.0 (Figure 4.11). PEG-*b*-PCL showed significantly higher drug release at both pH 7.4 and pH 5.0 over PEG-*b*-PBCL, which is believed to be due to the favorable interactions of the DOX with the benzyl substituents causing a slower release. After 12 h, PEG-*b*-PCL showed cumulative release over 90% for pH 5 and over 80% for pH 7.4. On the other hand, PEG-*b*-PBCL showed cumulative release around 60% at pH 5 and 50% around pH 7.4, indicating that the PEG-*b*-PBCL micelles were more stable and had a more controlled release over time. The release at pH 5 is faster for both PEG-*b*-PCL and PEG-*b*-PBCL, due to the

degradation of the polymer backbones from hydrolysis of the ester groups. The micelles were fairly stable up to 4 hours with minimal release, and highest release beginning around 12 h.

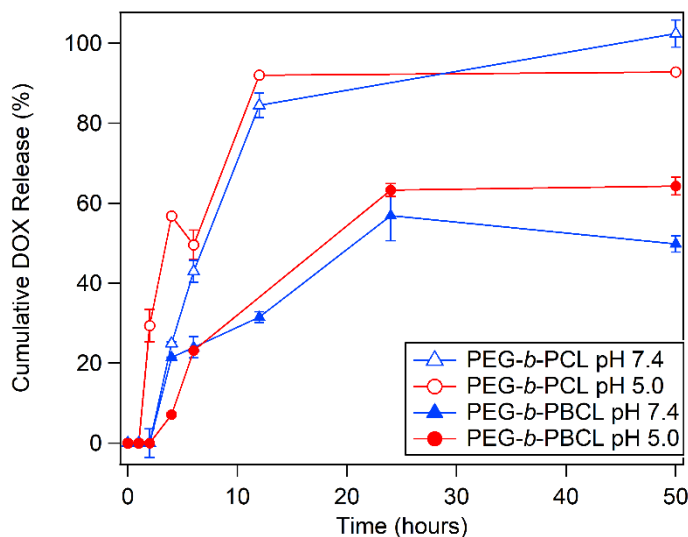


Figure 4.11. *In vitro* drug release over time of DOX from PEG-*b*-PCL and PEG-*b*-PBCL micelles at 37 °C.

4.4.6 Cytotoxicity of Empty and Combination Loaded Micelles

The cytotoxicity of empty micelles was measured using human cervical cancer cells (HeLa) over a 24 h period with doses ranging from 0.02 mg mL⁻¹ to 0.2 mg mL⁻¹ polymer in PBS (pH 7.4) (Figure 4.12). The cells showed high viability after being exposed to the polymer for 24 hours indicating that the polymers themselves were not cytotoxic. In order to assess the effect of the co-loading of the DOX and RSV in cytotoxicity experiments, HeLa cells were exposed to polymers loaded with DOX only, RSV only, and a combination of the two at different dosing concentrations ranging from 0.02 mg mL⁻¹ to 0.2 mg mL⁻¹ polymer in PBS (Figures 4.13 and 4.14). The loaded micelles were compared with free dosing of DOX, RSV, and a combination of DOX

and RSV that was dosed based on the amount of drug loaded in the micelles according to drug loading determinations. It was shown that the cells treated with either RSV loaded micelles or free RSV did not show decreased cell viability when compared with those of the empty polymer. Micelles loaded with DOX only and free DOX were shown to have decreased cell viability for both polymers, with DOX loaded PEG-*b*-PCL micelles having lower cytotoxicity than PEG-*b*-PBCL micelles due to their decreased DOX loading. However, the cells that were treated with combination loaded micelles or a combination of free DOX and RSV had the lowest viability. This was expected, as previous studies have shown that RSV can act as a chemosensitizing agent.¹⁶⁸ In addition, as shown with previous loading studies, the combination loaded micelles also contained the highest loading of DOX which should result in higher cytotoxicity to the cancer cells. Overall, the combination loaded PEG-*b*-PBCL micelles performed the best in the cytotoxicity studies as expected due to the highest DOX content of the micelles.

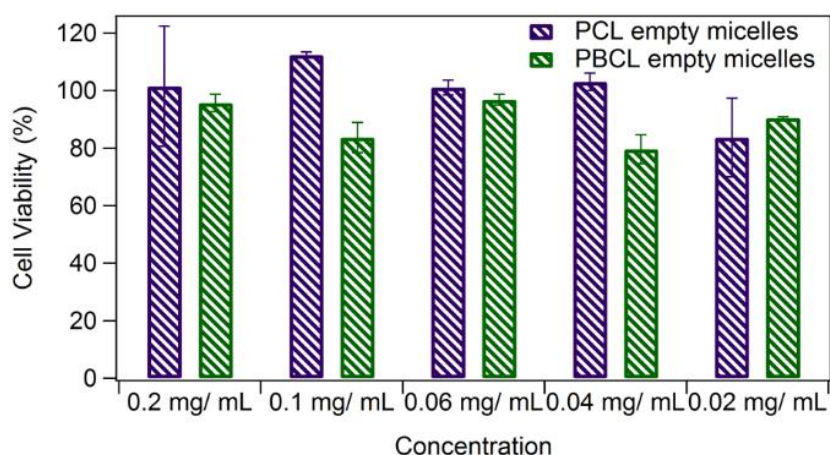


Figure 4.12. Cytotoxicity of PEG-*b*-PCL and PEG-*b*-PBCL empty micelles on HeLa cells after 24 hours.

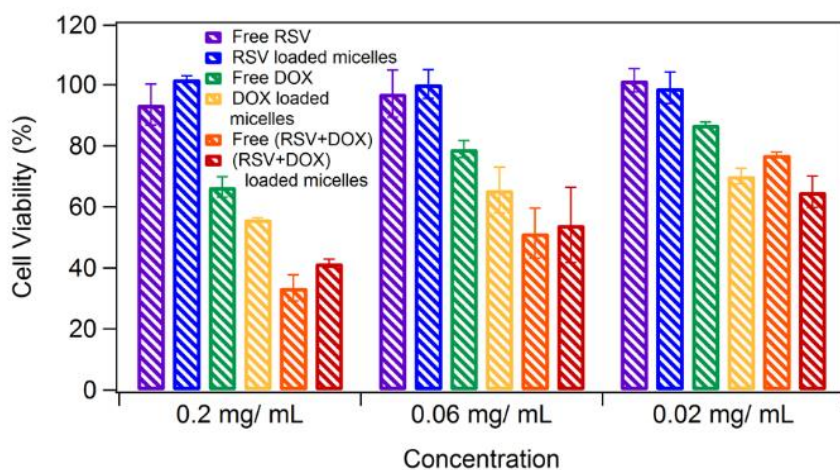


Figure 4.13. Cytotoxicity of DOX, RSV, and combination loaded PEG-*b*-PCL micelles on HeLa cells after 24 hours.

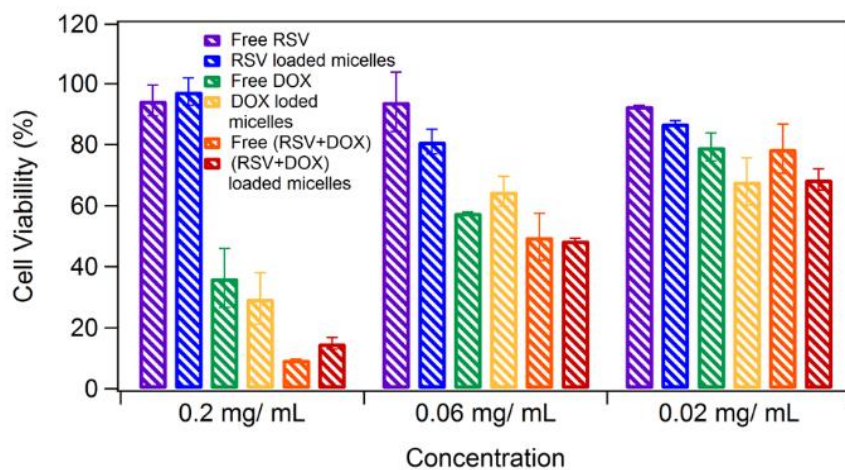


Figure 4.14. Cytotoxicity of DOX, RSV, and combination loaded PEG-*b*-PBCL micelles on HeLa cells after 24 hours.

4.4.7 Cellular Uptake

Cellular uptake studies were performed with combination loaded micelles of PEG-*b*-PCL and PEG-*b*-PBCL. HeLa cells were plated in 35-mm glass bottom cell culture dishes and dosed

with combination loaded micelles. After 2 h, the cells were fixed with paraformaldehyde and the nuclei were stained with DAPI. The cells were imaged to confirm the uptake of the micelles into the cancer cells (Figure 4.15). It was shown that the polymeric micelles were taken into the cells through endocytosis, with the DOX accumulating in the nucleus of the cells. It appears that the RSV is contained throughout the cells and does not preferentially accumulate in the nucleus.

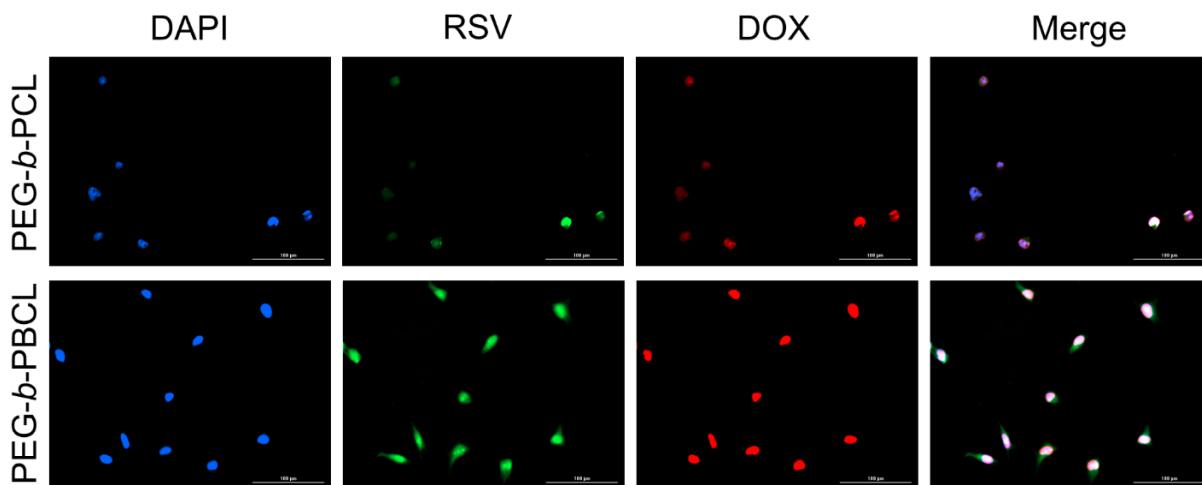


Figure 4.15. Cellular uptake of combination loaded micelles into HeLa cells after 2 hours.

4.5 Conclusions

The combination therapy of DOX and RSV has previously been shown as a way to improve cancer treatments through the synergy of the two drugs. RSV can act as a chemosensitizing agent, while also providing cardioprotection against the harmful effects of DOX treatment. As shown in this article, the combination loading of DOX and RSV into polymeric micelles provides further benefits with the use of RSV actually increasing the amount of DOX loaded into the micelles. The increased loading of DOX is beneficial in micellar drug delivery systems since often they are limited in their drug delivery capabilities. To the best of our knowledge, this is the first time an

increase in drug loading based on the combined use of DOX and RSV has been reported. This combination loading strategy is a new method that provides many benefits, enabling more efficient micellar drug delivery systems.

4.6 Acknowledgments

This work was completed through the equal contribution of Katherine and Ruvanthi. We would like to acknowledge financial support from NSF (CHE-1609880) and Welch Foundation (AT-1740).

REFERENCES

1. Chandra, R.; Rustgi, R., Biodegradable polymers. *Progress in Polymer Science* **1998**, 23 (7), 1273-1335.
2. Nair, L. S.; Laurencin, C. T., Biodegradable polymers as biomaterials. *Progress in Polymer Science* **2007**, 32 (8–9), 762-798.
3. Albertsson, A.C.; Varma, I. K., Aliphatic Polyesters: Synthesis, Properties and Applications. In *Degradable Aliphatic Polyesters*, Springer Berlin Heidelberg: Berlin, Heidelberg, **2002**; 1-40.
4. Vert, M., Aliphatic Polyesters: Great Degradable Polymers That Cannot Do Everything. *Biomacromolecules* **2005**, 6 (2), 538-546.
5. Jérôme, C.; Lecomte, P., Polyesters as Biomaterials: Synthesis and Fabrication. In *Encyclopedia of Biomedical Polymers and Polymeric Biomaterials*, Taylor & Francis: 2015; Vol. null, pp 6196-6224.
6. Zia, K. M.; Noreen, A.; Zuber, M.; Tabasum, S.; Mujahid, M., Recent developments and future prospects on bio-based polyesters derived from renewable resources: A review. *International Journal of Biological Macromolecules* **2016**, 82, 1028-1040.
7. Li, J.; Washington, M. A.; Bell, K. L.; Weiss, R. M.; Rothstein, S. N.; Little, S. R.; Edenborn, H. M.; Meyer, T. Y., Engineering Hydrolytic Degradation Behavior of Poly(lactic- co-glycolic acid) through Precise Control of Monomer Sequence. In *Sequence-Controlled Polymers: Synthesis, Self-Assembly, and Properties*, American Chemical Society: **2014**; Vol. 1170, 271-286.
8. Hakkarainen, M.; Höglund, A.; Odelius, K.; Albertsson, A.-C., Tuning the Release Rate of Acidic Degradation Products through Macromolecular Design of Caprolactone-Based Copolymers. *Journal of the American Chemical Society* **2007**, 129 (19), 6308-6312.
9. Xiong, X.-B.; Falamarzian, A.; Garg, S. M.; Lavasanifar, A., Engineering of amphiphilic block copolymers for polymeric micellar drug and gene delivery. *Journal of Controlled Release* **2011**, 155 (2), 248-261.
10. Hao, J.; Rainbolt, E.A.; Washington, K.; Biewer, M.C.; Stefan, M.C., Synthesis of Functionalized Poly(caprolactone)s and Their Application as Micellar Drug Delivery Systems. *Current Organic Chemistry* **2013**, 17 (9), 930-942.

11. Amass, W.; Amass, A.; Tighe, B., A review of biodegradable polymers: uses, current developments in the synthesis and characterization of biodegradable polyesters, blends of biodegradable polymers and recent advances in biodegradation studies. *Polymer International* **1998**, 47 (2), 89-144.
12. Mohamed, F.; van der Walle, C. F., Engineering biodegradable polyester particles with specific drug targeting and drug release properties. *Journal of Pharmaceutical Sciences* **2008**, 97 (1), 71-87.
13. Kumari, A.; Yadav, S. K.; Yadav, S. C., Biodegradable polymeric nanoparticles based drug delivery systems. *Colloids and Surfaces B: Biointerfaces* **2010**, 75 (1), 1-18.
14. Tian, H.; Tang, Z.; Zhuang, X.; Chen, X.; Jing, X., Biodegradable synthetic polymers: Preparation, functionalization and biomedical application. *Progress in Polymer Science* **2012**, 37 (2), 237-280.
15. Madhavan Nampoothiri, K.; Nair, N. R.; John, R. P., An overview of the recent developments in polylactide (PLA) research. *Bioresource Technology* **2010**, 101 (22), 8493-8501.
16. Edlund, U.; Albertsson, A.C., Degradable Polymer Microspheres for Controlled Drug Delivery. In *Degradable Aliphatic Polyesters*, Springer Berlin Heidelberg: Berlin, Heidelberg, **2002**, 67-112.
17. Makadia, H. K.; Siegel, S. J., Poly Lactic-co-Glycolic Acid (PLGA) as Biodegradable Controlled Drug Delivery Carrier. *Polymers* **2011**, 3 (3), 1377-1397.
18. Karavelidis, V.; Giliopoulos, D.; Karavas, E.; Bikiaris, D., Nanoencapsulation of a water soluble drug in biocompatible polyesters. Effect of polyesters melting point and glass transition temperature on drug release behavior. *European Journal of Pharmaceutical Sciences* **2010**, 41 (5), 636-643.
19. Alexis, F., Factors affecting the degradation and drug-release mechanism of poly(lactic acid) and poly[(lactic acid)-co-(glycolic acid)]. *Polymer International* **2005**, 54 (1), 36-46.
20. Lü, J.-M.; Wang, X.; Marin-Muller, C.; Wang, H.; Lin, P. H.; Yao, Q.; Chen, C., Current advances in research and clinical applications of PLGA-based nanotechnology. *Expert review of molecular diagnostics* **2009**, 9 (4), 325-341.
21. Wei, X.; Gong, C.; Gou, M.; Fu, S.; Guo, Q.; Shi, S.; Luo, F.; Guo, G.; Qiu, L.; Qian, Z., Biodegradable poly(ϵ -caprolactone)-poly(ethylene glycol) copolymers as drug delivery system. *International Journal of Pharmaceutics* **2009**, 381 (1), 1-18.
22. Woodruff, M. A.; Hutmacher, D. W., The return of a forgotten polymer—Polycaprolactone in the 21st century. *Progress in Polymer Science* **2010**, 35 (10), 1217-1256.

23. Dash, T. K.; Konkimalla, V. B., Poly- ϵ -caprolactone based formulations for drug delivery and tissue engineering: A review. *Journal of Controlled Release* **2012**, *158* (1), 15-33.
24. Rainbolt, E. A.; Miller, J. B.; Washington, K. E.; Senevirathne, S. A.; Biewer, M. C.; Siegwart, D. J.; Stefan, M. C., Fine-tuning thermoresponsive functional poly(ϵ -caprolactone)s to enhance micelle stability and drug loading. *Journal of Materials Chemistry B* **2015**, *3* (9), 1779-1787.
25. Senevirathne, S. A.; Boonsith, S.; Oupicky, D.; Biewer, M. C.; Stefan, M. C., Synthesis and characterization of valproic acid ester pro-drug micelles via an amphiphilic polycaprolactone block copolymer design. *Polymer Chemistry* **2015**, *6* (13), 2386-2389.
26. Senevirathne, S. A.; Washington, K. E.; Biewer, M. C.; Stefan, M. C., PEG based anti-cancer drug conjugated prodrug micelles for the delivery of anti-cancer agents. *Journal of Materials Chemistry B* **2016**, *4* (3), 360-370.
27. Senevirathne, S. A.; Washington, K. E.; Miller, J. B.; Biewer, M. C.; Oupicky, D.; Siegwart, D. J.; Stefan, M. C., HDAC inhibitor conjugated polymeric prodrug micelles for doxorubicin delivery. *Journal of Materials Chemistry B* **2017**, *5* (11), 2106-2114.
28. Vassiliou, A. A.; Papadimitriou, S. A.; Bikiaris, D. N.; Mattheolabakis, G.; Avgoustakis, K., Facile synthesis of polyester-PEG triblock copolymers and preparation of amphiphilic nanoparticles as drug carriers. *Journal of Controlled Release* **2010**, *148* (3), 388-395.
29. Moon, S. I.; Lee, C. W.; Taniguchi, I.; Miyamoto, M.; Kimura, Y., Melt/solid polycondensation of l-lactic acid: an alternative route to poly(l-lactic acid) with high molecular weight. *Polymer* **2001**, *42* (11), 5059-5062.
30. Papageorgiou, G. Z.; Bikiaris, D. N., Crystallization and melting behavior of three biodegradable poly(alkylene succinates). A comparative study. *Polymer* **2005**, *46* (26), 12081-12092.
31. Albertsson, A.C.; Varma, I. K., Recent Developments in Ring Opening Polymerization of Lactones for Biomedical Applications. *Biomacromolecules* **2003**, *4* (6), 1466-1486.
32. Dechy-Cabaret, O.; Martin-Vaca, B.; Bourissou, D., Controlled Ring-Opening Polymerization of Lactide and Glycolide. *Chemical Reviews* **2004**, *104* (12), 6147-6176.
33. Coulembier, O.; Degée, P.; Hedrick, J. L.; Dubois, P., From controlled ring-opening polymerization to biodegradable aliphatic polyester: Especially poly(β -malic acid) derivatives. *Progress in Polymer Science* **2006**, *31* (8), 723-747.
34. Kamber, N. E.; Jeong, W.; Waymouth, R. M.; Pratt, R. C.; Lohmeijer, B. G. G.; Hedrick, J. L., Organocatalytic Ring-Opening Polymerization. *Chemical Reviews* **2007**, *107* (12), 5813-5840.

35. Albertsson, A.C.; Srivastava, R. K., Recent developments in enzyme-catalyzed ring-opening polymerization. *Advanced Drug Delivery Reviews* **2008**, *60* (9), 1077-1093.
36. Liñares, G. G.; Baldessari, A., Lipases as efficient catalysts in the synthesis of monomers and polymers with biomedical applications. *Current Organic Chemistry* **2013**, *17* (7), 719-743.
37. Thomas, C. M., Stereocontrolled ring-opening polymerization of cyclic esters: synthesis of new polyester microstructures. *Chemical Society Reviews* **2010**, *39* (1), 165-173.
38. Kowalski, A.; Libiszowski, J.; Biela, T.; Cypriak, M.; Duda, A.; Penczek, S., Kinetics and Mechanism of Cyclic Esters Polymerization Initiated with Tin(II) Octoate. Polymerization of ϵ -Caprolactone and L-Lactide Co-initiated with Primary Amines. *Macromolecules* **2005**, *38* (20), 8170-8176.
39. Hao, P.; Yang, Z.; Li, W.; Ma, X.; Roesky, H. W.; Yang, Y.; Li, J., Aluminum Complexes Containing the C–O–Al–O–C Framework as Efficient Initiators for Ring-Opening Polymerization of ϵ -Caprolactone. *Organometallics* **2015**, *34* (1), 105-108.
40. Wei, Y.; Wang, S.; Zhou, S., Aluminum alkyl complexes: synthesis, structure, and application in ROP of cyclic esters. *Dalton Transactions* **2016**, *45* (11), 4471-4485.
41. Yang, Y.; Wang, H.; Ma, H., Stereoselective Polymerization of *rac*-Lactide Catalyzed by Zinc Complexes with Tetradentate Aminophenolate Ligands in Different Coordination Patterns: Kinetics and Mechanism. *Inorganic Chemistry* **2015**, *54* (12), 5839-5854.
42. Honrado, M.; Otero, A.; Fernández-Baeza, J.; Sánchez-Barba, L. F.; Garcés, A.; Lara-Sánchez, A.; Rodríguez, A. M., Copolymerization of Cyclic Esters Controlled by Chiral NNO-Scorpionate Zinc Initiators. *Organometallics* **2016**, *35* (2), 189-197.
43. Hao, J.; Granowski, P. C.; Stefan, M. C., Zinc Undecylenate Catalyst for the Ring-Opening Polymerization of Caprolactone Monomers. *Macromolecular Rapid Communications* **2012**, *33* (15), 1294-1299.
44. Jérôme, C.; Lecomte, P., Recent advances in the synthesis of aliphatic polyesters by ring-opening polymerization. *Advanced Drug Delivery Reviews* **2008**, *60* (9), 1056-1076.
45. De Jong, W. H.; Borm, P. J. A., Drug delivery and nanoparticles: Applications and hazards. *International Journal of Nanomedicine* **2008**, *3* (2), 133-149.
46. Peer, D.; Karp, J. M.; Hong, S.; Farokhzad, O. C.; Margalit, R.; Langer, R., Nanocarriers as an emerging platform for cancer therapy. *Nature Nanotechnology* **2007**, *2* (12), 751-760.

47. Cho, H. K.; Cheong, I. W.; Lee, J. M.; Kim, J. H., Polymeric nanoparticles, micelles and polymersomes from amphiphilic block copolymer. *Korean Journal of Chemical Engineering* **2010**, 27 (3), 731-740.
48. Elsabahy, M.; Wooley, K. L., Design of polymeric nanoparticles for biomedical delivery applications. *Chemical Society Reviews* **2012**, 41 (7), 2545-2561.
49. Lee, J. S. F., Jan, Polymersomes for drug delivery: Design, formation and characterization. *Journal of Controlled Release* **2012**, 161 (2), 473-483.
50. Brinkhuis, R. P.; Rutjes, F. P. J. T.; van Hest, J. C. M., Polymeric vesicles in biomedical applications. *Polymer Chemistry* **2011**, 2 (7), 1449-1462.
51. Bleul, R.; Thiermann, R.; Maskos, M., Techniques to Control Polymersome Size. *Macromolecules* **2015**, 48 (20), 7396-7409.
52. Torchilin, V. P., Passive and Active Drug Targeting: Drug Delivery to Tumors as an Example. In *Drug Delivery*, Schäfer-Korting, M., Ed. Springer Berlin Heidelberg: Berlin, Heidelberg, **2010**; 3-53.
53. Bertrand, N.; Wu, J.; Xu, X.; Kamaly, N.; Farokhzad, O. C., Cancer nanotechnology: The impact of passive and active targeting in the era of modern cancer biology. *Advanced Drug Delivery Reviews* **2014**, 66, 2-25.
54. Movassaghian, S.; Merkel, O. M.; Torchilin, V. P., Applications of polymer micelles for imaging and drug delivery. *Wiley Interdisciplinary Reviews: Nanomedicine and Nanobiotechnology* **2015**, 7 (5), 691-707.
55. Sawant, R. R.; Jhaveri, A. M.; Torchilin, V. P., Immunomicelles for advancing personalized therapy. *Advanced Drug Delivery Reviews* **2012**, 64 (13), 1436-1446.
56. Zhang, L.; Chen, Z.; Yang, K.; Liu, C.; Gao, J.; Qian, F., β -Lapachone and Paclitaxel Combination Micelles with Improved Drug Encapsulation and Therapeutic Synergy as Novel Nanotherapeutics for NQO1-Targeted Cancer Therapy. *Molecular Pharmaceutics* **2015**, 12 (11), 3999-4010.
57. Ouahab, A.; Shao, C.; Shen, Y.; Tu, J., Development and characterization of stabilized double loaded mPEG-PDLLA micelles for simultaneous delivery of paclitaxel and docetaxel. *Drug Development & Industrial Pharmacy* **2014**, 40 (7), 860-868.
58. Lee, K.-Y.; Chiu, Y.-T.; Lo, C.-L., Preparation and characterization of potential doxorubicin-loaded mixed micelles formed from vitamin E containing graft copolymers and PEG-*b*-PLA diblock copolymers. *RSC Advances* **2015**, 5 (102), 83825-83836.

59. Wan, C. P. L.; Letchford, K.; Leung, D.; Jackson, J. K.; Burt, H. M., Mixed Molecular Weight Copolymer Nanoparticles for the Treatment of Drug-Resistant Tumors: Formulation Development and Cytotoxicity. *Journal of Pharmaceutical Sciences* **2014**, *103* (12), 3966-3976.
60. Zhao, L.; Yang, C.; Dou, J.; Xi, Y.; Lou, H.; Zhai, G., Development of RGD-Functionalized PEG-PLA Micelles for Delivery of Curcumin. *Journal of Biomedical Nanotechnology* **2015**, *11* (3), 436-446.
61. Guan, X.; Guan, X.; Tong, H.; Ma, J.; Sun, X., Target Delivery of Daunorubicin to Glioblastoma by Cyclic RGD-Linked PEG-PLA Micelles. *Journal of Macromolecular Science, Part A* **2015**, *52* (5), 401-406.
62. Yin, L.; Chen, Y.; Zhang, Z.; Yin, Q.; Zheng, N.; Cheng, J., Biodegradable Micelles Capable of Mannose-Mediated Targeted Drug Delivery to Cancer Cells. *Macromolecular Rapid Communications* **2015**, *36* (5), 483-489.
63. Siafaka, P.; Betsiou, M.; Tsolou, A.; Angelou, E.; Agianian, B.; Koffa, M.; Chaitidou, S.; Karavas, E.; Avgoustakis, K.; Bikiaris, D., Synthesis of folate-pegylated polyester nanoparticles encapsulating ixabepilone for targeting folate receptor overexpressing breast cancer cells. *Journal of Materials Science: Materials in Medicine* **2015**, *26* (12), 1-14.
64. Xu, Z.; Liu, S.; Liu, H.; Yang, C.; Kang, Y.; Wang, M., Unimolecular micelles of amphiphilic cyclodextrin-core star-like block copolymers for anticancer drug delivery. *Chemical Communications* **2015**, *51* (87), 15768-15771.
65. Jelonek, K.; Li, S.; Wu, X.; Kasperczyk, J.; Marcinkowski, A., Self-assembled filomicelles prepared from polylactide/poly(ethylene glycol) block copolymers for anticancer drug delivery. *International Journal of Pharmaceutics* **2015**, *485* (1-2), 357-364.
66. Sui, X.; Kujala, P.; Janssen, G.-J.; de Jong, E.; Zuhorn, I. S.; van Hest, J. C. M., Robust formation of biodegradable polymersomes by direct hydration. *Polymer Chemistry* **2015**, *6* (5), 691-696.
67. Qiao, Z.-Y.; Qiao, S.-L.; Fan, G.; Fan, Y.-S.; Chen, Y.; Wang, H., One-pot synthesis of pH-sensitive poly(RGD-co- β -amino ester)s for targeted intracellular drug delivery. *Polymer Chemistry* **2014**, *5* (3), 844-853.
68. Deng, H.; Liu, J.; Zhao, X.; Zhang, Y.; Liu, J.; Xu, S.; Deng, L.; Dong, A.; Zhang, J., PEG-*b*-PCL Copolymer Micelles with the Ability of pH-Controlled Negative-to-Positive Charge Reversal for Intracellular Delivery of Doxorubicin. *Biomacromolecules* **2014**, *15* (11), 4281-4292.
69. Mura, S.; Nicolas, J.; Couvreur, P., Stimuli-responsive nanocarriers for drug delivery. *Nature Materials* **2013**, *12* (11), 991-1003.

70. Zhang, C. Y.; Xiong, D.; Sun, Y.; Zhao, B.; Lin, W. J.; Zhang, L. J., Self-assembled micelles based on pH-sensitive PAE-g-MPEG-cholesterol block copolymer for anticancer drug delivery. *International Journal of Nanomedicine* **2014**, 9, 4923-4933, 11 pp.
71. Liu, Q.; Chen, J.; Du, J., Asymmetrical polymer vesicles with a "stealthy" outer corona and an endosomal-escape-accelerating inner corona for efficient intracellular anticancer drug delivery. *Biomacromolecules* **2014**, 15 (8), 3072-3082.
72. Liu, H.; Miao, K.; Zhao, G.; Li, C.; Zhao, Y., Synthesis of an amphiphilic PEG-PCL-PSt-PLLA-PAA star quintopolymer and its self-assembly for pH-sensitive drug delivery. *Polymer Chemistry* **2014**, 5 (8), 3071-3080.
73. Hwang, G. H.; Min, K. H.; Lee, H. J.; Nam, H. Y.; Choi, G. H.; Kim, B. J.; Jeong, S. Y.; Lee, S. C., pH-Responsive robust polymer micelles with metal-ligand coordinated core cross-links. *Chemical. Communications* **2014**, 50 (33), 4351-4353.
74. Ko, N. R.; Oh, J. K., Glutathione-Triggered Disassembly of Dual Disulfide Located Degradable Nanocarriers of Polylactide-Based Block Copolymers for Rapid Drug Release. *Biomacromolecules* **2014**, 15 (8), 3180-3189.
75. Shi, C.; Guo, X.; Qu, Q.; Tang, Z.; Wang, Y.; Zhou, S., Actively targeted delivery of anticancer drug to tumor cells by redox-responsive star-shaped micelles. *Biomaterials* **2014**, 35 (30), 8711-8722.
76. Guerry, A.; Cottaz, S.; Fleury, E.; Bernard, J.; Halila, S., Redox-stimuli responsive micelles from DOX-encapsulating polycaprolactone-g-chitosan oligosaccharide. *Carbohydrate Polymers* **2014**, 112, 746-752.
77. Yameen, B.; Vilos, C.; Choi, W. I.; Whyte, A.; Huang, J.; Pollit, L.; Farokhzad, O. C., Drug Delivery Nanocarriers from Fully Degradable PEG-Conjugated Polyester with Reduction-Responsive Backbone. *Chemistry – A European Journal* **2015**, 21 (32), 11325-11329.
78. Cunningham, A.; Ko, N. R.; Oh, J. K., Synthesis and reduction-responsive disassembly of PLA-based mono-cleavable micelles. *Colloids and Surfaces B: Biointerfaces* **2014**, 122, 693-700.
79. Zhu, W.; Wang, Y.; Cai, X.; Zha, G.; Luo, Q.; Sun, R.; Li, X.; Shen, Z., Reduction-triggered release of paclitaxel from *in situ* formed biodegradable core-cross-linked micelles. *Journal of Materials Chemistry B* **2015**, 3 (15), 3024-3031.
80. Sun, R.; Luo, Q.; Gao, C.; Wang, Y.; Gao, L.; Du, H.; Huang, Y.; Li, X.; Shen, Z.; Zhu, W., Facile fabrication of reduction-responsive nanocarriers for controlled drug release. *Polymer Chemistry* **2014**, 5 (17), 4879-4883.

81. Zhao, X.; Liu, P., Reduction-Responsive Core-Shell-Corona Micelles Based on Triblock Copolymers: Novel Synthetic Strategy, Characterization, and Application As a Tumor Microenvironment-Responsive Drug Delivery System. *ACS Applied Materials & Interfaces* **2015**, 7 (1), 166-174.
82. Li, W.; Huang, L.; Ying, X.; Jian, Y.; Hong, Y.; Hu, F.; Du, Y., Antitumor drug delivery modulated by a polymeric micelle with an upper critical solution temperature. *Angewandte Chemie International Edition* **2015**, 54 (10), 3126-3131.
83. Karavelidis, V.; Bikiaris, D.; Avgoustakis, K., New thermosensitive nanoparticles prepared by biocompatible pegylated aliphatic polyester block copolymers for local cancer treatment. *Journal of Pharmacy and Pharmacology* **2015**, 67 (2), 215-230.
84. Li, M.; Pan, P.; Shan, G.; Bao, Y., Thermoresponsive poly(ϵ -caprolactone)-*graft*-poly(N-isopropylacrylamide) graft copolymers prepared by a combination of ring-opening polymerization and sequential azide-alkyne click chemistry. *Polymer International* **2015**, 64 (3), 389-396.
85. Rainbolt, E. A.; Washington, K. E.; Biewer, M. C.; Stefan, M. C., Towards smart polymeric drug carriers: self-assembling γ -substituted polycaprolactones with highly tunable thermoresponsive behavior. *Journal of Materials Chemistry B* **2013**, 1 (47), 6532-6537.
86. Dan, K.; Ghosh, S., Stimuli responsive triblock copolymers by chain-growth polymerization from telechelic macroinitiators prepared via a step-growth polymerization. *Polymer Chemistry* **2014**, 5 (12), 3901-3909.
87. Lee, R.S.; Li, Y.C.; Wang, S.W., Synthesis and characterization of amphiphilic photocleavable polymers based on dextran and substituted- ϵ -caprolactone. *Carbohydrate Polymers* **2015**, 117, 201-10.
88. Li, Y.; Niu, Y.; Hu, D.; Song, Y.; He, J.; Liu, X.; Xia, X.; Lu, Y.; Xu, W., Preparation of Light-Responsive Polyester Micelles via Ring-Opening Polymerization of *O*-Carboxyanhydride and Azide-Alkyne Click Chemistry. *Macromolecular Chemistry and Physics* **2015**, 216 (1), 77-84.
89. Chen, C.-Y.; Kim, T. H.; Wu, W.-C.; Huang, C.-M.; Wei, H.; Mount, C. W.; Tian, Y.; Jang, S.-H.; Pun, S. H.; Jen, A. K. Y., pH-dependent, thermosensitive polymeric nanocarriers for drug delivery to solid tumors. *Biomaterials* **2013**, 34 (18), 4501-4509.
90. Li, Y.; Wang, F.; Sun, T. M.; Du, J. Z.; Yang, X. Z.; Wang, J., Surface-modulated and thermoresponsive polyphosphoester nanoparticles for enhanced intracellular drug delivery. *Science China: Chemistry* **2014**, 57 (4), 579-585.

91. Wu, Q.; Tang, X.; Liu, X.; Hou, Y.; Li, H.; Yang, C.; Yi, J.; Song, X.; Zhang, G., Thermo/pH dual responsive mixed-shell polymeric micelles based on the complementary multiple hydrogen bonds for drug delivery. *Chemistry – An Asian Journal* **2016**, *11* (1), 112-119.
92. Zhu, A.; Miao, K.; Deng, Y.; Ke, H.; He, H.; Yang, T.; Guo, M.; Li, Y.; Guo, Z.; Wang, Y.; Yang, X.; Zhao, Y.; Chen, H., Dually pH/reduction-responsive vesicles for ultrahigh-contrast fluorescence imaging and thermo-chemotherapy-synergized tumor ablation. *ACS Nano* **2015**, *9* (8), 7874-7885.
93. Guo, X.; Shi, C.; Yang, G.; Wang, J.; Cai, Z.; Zhou, S., Dual-responsive polymer micelles for target-cell-specific anticancer drug delivery. *Chemistry of Materials* **2014**, *26* (15), 4405-4418.
94. Ye, L.; Liu, X.; Ito, K.; Feng, Z., The preparation of an azo-substituted polyrotaxane end-capped with PNIPPAAm and its dual stimuli-responsive behavior for drug delivery applications. *Journal of Materials Chemistry B* **2014**, *2* (35), 5746-5757.
95. Yuan, W.; Wang, J.; Li, L.; Zou, H.; Yuan, H.; Ren, J., Synthesis, Self-Assembly, and Multi-Stimuli Responses of a Supramolecular Block Copolymer. *Macromolecular Rapid Communications* **2014**, *35* (20), 1776-1781.
96. Dash, T. K.; Konkimalla, V. B., Polymeric Modification and Its Implication in Drug Delivery: Poly- ϵ -caprolactone (PCL) as a Model Polymer. *Molecular Pharmaceutics* **2012**, *9* (9), 2365-2379.
97. Oh, J. K., Polylactide (PLA)-based amphiphilic block copolymers: synthesis, self-assembly, and biomedical applications. *Soft Matter* **2011**, *7* (11), 5096-5108.
98. Rainbolt, E. A.; Washington, K. E.; Biewer, M. C.; Stefan, M. C., Recent developments in micellar drug carriers featuring substituted poly(ϵ -caprolactone)s. *Polymer Chemistry* **2015**, *6* (13), 2369-2381.
99. Seyednejad, H.; Ghassemi, A. H.; van Nostrum, C. F.; Vermonden, T.; Hennink, W. E., Functional aliphatic polyesters for biomedical and pharmaceutical applications. *Journal of Controlled Release* **2011**, *152* (1), 168-176.
100. Gaucher, G.; Dufresne, M.H.; Sant, V. P.; Kang, N.; Maysinger, D.; Leroux, J.C., Block copolymer micelles: preparation, characterization and application in drug delivery. *Journal of Controlled Release* **2005**, *109* (1-3), 169-188.
101. Tyrrell, Z. L.; Shen, Y.; Radosz, M., Fabrication of micellar nanoparticles for drug delivery through the self-assembly of block copolymers. *Progress in Polymer Science* **2010**, *35* (9), 1128-1143.

102. Hao, J.; Servello, J.; Sista, P.; Biewer, M. C.; Stefan, M. C., Temperature-sensitive aliphatic polyesters: synthesis and characterization of γ -substituted caprolactone monomers and polymers. *Journal of Materials Chemistry* **2011**, *21* (29), 10623-10628.
103. Hao, J.; Cheng, Y.; Ranatunga, R. J. K. U.; Senevirathne, S.; Biewer, M. C.; Nielsen, S. O.; Wang, Q.; Stefan, M. C., A Combined Experimental and Computational Study of the Substituent Effect on Micellar Behavior of γ -Substituted Thermoresponsive Amphiphilic Poly(ϵ -caprolactone)s. *Macromolecules* **2013**, *46* (12), 4829-4838.
104. Knop, K.; Hoogenboom, R.; Fischer, D.; Schubert, U. S., Poly(ethylene glycol) in Drug Delivery: Pros and Cons as Well as Potential Alternatives. *Angewandte Chemie International Edition* **2010**, *49* (36), 6288-6308.
105. Cheng, Y.; Hao, J.; Lee, L. A.; Biewer, M. C.; Wang, Q.; Stefan, M. C., Thermally Controlled Release of Anticancer Drug from Self-Assembled γ -Substituted Amphiphilic Poly(ϵ -caprolactone) Micellar Nanoparticles. *Biomacromolecules* **2012**, *13* (7), 2163-2173.
106. Lim, H. J.; Lee, H.; Kim, K. H.; Huh, J.; Ahn, C.-H.; Kim, J. W., Effect of molecular architecture on micellization, drug loading and releasing of multi-armed poly(ethylene glycol)-*b*-poly(ϵ -caprolactone) star polymers. *Colloid and Polymer Science* **2013**, *291* (8), 1817-1827.
107. Wu, W.; Wang, W.; Li, J., Star polymers: Advances in biomedical applications. *Progress in Polymer Science* **2015**, *46*, 55-85.
108. Kim, K. H.; Cui, G. H.; Lim, H. J.; Huh, J.; Ahn, C.-H.; Jo, W. H., Synthesis and Micellization of Star-Shaped Poly(ethylene glycol)-*block*-Poly(ϵ -caprolactone). *Macromolecular Chemistry and Physics* **2004**, *205* (12), 1684-1692.
109. Cameron, D. J. A.; Shaver, M. P., Aliphatic polyester polymer stars: synthesis, properties and applications in biomedicine and nanotechnology. *Chemical Society Reviews* **2011**, *40* (3), 1761-1776.
110. Trollsås, M.; Hedrick, J. L., Dendrimer-like Star Polymers. *Journal of the American Chemical Society* **1998**, *120* (19), 4644-4651.
111. Wang, F.; Bronich, T. K.; Kabanov, A. V.; Rauh, R. D.; Roovers, J., Synthesis and Evaluation of a Star Amphiphilic Block Copolymer from Poly(ϵ -caprolactone) and Poly(ethylene glycol) as a Potential Drug Delivery Carrier. *Bioconjugate Chemistry* **2005**, *16* (2), 397-405.
112. Inoue, K., Functional dendrimers, hyperbranched and star polymers. *Progress in Polymer Science* **2000**, *25* (4), 453-571.

113. Pu, Y.; Zhang, L.; Zheng, H.; He, B.; Gu, Z., Synthesis and Drug Release of Star-Shaped Poly(benzyl L-aspartate)-*block*-poly(ethylene glycol) Copolymers with POSS Cores. *Macromolecular Bioscience* **2014**, *14* (2), 289-297.
114. Khanna, K.; Varshney, S.; Kakkar, A., Miktoarm star polymers: advances in synthesis, self-assembly, and applications. *Polymer Chemistry* **2010**, *1* (8), 1171-1185.
115. Matyjaszewski, K., The synthesis of functional star copolymers as an illustration of the importance of controlling polymer structures in the design of new materials. *Polymer International* **2003**, *52* (10), 1559-1565.
116. Gao, X.; Wang, B.; Wei, X.; Rao, W.; Ai, F.; Zhao, F.; Men, K.; Yang, B.; Liu, X.; Huang, M.; Gou, M.; Qian, Z.; Huang, N.; Wei, Y., Preparation, characterization and application of star-shaped PCL/PEG micelles for the delivery of doxorubicin in the treatment of colon cancer. *International Journal of Nanomedicine* **2013**, *8*, 971-982.
117. Nabid, M. R.; Tabatabaei Rezaei, S. J.; Sedghi, R.; Niknejad, H.; Entezami, A. A.; Oskooie, H. A.; Heravi, M. M., Self-assembled micelles of well-defined pentaerythritol-centered amphiphilic A4B8 star-block copolymers based on PCL and PEG for hydrophobic drug delivery. *Polymer* **2011**, *52* (13), 2799-2809.
118. Quaglia, F.; Ostacolo, L.; Nese, G.; Canciello, M.; De Rosa, G.; Ungaro, F.; Palumbo, R.; La Rotonda, M. I.; Maglio, G., Micelles based on amphiphilic PCL-PEO triblock and star-shaped diblock copolymers: Potential in drug delivery applications. *Journal of Biomedical Materials Research Part A* **2008**, *87A* (3), 563-574.
119. Storey, R. F.; Sherman, J. W., Kinetics and Mechanism of the Stannous Octoate-Catalyzed Bulk Polymerization of ϵ -Caprolactone. *Macromolecules* **2002**, *35* (5), 1504-1512.
120. Tanzi, M. C.; Verderio, P.; Lampugnani, M. G.; Resnati, M.; Dejana, E.; Sturani, E., Cytotoxicity of some catalysts commonly used in the synthesis of copolymers for biomedical use. *Journal of Materials Science: Materials in Medicine* **1994**, *5* (6), 393-396.
121. Se, K.; Sakakibara, T.; Ogawa, E., Molecular weight determination of star polymers and star block copolymers using GPC equipped with low-angle laser light-scattering. *Polymer* **2002**, *43* (20), 5447-5453.
122. Choi, J.; Kwak, S.-Y., Synthesis and Characterization of Hyperbranched Poly(ϵ -caprolactone)s Having Different Lengths of Homologous Backbone Segments. *Macromolecules* **2003**, *36* (23), 8630-8637.
123. Singal, P. K.; Iliskovic, N., Doxorubicin-Induced Cardiomyopathy. *New England Journal of Medicine* **1998**, *339* (13), 900-905.

124. Shuai, X.; Ai, H.; Nasongkla, N.; Kim, S.; Gao, J., Micellar carriers based on block copolymers of poly(ϵ -caprolactone) and poly(ethylene glycol) for doxorubicin delivery. *Journal of Controlled Release* **2004**, 98 (3), 415-426.
125. Chen, Y.; Zhang, Y. X.; Wu, Z. F.; Peng, X. Y.; Su, T.; Cao, J.; He, B.; Li, S., Biodegradable poly(ethylene glycol)-poly(ϵ -caprolactone) polymeric micelles with different tailored topological amphiphilicities for doxorubicin (DOX) drug delivery. *RSC Advances* **2016**, 6 (63), 58160-58172.
126. Kataoka, K.; Harada, A.; Nagasaki, Y., Block copolymer micelles for drug delivery: design, characterization and biological significance. *Advanced Drug Delivery Reviews* **2001**, 47 (1), 113-131.
127. Ahmad, Z.; Shah, A.; Siddiq, M.; Kraatz, H.-B., Polymeric micelles as drug delivery vehicles. *RSC Advances* **2014**, 4 (33), 17028-17038.
128. Biswas, S.; Kumari, P.; Lakhani, P. M.; Ghosh, B., Recent advances in polymeric micelles for anti-cancer drug delivery. *European Journal of Pharmaceutical Sciences* **2016**, 83, 184-202.
129. Rösler, A.; Vandermeulen, G. W. M.; Klok, H. A., Advanced drug delivery devices via self-assembly of amphiphilic block copolymers. *Advanced Drug Delivery Reviews* **2012**, 64, Supplement, 270-279.
130. Allen, T. M.; Cullis, P. R., Drug Delivery Systems: Entering the Mainstream. *Science* **2004**, 303 (5665), 1818.
131. Rahikkala, A.; Aseyev, V.; Tenhu, H.; Kauppinen, E. I.; Raula, J., Thermoresponsive Nanoparticles of Self-Assembled Block Copolymers as Potential Carriers for Drug Delivery and Diagnostics. *Biomacromolecules* **2015**, 16 (9), 2750-2756.
132. Schmaljohann, D., Thermo- and pH-responsive polymers in drug delivery. *Advanced Drug Delivery Reviews* **2006**, 58 (15), 1655-1670.
133. Stuart, M. A. C.; Huck, W. T. S.; Genzer, J.; Muller, M.; Ober, C.; Stamm, M.; Sukhorukov, G. B.; Szleifer, I.; Tsukruk, V. V.; Urban, M.; Winnik, F.; Zauscher, S.; Luzinov, I.; Minko, S., Emerging applications of stimuli-responsive polymer materials. *Nature Materials* **2010**, 9 (2), 101-113.
134. Torchilin, V. P., Multifunctional, stimuli-sensitive nanoparticulate systems for drug delivery. *Nature Reviews Drug Discovery* **2014**, 13 (11), 813-827.
135. Washington, K. E.; Kularatne, R. N.; Karmegam, V.; Biewer, M. C.; Stefan, M. C., Recent advances in aliphatic polyesters for drug delivery applications. *Wiley Interdisciplinary Reviews: Nanomedicine and Nanobiotechnology* **2016**, DOI:10.1002/wnan.1446.

136. Adams, M. L.; Lavasanifar, A.; Kwon, G. S., Amphiphilic block copolymers for drug delivery. *Journal of Pharmaceutical Sciences* **2003**, 92 (7), 1343-1355.
137. Maeda, H.; Nakamura, H.; Fang, J., The EPR effect for macromolecular drug delivery to solid tumors: Improvement of tumor uptake, lowering of systemic toxicity, and distinct tumor imaging *in vivo*. *Advanced Drug Delivery Reviews* **2013**, 65 (1), 71-79.
138. Wang, J.; Mao, W.; Lock, L. L.; Tang, J.; Sui, M.; Sun, W.; Cui, H.; Xu, D.; Shen, Y., The Role of Micelle Size in Tumor Accumulation, Penetration, and Treatment. *ACS Nano* **2015**, 9 (7), 7195-7206.
139. Maeda, H., Toward a full understanding of the EPR effect in primary and metastatic tumors as well as issues related to its heterogeneity. *Advanced Drug Delivery Reviews* **2015**, 91, 3-6.
140. Roy, D.; Brooks, W. L. A.; Sumerlin, B. S., New directions in thermoresponsive polymers. *Chemical Society Reviews* **2013**, 42 (17), 7214-7243.
141. Ren, J. M.; McKenzie, T. G.; Fu, Q.; Wong, E. H. H.; Xu, J.; An, Z.; Shanmugam, S.; Davis, T. P.; Boyer, C.; Qiao, G. G., Star Polymers. *Chemical Reviews* **2016**, 116 (12), 6743-6836.
142. Basu Ray, G.; Chakraborty, I.; Moulik, S. P., Pyrene absorption can be a convenient method for probing critical micellar concentration (cmc) and indexing micellar polarity. *Journal of Colloid and Interface Science* **2006**, 294 (1), 248-254.
143. Kim, J. K.; Yang, S. Y.; Lee, Y.; Kim, Y., Functional nanomaterials based on block copolymer self-assembly. *Progress in Polymer Science* **2010**, 35 (11), 1325-1349.
144. Washington, K. E.; Kularatne, R. N.; Du, J.; Gillings, M. J.; Webb, J. C.; Doan, N. C.; Biewer, M. C.; Stefan, M. C., Synthesis of linear and star-like poly(ϵ -caprolactone)-*b*-poly{ γ -2-[2-(2-methoxy-ethoxy)ethoxy]ethoxy- ϵ -caprolactone} amphiphilic block copolymers using zinc undecylenate. *Journal of Polymer Science Part A: Polymer Chemistry* **2016**, 54 (22), 3601-3608.
145. Burke, J.; Donno, R.; d'Arcy, R.; Cartmell, S.; Tirelli, N., The Effect of Branching (Star Architecture) on Poly(d,l-lactide) (PDLLA) Degradation and Drug Delivery. *Biomacromolecules* **2017**, 18 (3), 728-739.
146. Tacar, O.; Sriamornsak, P.; Dass, C. R., Doxorubicin: an update on anticancer molecular action, toxicity and novel drug delivery systems. *Journal of Pharmacy and Pharmacology* **2013**, 65 (2), 157-170.

147. Cappetta, D.; Rossi, F.; Piegari, E.; Quaini, F.; Berrino, L.; Urbanek, K.; De Angelis, A., Doxorubicin targets multiple players: A new view of an old problem. *Pharmacological Research* **2012**.
148. Kasiotis, K. M.; Pratsinis, H.; Kletsas, D.; Haroutounian, S. A., Resveratrol and related stilbenes: Their anti-aging and anti-angiogenic properties. *Food and Chemical Toxicology* **2013**, *61*, 112-120.
149. Carrizzo, A.; Forte, M.; Damato, A.; Trimarco, V.; Salzano, F.; Bartolo, M.; Maciag, A.; Puca, A. A.; Vecchione, C., Antioxidant effects of resveratrol in cardiovascular, cerebral and metabolic diseases. *Food and Chemical Toxicology* **2013**, *61*, 215-226.
150. Pangeni, R.; Sahni, J. K.; Ali, J.; Sharma, S.; Baboota, S., Resveratrol: review on therapeutic potential and recent advances in drug delivery. *Expert Opinion on Drug Delivery* **2014**, *11* (8), 1285-1298.
151. Nassiri-Asl, M.; Hosseinzadeh, H., Review of the pharmacological effects of *Vitis vinifera* (Grape) and its bioactive compounds. *Phytotherapy Research* **2009**, *23* (9), 1197-1204.
152. Carlson, L. J.; Cote, B.; Alani, A. W. G.; Rao, D. A., Polymeric Micellar Co-delivery of Resveratrol and Curcumin to Mitigate *In Vitro* Doxorubicin-Induced Cardiotoxicity. *Journal of Pharmaceutical Sciences* **2014**, *103* (8), 2315-2322.
153. Rezk, Y. A.; Balulad, S. S.; Keller, R. S.; Bennett, J. A., Use of Resveratrol to improve the effectiveness of cisplatin and doxorubicin: Study in human gynecologic cancer cell lines and in rodent heart. *American Journal of Obstetrics and Gynecology* **2006**, *194* (5), e23-e26.
154. Meng, J.; Guo, F.; Xu, H.; Liang, W.; Wang, C.; Yang, X.-D., Combination Therapy using Co-encapsulated Resveratrol and Paclitaxel in Liposomes for Drug Resistance Reversal in Breast Cancer Cells *in vivo*. *Scientific Reports* **2016**, *6*, 22390.
155. Tatlıdede, E.; Sehirli, O.; Velioğlu-Oğünç, A.; Cetinel, S.; Yeğen, B. C.; Yarat, A.; Süleymanoğlu, S.; Sener, G., Resveratrol treatment protects against doxorubicin-induced cardiotoxicity by alleviating oxidative damage. *Free Radical Research* **2009**, 43.
156. Al-Abd, A. M.; Mahmoud, A. M.; El-Sherbiny, G. A.; El-Moselhy, M. A.; Nofal, S. M.; El-Latif, H. A.; El-Eraky, W. I.; El-Shemy, H. A., Resveratrol enhances the cytotoxic profile of docetaxel and doxorubicin in solid tumour cell lines *in vitro*. *Cell Proliferation* **2011**, *44* (6), 591-601.
157. Osman, A. M.; Bayoumi, H. M.; Al-Harthy, S. A.; Damanhour, Z. A.; AlShal, M., Modulation of doxorubicin cytotoxicity by resveratrol in a human breast cancer cell line. *Cancer Cell International* **2012**, 12.

158. Cote, B.; Carlson, L. J.; Rao, D. A.; Alani, A. W. G., Combinatorial resveratrol and quercetin polymeric micelles mitigate doxorubicin induced cardiotoxicity *in vitro* and *in vivo*. *Journal of Controlled Release* **2015**, *213*, 128-133.
159. Mi-Hua, L. I. U.; Jian, S.; Jian, L. I.; Yuan, Z.; Xiao-Long, L. I. N., Resveratrol inhibits doxorubicin-induced cardiotoxicity via sirtuin 1 activation in H9c2 cardiomyocytes. *Experimental & Therapeutic Medicine* **2016**, *12* (2), 1113-1118.
160. Rai, G.; Mishra, S.; Suman, S.; Shukla, Y., Resveratrol improves the anticancer effects of doxorubicin *in vitro* and *in vivo* models: A mechanistic insight. *Phytomedicine* **2016**, *23* (3), 233-242.
161. Gu, J.; Hu, W.; Zhang, D.-d., Resveratrol, a polyphenol phytoalexin, protects against doxorubicin-induced cardiotoxicity. *Journal of Cellular and Molecular Medicine* **2015**, *19* (10), 2324-2328.
162. Zhao, Y.; Huan, M.-l.; Liu, M.; Cheng, Y.; Sun, Y.; Cui, H.; Liu, D.-z.; Mei, Q.-b.; Zhou, S.-y., Doxorubicin and resveratrol co-delivery nanoparticle to overcome doxorubicin resistance. *Scientific Reports* **2016**, *6*, 35267.
163. Wang, W.; Zhang, L.; Le, Y.; Wang, J.; Chen, J.-F., Doxorubicin-loaded pH-sensitive polymeric blends for synergistic cancer treatment. *RSC Advances* **2016**, *6* (37), 31167-31176.
164. Gaucher, G.; Dufresne, M.-H.; Sant, V. P.; Kang, N.; Maysinger, D.; Leroux, J.-C., Block copolymer micelles: preparation, characterization and application in drug delivery. *Journal of Controlled Release* **2005**, *109* (1-3), 169-188.
165. Owen, S. C.; Chan, D. P. Y.; Shoichet, M. S., Polymeric micelle stability. *Nano Today* **2012**, *7* (1), 53-65.
166. Kim, S.; Shi, Y.; Kim, J. Y.; Park, K.; Cheng, J.-X., Overcoming the barriers in micellar drug delivery: loading efficiency, *in vivo* stability, and micelle-cell interaction. *Expert Opinion on Drug Delivery* **2010**, *7* (1), 49-62.
167. Cabral, H.; Matsumoto, Y.; Mizuno, K.; Chen, Q.; Murakami, M.; Kimura, M.; Terada, Y.; Kano, M. R.; Miyazono, K.; Uesaka, M.; Nishiyama, N.; Kataoka, K., Accumulation of sub-100 nm polymeric micelles in poorly permeable tumours depends on size. *Nature Nanotechnology* **2011**, *6* (12), 815-823.
168. Osman, A.-M. M.; Al-Harathi, S. E.; AlArabi, O. M.; Elshal, M. F.; Ramadan, W. S.; Alaama, M. N.; Al-Kreathy, H. M.; Damanhour, Z. A.; Osman, O. H., Chemosensitizing and cardioprotective effects of resveratrol in doxorubicin- treated animals. *Cancer Cell International* **2013**, *13* (1), 52.

BIOGRAPHICAL SKETCH

Katherine E. Washington was born and raised in New Mexico. She moved to the Dallas area and finished her undergraduate studies at The University of Texas at Dallas where she received her BS in Chemistry in 2012. During her undergraduate studies, she conducted research under Dr. Michael Biewer on the synthesis of poly(3-hexylthiophene) block copolymers. After studying polymer chemistry, she decided to join Dr. Mihaela Stefan's group and continue her graduate studies at The University of Texas at Dallas in the fall of 2012. It was during this time that she began working on substituted poly(caprolactone)s for micellar drug delivery systems. After completing her PhD studies, Katherine plans to work in an industry position.

CURRICULUM VITAE

Katherine E. Washington

Address: Department of Chemistry and Biochemistry, BE 26
The University of Texas at Dallas
800 W Campbell Rd, Richardson, TX 75080
Email: kew084000@utdallas.edu

Education:

The University of Texas at Dallas, Richardson, TX Aug. 2012 - June 2017

Ph.D. candidate in Chemistry

Dissertation: 'Linear and Star-Like Substituted Polycaprolactones for Enhanced Delivery of Doxorubicin'

Advisor: Prof. Mihaela C. Stefan

The University of Texas at Dallas, Richardson, TX Aug. 2008 – May 2012

B.S. in Chemistry

Graduate Research Experience:

Developed biodegradable linear and star-like amphiphilic diblock poly(ϵ -caprolactone)s for micellar drug delivery applications

- Focused on synthesis, purification, and characterization of small molecules and polymers
- Studied self-assembly of amphiphilic copolymers and encapsulation of hydrophobic molecules

Publications:

1. **Washington, K.E.**; Kularatne, R.N.; Biewer, M.C.; Stefan, M.C., Combination Loading of Doxorubicin and Resveratrol in Polymeric Micelles to Increase Efficiency and Efficacy. *Biomacromolecules*, **2017**, Submitted.
2. **Washington, K.E.**; Kularatne, R.N.; Du, J.; Ren, Y.; Gillings, M.J.; Geng, C.X.; Biewer, M.C.; Stefan, M.C., Thermoresponsive star-like γ -substituted poly(caprolactone)s for micellar drug delivery. *Journal of Materials Chemistry B*, **2017**, Submitted.
3. Quiram, G.; Mantagner, F.; Palmer, K.L.; Stefan, M.C.; **Washington, K.E.**; Rodrigues, D.C., Synthesis and Characterization of Chlorhexidine-Containing Polymeric Trilayer Nanoparticles for Intracanal Medicament. *Dental Materials*, **2017**, Submitted.
4. **Washington, K.E.**; Kularatne, R.N.; Karmegam, V.; Biewer, M.C.; Stefan, M.C., Stimuli-responsive poly(ϵ -caprolactone)s for drug delivery applications. Book chapter for Stimuli

Responsive Polymeric Nanocarriers for Drug Delivery Applications: Types and Triggers, Elsevier Publishing, 2017, Accepted.

5. Senevirathne, S.A.*; **Washington, K.E.***; Miller, J.B.; Biewer, M.C.; Oupicky, D.; Siegwart, D.J.; Stefan, M.C.; HDAC Inhibitor Conjugated Polymeric Prodrug Micelles for Doxorubicin Delivery. *J. Mater. Chem. B.*, **2017**, 5, 2106-2114. [*Equal contribution of authors]
6. Bulumulla, C.; Du, J.; **Washington, K.E.**; Kularatne, R.N.; Nguyen, H.Q.; Biewer, M.C.; Stefan, M.C.; Influence of Functionalized Side Chains of Polythiophene Diblock Copolymers on the Performance of CdSe Quantum Dot Hybrid Solar Cells. *J. Mater. Chem. A.*; **2017**, 5, 2473-2477.
7. Du, J.; Fortney, A.; **Washington, K.E.**; Bulumulla, C.; Huang, P.; Dissanayake, D.; Biewer, M.C.; Kowalewski, T.; Stefan, M.C.; Systematic Investigation of Benzodithiophene-Benzothiadiazole Isomers for Organic Photovoltaics. *ACS Applied Materials & Interfaces*, **2016**, 8, 33025-33033.
8. Pathiranage, T.M.S.K.; Kim, M.; Nguyen, H.Q.; **Washington, K.E.**; Biewer, M.C.; Stefan, M.C.; Enhancing Long-Range Ordering of P3HT by Incorporating Thermotropic Biphenyl Mesogens via ATRP. *Macromolecules*, **2016**, 49, 6846-6857.
9. **Washington, K.E.**; Kularatne, R.N.; Karmegam, V.; Biewer, M.C.; Stefan, M.C.; Recent advances in aliphatic polyesters for drug delivery applications. *WIREs Nanomedicine and Nanobiotechnology*, **2016**, DOI: 10.1002/wnan.1446
10. **Washington, K.E.**; Kularatne, R.N.; Du, J.; Gillings, M.J.; Webb, J.C.; Doan, N.C.; Biewer, M.C.; Stefan, M.C.; Synthesis of linear and star-like poly(ϵ -caprolactone)-*b*-poly{ γ -2-[2-(2-methoxy-ethoxy)ethoxy]ethoxy- ϵ -caprolactone} amphiphilic block copolymers using zinc undecylenate, *Journal of Polymer Science Part A: Polymer Chemistry*, **2016**, 54, 3601-3608.
11. Senevirathne, S.A.; **Washington, K.E.**; Biewer, M.C.; Stefan, M.C.; PEG based anti-cancer drug conjugated prodrug micelles for the delivery of anti-cancer agents. *J. Mater. Chem. B.*, **2016**, 4, 360-370.
12. Rainbolt, E.A.; Miller, J.B.; **Washington, K.E.**; Senevirathne, S.A.; Biewer, M.C.; Siegwart, D.J.; Stefan, M.C. Fine-tuning thermoresponsive functional poly(ϵ -caprolactone)s to enhance micelle stability and drug loading. *J. Mater. Chem. B.*, **2015**, 3, 1779-1787.
13. Rainbolt, E.A.; **Washington, K.E.**; Biewer, M.C.; Stefan, M.C. Recent developments in micellar drug carriers featuring substituted poly(ϵ -caprolactone)s. *Polymer Chemistry*, **2015**, 6, 2369-2381.
14. Kapallani, A.; Dillard, C.; **Washington, K.E.**; Biewer, M.C.; Stefan, M.C.; Kalra, V. Self-Assembly of Poly(3-hexylthiophene)-block-poly(γ -benzyl-L-glutamate) within Solution-Cast Films and Nanofibers. *Macromolecular Materials and Engineering*, **2014**, 299, 1484-1493.
15. Rainbolt, E.A.; **Washington, K.E.**; Biewer, M.C.; Stefan, M.C. Towards smart polymeric drug carriers: self-assembling γ -substituted polycaprolactones with highly tunable thermoresponsive behavior. *Journal of Materials Chemistry B: Materials for Biology and Medicine*, **2013**, 1, 6532-6537.
16. Hao, J.; Rainbolt, E.A.; **Washington, K.E.**; Biewer, M.C.; Stefan, M.C. Synthesis of Functionalized Poly(caprolactone)s and Their Application as Micellar Drug Delivery Systems. *Current Organic Chemistry* **2013**, 17, 930-942.

Presentations:

1. **Washington, K.E.**; Kularatne, R.N.; Ren, Y.X.; Biewer, M.C.; Stefan, M.C.; Functionalized star-like ϵ -caprolactone amphiphilic block copolymers for thermoresponsive micellar drug delivery systems. Oral presentation in the Excellence in Graduate Polymer Research Symposium, 253rd ACS National Meeting, San Francisco, CA (**March 2017**).
2. **Washington, K.E.**; Kularatne, R.N.; Gillings, M.J.; Geng, C.X.; Biewer, M.C.; Stefan, M.C.; Comparison of star-like and linear amphiphilic γ -substituted ϵ -caprolactone block copolymers for drug delivery applications. Oral presentation at the 252nd ACS National Meeting, Philadelphia, PA (**August 2016**).
3. **Washington, K.E.** Comparison of Linear and Star-like Poly(ϵ -caprolactone)-*b*-poly{ γ -2-[2-(2-methoxy-ethoxy)ethoxy]ethoxy- ϵ -caprolactone} Amphiphilic Block Copolymers for Drug Delivery Applications. Oral presentation at the 2016 Texas Soft Matter Meeting, Dallas, TX. (**August 2016**)
4. **Washington, K.E.**; Kularatne, R.N.; Doan, N.C.; Webb, J.C.; Gillings, M.J.; Biewer, M.C.; Stefan, M.C. Star-like amphiphilic γ -substituted ϵ -caprolactone block copolymers for drug delivery applications. Oral presentation at the 250th ACS National Meeting, Boston, MA. (**August 2015**)

Posters:

1. **Washington, K.E.**; Rainbolt, E.A.; Senevirathne, S.A.; Biewer, M.C.; Stefan, M.C.; γ -Substituted ϵ -caprolactone monomers for the synthesis of diblock copolymers for micellar drug delivery applications. Poster presentation at the 247th ACS National Meeting, Dallas, TX (**March 2014**).

Awards, Honors & Professional Association:

American Chemical Society Member (Jan. 2014 - Present)
Graduate Studies Scholarship, The University of Texas at Dallas (Aug. 2012 - Present)
Betty and Gifford Johnson Scholarship (April 2017)
Excellence in Graduate Polymer Research (ACS, March 2017)
PhD Research Small Grant (January 2017)
Eric Moore Chemistry Graduate Student Scholarship (June, 2015)